MARTIN MARIETTA ENERGY SYSTEMS LIBRARIES
3 4456 0363128 3

ornl

ORNL/TM-11918

OAK RIDGE NATIONAL LABORATORY

MARTIN MARIETTA

Analysis of the Spring-1991 Two-Meter Box Test Bed Experiments Performed at the Army Pulse Radiation Facility (APRF)

J. O. Johnson
J. D. Drischler
J. M. Barnes

OAK RIDGE NATIONAL LABORATORY
CENTRAL RESEARCH LIBRARY
CIRCULATION SECTION
4500N ROOM 175
LIBRARY LOAN COPY
DO NOT TRANSFER TO ANOTHER PERSON
If you wish someone else to see this report, send in name with report and the library will arrange a loan.

MANAGED BY
MARTIN MARIETTA ENERGY SYSTEMS, INC.
FOR THE UNITED STATES
DEPARTMENT OF ENERGY

This report has been reproduced directly from the best available copy.

Available to DOE and DOE contractors from the Office of Scientific and Technical Information, P.O. Box 62, Oak Ridge, TN 37831; prices available from (615) 576-8401, FTS 626-8401.

Available to the public from the National Technical Information Service, U.S. Department of Commerce, 5285 Port Royal Rd., Springfield, VA 22161.

This report was prepared as an account of work sponsored by an agency of the United States Government. Neither the United States Government nor any agency thereof, nor any of their employees, makes any warranty, express or implied, or assumes any legal liability or responsibility for the accuracy, completeness, or usefulness of any information, apparatus, product, or process disclosed, or represents that its use would not infringe privately owned rights. Reference herein to any specific commercial product, process, or service by trade name, trademark, manufacturer, or otherwise, does not necessarily constitute or imply its endorsement, recommendation, or favoring by the United States Government or any agency thereof. The views and opinions of authors expressed herein do not necessarily state or reflect those of the United States Government or any agency thereof.

ORNL/TM-11918

Engineering Physics and Mathematics Division

ANALYSIS OF THE SPRING-1991 TWO-METER BOX TEST BED EXPERIMENTS PERFORMED AT THE ARMY PULSE RADIATION FACILITY (APRF)

J. O. Johnson
J. D. Drischler
J. M. Barnes*

*Computing and Telecommunications Division

DATE PUBLISHED - September 1992

NOTICE This document contains information of a preliminary nature. It is subject to revision or correction and therefore does not represent a final report.

This work is sponsored by the Defense Nuclear Agency under DNA MIPR #92-524, Work Unit 00001 and DOE Interagency Agreement No 1205-E097-A1

Prepared by
Oak Ridge National Laboratory
Oak Ridge, Tennessee 37831
managed by
MARTIN MARIETTA ENERGY SYSTEMS, INC.
for the
U.S. DEPARTMENT OF ENERGY
under Contract No. DE-AC05 84OR21400

MARTIN MARIETTA ENERGY SYSTEMS LIBRARIES

3 4456 0363128 3

)OE F 1332.15
10-90)
ll other editions
'e obsolete

U.S. DEPARTMENT OF ENERGY

DOE AND MAJOR CONTRACTOR RECOMMENDATIONS FOR ANNOUNCEMENT AND DISTRIBUTION OF DOCUMENTS

(See Instructions on Reverse Side)

OMB Control No. 1910-1400
Burden Disclosure Statement on back

. DOE Report No.	2. DOE Contract No.	3. DOE Funding Office	4. OSTI UC or C Category No.
)RNL/TM-11918	DE-AC05-84OR21400	43 0C 08 40 3	UC-000

. Title ANALYSIS OF THE SPRING -1991 TWO-METER BOX TEST BED EXPERIMENTS PERFORMED AT THE ARMY PULSE RADIATION FACILITY (APRF)

. **Type of Document ("x" one)**

a. Scientific and technical report: ❒ monthly ❒ quarterly ❒ annual ❒ final ☒ topical ❒ special/public interest ❒ other

b. Conference paper: Name of conference (no abbreviations) _____

Location (city/st/ctry) _____

Date (mo/day/yr) _____ Sponsor _____

Contents: ❒ proceedings ❒ viewgraphs ❒ paper ❒ poster sessions

c. Computer Media:

Document is accompanied by ❒ magnetic tape(s) _____
❒ diskette(s) _____
❒ other (specify) _____

d. Other (e.g., journal article, manuscript, manual, etc.) (specify) _____

. **Copies Transmitted to OSTI ("x" one or more). See instructions on Reverse.**

❒ a. Copies for unclassified distribution.
☒ b. Twelve copies for OSTI processing and NTIS sales.
❒ c. Twenty-five additional copies for special/public interest.
❒ d. Two reproducible copies for OSTI processing.
❒ e. Copies for special distribution.
❒ f. Copies for classified distribution as defined in M-3679.
❒ g. One copy for OSTI classified processing.

. **Document contains information pertaining to any of the following:**

❒ Yes ("x" one or more) ☒ No (If no, unlimited distribution may be made within the U.S. In addition, copies may be made available to foreign requestors through exchange agreements or NTIS sales.)

❒ a. Classified
(Announce to appropriate recipients as listed in M-3679, "Standard Distribution for Classified Scientific and Technical Reports")
❒ b. Export Control/ITAR/EAR
❒ c. Proprietary Data
❒ d. Small Business Innovation Research (SBIR)
❒ e. Unclassified Controlled Nuclear Information (UCNI)
❒ f. Patent Hold
❒ g. Translations of copyrighted material
(Boxes b–g will be announced to Government agencies and their contractors)
❒ h. Cooperative Research and Development Agreement (CRADA)
❒ i. Other (explain) _____
(This designation must be in accordance with written DOE Program Office guidance. Attach copy of guidance.)

Upon demand, OSTI will make distribution of these documents in accordance with existing laws, regulations, and/or written program office guidance.

). **Patent Information**

a. Does this information product disclose any new equipment, process, or material? ☒ No ❒ Yes If so, identify page nos. _____

b. Has an invention disclosure been submitted to DOE covering any aspect of this information product? ☒ No ❒ Yes
If so, identify the DOE (or other) disclosure number and to whom the disclosure was submitted.

c. Are there any patent-related objections to the release of this information product? ☒ No ❒ Yes If so, state these objections.

0. **Additional information, remarks, and special handling instructions. (*Do not* identify Sigma categories for Nuclear Weapon Data reports, and *do not* provide additional instructions which are inconsistent with item 8 above.) (Continue on separate sheet, if necessary.)**

1. Submitted by (Name and Position) (Please print or type)		Phone
R. A. Lawson, Laboratory Records Department Head		574-6764
Organization	**Signature**	**Date**
Oak Ridge National Laboratory	R. A. Lawson (KB)	10-1-92

TABLE OF CONTENTS

Page

LIST OF FIGURES v

LIST OF TABLES vii

ACKNOWLEDGEMENTS xi

EXECUTIVE SUMMARY xiii

ABSTRACT xv

1.0 INTRODUCTION 1

1.1 Objective 1

2.0 THE TWO-METER BOX TEST BED EXPERIMENTS 2

2.1 The APRF Reactor Source 2
2.2 The Two-Meter Box Test Bed 2
2.3 The RT-200 Anthropomorphic Phantom 3
2.4 Details of the Measurements 3
2.5 Experimental Equipment 4

3.0 MASH CALCULATIONAL TECHNIQUES 5

3.1 Definition of Protection and Reduction Factors 5
3.2 Air-Over-Ground Environment 5
3.3 The Two-Meter Box and Phantom Geometry Models 11
3.4 The Two-Meter Box Calculations 17

4.0 DISCUSSION OF RESULTS 19

4.1 Neutron Dose and Reduction Factors 19
4.2 Gamma-Ray Dose and Reduction Factors 21

5.0 MONTE CARLO STATISTICAL UNCERTAINTY 43

6.0 CONCLUSIONS 44

7.0 RECOMMENDATIONS 47

8.0 REFERENCES 48

APPENDIX A - Comparisons of the Calculated (MASH) and Measured Neutron Dose Reduction Factors for the Spring 1991 Two-Meter Box Test Bed Experiments Performed at the APRF 49

APPENDIX B - Comparisons of the Calculated (MASH) and Measured Gamma-Ray Dose and Reduction Factors for the Spring 1991 Two-Meter Box Test Bed Experiments Performed at the APRF 56

APPENDIX C - Sample Input Decks for MORSE Used in the MASH Analysis of the Spring 1991 Two-Meter Box Test Bed Experiments Performed at the APRF 70

LIST OF FIGURES

Figure — Page

1. Isometric View of the Two-Meter Box Test Bed with a 5% Borated Polyethylene Liner 12

2. Isometric View of the Combinatorial Geometry Phantom Model Used in the MASH Analysis 13

3. Isometric View of the MASH Geometry Model of the Combinatorial Geometry Phantom Standing Inside the Lined (5% Borated Polyethylene) Two-Meter Box Test Bed 14

C-1. Sample MORSE Input for the MASH Analysis of the Empty Lined (5% Borated Polyethylene) Two-Meter Box Used in the APRF Spring 1991 Two-Meter Box Test Bed Experiments 71

C-2. Sample Geometry Input for the MASH Analysis of the Empty Lined (5% Borated Polyethylene) Two-Meter Box Used in the APRF Spring 1991 Two-Meter Box Test Bed Experiments. 73

C-3. Sample MORSE Input for the MASH Analysis of the Combinatorial Geometry Phantom (with BD-100R Detectors) Used in the APRF Spring 1991 Two-Meter Box Test Bed Experiments 76

C-4. Sample Geometry Input for the MASH Analysis of the Combinatorial Geometry Phantom (with BD-100R Detectors) Used in the APRF Spring 1991 Two-Meter Box Test Bed Experiments 78

C-5. Sample MORSE Input for the MASH Analysis of the Combinatorial Geometry Phantom (with BD-100R Detectors) Standing in the Lined (5% Borated Polyethylene) Two-Meter Box Used in the APRF Spring 1991 Two-Meter Box Test Bed Experiments 85

C-6. Sample Geometry Input for the MASH Analysis of the Combinatorial Geometry Phantom (with BD-100R Detectors) Standing in the Lined (5% Borated Polyethylene) Two-Meter Box Used in the APRF Spring 1991 Two-Meter Box Test Bed Experiments 87

LIST OF TABLES

Table | Page

1. Definitions of Radiation Protection Factors and Reduction Factors 6

2. APRF Reactor Neutron Leakage Spectrum (number of neutrons per energy bin) and DABL69 Free-In-Air Tissue Kerma Response Function (Gy-cm^2/n) Used in the MASH Analysis 8

3. APRF Reactor Gamma-Ray Leakage Spectrum (number of gamma rays per energy bin) and DABL69 Free-In-Air Tissue Kerma Response Function (Gy-cm^2/γ) Used in the MASH Analysis 9

4. Meteorological Data and Air Number Densities Used in the MASH Analysis of the APRF Spring 1991 Two-Meter Box Test Bed Experiments 10

5. Compositions of the Materials Used in the MASH Analysis of the APRF Spring 1991 Two-Meter Box Test Bed Experiments 15

6. MASH Coordinate Positions for the Analysis of the APRF Spring 1991 Two-Meter Box Test Bed Experiments BD-100R Bubble Dosimeter Locations on the RT-200 Humanoid Phantom and Inside the Two-Meter Box . . . 16

7. MASH Geometry Regions and Cross-Section Materials Used in the Analysis of the APRF Spring 1991 Two-Meter Box Test Bed Experiments 18

8. Comparisons of Calculated and APRF Measured Neutron Dose Averaged Over External, Internal, and All Detector Locations On or Inside the RT-200 Humanoid Phantom at the 400 Meter Test Site at the APRF . . 25

9. Comparisons of Calculated and APRF Measured Neutron Reduction Factors Averaged Over External, Internal, and All Detector Locations On or Inside the RT-200 Humanoid Phantom at the 400 Meter Test Site at the APRF 26

10. Comparisons of Calculated and ETCA Measured Neutron Dose Averaged Over External, Internal, and All Detector Locations On or Inside the RT-200 Humanoid Phantom at the 400 Meter Test Site at the APRF 27

11. Comparisons of Calculated and ETCA Measured Neutron Reduction Factors Averaged Over External, Internal, and All Detector Locations On or Inside the RT-200 Humanoid Phantom at the 400 Meter Test Site at the APRF 28

12. Comparisons of Calculated and Average Experimentally Measured Neutron Dose Averaged Over External, Internal, and All Detector Locations On or Inside the RT-200 Humanoid Phantom at the 400 Meter Test Site at the APRF 29

13. Comparisons of Calculated and Average Experimentally Measured Neutron Reduction Factors Averaged Over External, Internal, and All Detector Locations On or Inside the RT-200 Humanoid Phantom at the 400 Meter Test Site at the APRF 30

14. Comparisons of Calculated and HDL Measured Gamma-Ray Dose Averaged Over External, Internal, and All Detector Locations On or Inside the RT-200 Humanoid Phantom at the 400 Meter Test Site at the APRF 31

15. Comparisons of Calculated and HDL Measured Gamma-Ray Reduction Factors Averaged Over External, Internal, and All Detector Locations On or Inside the RT-200 Humanoid Phantom at the 400 Meter Test Site at the APRF 32

16. Comparisons of Calculated and APRF Measured Gamma-Ray Dose Averaged Over External, Internal, and All Detector Locations On or Inside the RT-200 Humanoid Phantom at the 400 Meter Test Site at the APRF. (Small TLD) 33

17. Comparisons of Calculated and APRF Measured Gamma-Ray Reduction Factors Averaged Over External, Internal, and All Detector Locations On or Inside the RT-200 Humanoid Phantom at the 400 Meter Test Site at the APRF. (Small TLD) 34

18. Comparisons of Calculated and APRF Measured Gamma-Ray Dose Averaged Over External, Internal, and All Detector Locations On or Inside the RT-200 Humanoid Phantom at the 400 Meter Test Site at the APRF. (Large TLD) 35

19. Comparisons of Calculated and APRF Measured Gamma-Ray Reduction Factors Averaged Over External, Internal, and All Detector Locations On or Inside the RT-200 Humanoid Phantom at the 400 Meter Test Site at the APRF. (Large TLD) 36

20. Comparisons of Calculated and ETCA Measured Gamma-Ray Dose Averaged Over External, Internal, and All Detector Locations On or Inside the RT-200 Humanoid Phantom at the 400 Meter Test Site at the APRF 37

21. Comparisons of Calculated and ETCA Measured Gamma-Ray Reduction Factors Averaged Over External, Internal, and All Detector Locations On or Inside the RT-200 Humanoid Phantom at the 400 Meter Test Site at the APRF 38

22. Comparisons of Calculated and AFRRI Measured Gamma-Ray Dose Averaged Over External, Internal, and All Detector Locations On or Inside the RT-200 Humanoid Phantom at the 400 Meter Test Site at the APRF 39

23. Comparisons of Calculated and AFRRI Measured Gamma-Ray Reduction Factors Averaged Over External, Internal, and All Detector Locations On or Inside the RT-200 Humanoid Phantom at the 400 Meter Test Site at the APRF 40

24. Comparisons of Calculated and Average Experimentally Measured Gamma-Ray Dose(Tissue) Averaged Over External, Internal, and All Detector Locations On or Inside the RT-200 Humanoid Phantom at the 400 Meter Test Site at the APRF 41

25. Comparisons of Calculated and Average Experimentally Measured Gamma-Ray Reduction Factors(Tissue) Averaged Over External, Internal, and All Detector Locations On or Inside the RT-200 Humanoid Phantom at the 400 Meter Test Site at the APRF 42

26. Overall Comparisons of Calculated and Average Experimentally Measured Neutron and Gamma-Ray Dose and Reduction Factors Averaged Over External, Internal, and All Detector Locations On or Inside the RT-200 Humanoid Phantom, and Phantom Orientation Free-Field or Inside the Two-Meter Box, at the 400 Meter Test Site at the APRF 46

A-1. MASH VS. APRF: Phantom Free-Field Neutron Dose and Reduction Factors 50

A-2. MASH VS. APRF: Phantom In 2m Box Neutron Dose 51

A-3. MASH VS. APRF: Phantom In 2m Box Neutron Reduction Factors . . . 52

A-4. MASH VS. ETCA: Phantom Free-Field Neutron Dose and Reduction Factors 53

A-5. MASH VS. ETCA: Phantom In 2m Box Neutron Dose 54

A-6. MASH VS. ETCA: Phantom In 2m Box Neutron Reduction Factors . . . 55

B-1. MASH VS. HDL: Phantom Free-Field Gamma-Ray Dose and Reduction Factors 57

B-2. MASH VS. HDL: Phantom In 2m Box Gamma-Ray Dose 58

B-3. MASH VS. HDL: Phantom In 2m Box Gamma-Ray Reduction Factors 59

B-4. MASH VS. APRF: Phantom Free-Field Gamma-Ray Dose and Reduction Factors 60

B-5. MASH VS. APRF (Small TLD): Phantom In 2m Box Gamma-Ray Dose 61

B-6. MASH VS. APRF (Small LTD): Phantom In 2m Box Gamma-Ray Reduction Factors 62

B-7. MASH VS: APRF (Large LTD): Phantom In 2m Box Gamma-Ray Dose 63

B-8. MASH VS. APRF (Large LTD): Phantom In 2m Box Gamma-Ray Reduction Factors 64

B-9 MASH VS. ETCA: Phantom Free-Field Gamma-Ray Dose and Reduction Factors 65

B-10. MASH VS. ETCA: Phantom In 2m Box Gamma-Ray Dose 66

B-11. MASH VS. ETCA: Phantom In 2m Box Gamma-Ray Reduction Factors 67

B-12. MASH VS. AFRRI: Phantom In 2m Box Gamma-Ray Dose 68

B-13. MASH VS. AFRRI: Phantom In 2m Box Gamma-Ray Reduction Factors 69

ACKNOWLEDGEMENTS

The authors would first like to express their gratitude to the Defense Nuclear Agency for continuously supporting and patiently monitoring the development, verification, and validation of the MASH code system. Also, the authors would like to thank Mrs. Sue Shriner for her significant efforts in preparing this manuscript for publication.

EXECUTIVE SUMMARY

This report summarizes the results of a "benchmark" analysis of the Monte Carlo Adjoint Shielding Code system (MASH) against a series of experiments performed at the Army Pulse Radiation Facility (APRF) in Aberdeen Proving Ground, Maryland. This series of experiments was performed during the period from April 26, 1991 through May 9, 1991 and involved experimentalists from APRF, the Armed Forces Radiobiological Research Institute (AFRRI), Harry Diamond Laboratories (HDL), and the Establissement Technique Central de l'Armement, France (ETCA). The "benchmark" analysis of MASH is being performed at Oak Ridge National Laboratory (ORNL) and Science Applications International Corporation (SAIC) and is designed to determine the capability of MASH in reproducing the measured neutron and gamma-ray integral and spectral data. This effort is one of the primary objectives of the MASH Verification and Validation Subtask of the Defense Nuclear Agency (DNA) Radiation Environments Program (REP). Results of the "benchmark" analyses were used in the recommendations to the North Atlantic Treaty Organization (NATO) Panel VII Ad Hoc Group of Shielding Experts for replacing the Vehicle Code System (VCS) with MASH as the reference code for future armored vehicle nuclear vulnerability calculations.

The reactor was operated in the steady state mode for all of the measurements. Environmental effects due to terrain, meteorological data, and ground moisture were assessed for inclusion in the MASH analysis. Two different detectors were used by the experimentalists to measure the radiation environments in the free-field and inside the two-meter box test bed, including the BD-100R Bubble Dosimeters for neutron measurements and Thermoluminescent Dosimeters (TLDs) for gamma-ray measurements. Integral measurements were made at a distance of 400 meters from the APRF reactor. In particular, free-field environments were measured along with measurements made using the "NATO standard test bed" with an interior 5.08-cm-thick 5% borated polyethylene liner and the RT-200 humanoid phantom standing in the free-field and inside the lined test bed at the "NATO standard reference point" at 400 meters. The "NATO standard test bed" is a large cubical steel walled box having interior dimensions of 200 cm x 200 cm x 200 cm and wall thickness (top and sides) of 5.08 cm. The bottom plate is 10.16 cm thick. The top and side wall thicknesses can be increased to 10.16 cm by the addition of 5.08-cm-thick steel plates. The two-meter box test bed was chosen because the geometry provides a simplistic assembly for experimental and theoretical (MASH) comparisons of radiation transmission through material types and thicknesses indicative of modern armored vehicles. The RT-200 anthropomorphic phantom approximates the size, height, and weight of the typical U. S. armored vehicle crewman. The RT-200 stands 175.0 cm tall, and weighs 74.0 kg. The chest depth and width are 21.4 cm and 33.8 cm respectively, and the head depth and width are 20.8 cm and 14.8 cm. The RT-200 has non-articulating arms and legs as separate solid members and a physical appearance that closely resembles the male human form.

The MASH calculational technique employs a forward discrete ordinates calculation to determine the neutron and gamma-ray flux on a coupling surface surrounding the armored

vehicle or shielded structure and an adjoint Monte Carlo calculation to determine the dose importance of the surface flux. MASH then folds the flux together with the dose importance to yield the desired detector response(s). MASH was specifically designed to calculate the neutron and gamma-ray radiation environments and shielding protection factors of vehicles, structures, trenches, and other shield configurations. All calculations utilized a P_5 Legendre expansion of the cross sections, the reference DNA DABL69 69 group (46n/23γ) cross-section library, and the Kerr fluence-to-dose free-in-air tissue dose conversion factors (from the DABL69 library).

In general, the calculational results show mixed agreement with the measured data reported by the different teams of experimentalists. The neutron dose results indicate good agreement (typically ±20%) for the phantom standing in the free-field and excellent agreement (typically ±10%) for the phantom standing inside the two-meter box. The neutron reduction factors however, agreed for the phantom standing in the free-field but exhibited significant differences for the phantom standing inside the box. With respect to the gamma-ray data, there were individual discrepancies between calculations and measurements however, typical agreement was within ±20%. The C/E comparisons for the gamma-ray free-field environment at 400 meters showed improved agreement between calculation and experiment relative to the same comparisons in the Fall 1989 and Spring 1990 studies. To determine the overall quality of the comparisons between MASH and the measurements, the data (both calculational and experimental) was averaged over detector position (internal and external), response function (tissue and CaF_2:Mn), radiation type (neutron and gamma-ray), and phantom orientation (front facing and left side toward reactor). This averaging procedure produced one set of data for the phantom standing in the free-field, and one set of data for the phantom standing inside the lined two-meter box. Overall, the calculations agreed quite well with most of the measured data supplied by the teams of experimentalists. Generally, the agreement was within the ±20% limit deemed as acceptable by the DNA.

This was the third concerted effort aimed at benchmarking the MASH code against experimental measurements, and again there were some glitches in the effort. The most significant problem occurred in the reporting of the gamma-ray dose data. The calculational and experimental results must report the same data for a meaningful comparison to be made. For TLD data, all corrections to the data for spectral effects (calibration field versus radiation field), response functions [dose(tissue) or dose(TLD)], and contributions due to thermal neutrons must be accounted for or removed from both sets of data. This will allow a true "benchmark" comparison of the MASH code system and reduce the possible sources of discrepancies. The comparisons again indicate multiple teams of experimentalists performing the same set of measurements yield a better indication of the quality of the comparison. By averaging the different sets of experimental data together, the anomalies and inconsistencies associated with any one measurement will not manifest itself in the overall comparison, yet the trends and results consistent in all of the sets of experimental data will remain. The consistent discrepancy associated with the calculated and measured free-field gamma-ray data (from the Fall 1989 and Spring 1990 studies) was less significant in this effort, but still must be addressed before the overall quality of the gamma-ray data comparisons can be improved. To resolve discrepancies with the comparisons on or inside the phantom, future experiments should consider including the use of a simplified phantom model of known dimensions, simple geometric shapes, and known materials, e.g. a cylindrical water-filled lucite phantom.

ABSTRACT

The capability to accurately assess and predict the effectiveness of radiation shielding materials in vehicles, structures, trenches, and other configurations is of considerable interest to the DoD and the DNA. A research effort involving several institutions has worked towards providing this capability for several years, resulting in the Monte Carlo Adjoint Shielding Code system - MASH. The purpose of this report is to present the results of a "benchmark" analysis of MASH against a third set of measurements performed in the Spring of 1991 at the APRF and determine the capability of MASH in reproducing the measured neutron and gamma-ray integral data. In particular, the free-field environment was calculated along with measurements made using the "NATO standard test bed" (i.e. a two-meter box) and the RT-200 anthropormorphic phantom standing in the free-field and inside the two-meter box lined with 5% borated polyethylene at the "NATO standard reference point" at 400 meters.

The calculational results show mixed agreement with the measured data reported by the different teams of experimentalists. The neutron dose results indicate good agreement (typically ±20%) for the phantom standing in the free-field and excellent agreement (typically ±10%) for the phantom standing inside the two-meter box. The neutron reduction factors however, agreed for the phantom standing in the free-field but exhibited significant differences for the phantom standing inside the box. With respect to the gamma-ray data, there were individual discrepancies between calculations and measurements; however, typical agreement was within ±20%. The C/E comparisons for the gamma-ray free-field environment at 400 meters showed improved agreement between calculation and experiment relative to the same comparisons in the Fall 1989 and Spring 1990 studies.

To determine the overall quality of the comparisons between MASH and the measurements, the data (both calculational and experimental) was averaged over detector position (internal and external), response function (tissue and CaF_2:Mn), radiation type (neutron and gamma-ray), and phantom orientation (front facing and left side toward reactor). This averaging procedure produced one set of data for the phantom standing in the free-field, and one set of data for the phantom standing inside the lined two-meter box. In general, the calculations agreed quite well with most of the measured data supplied by the teams of experimentalists. The agreement was within the ±20% limit deemed as acceptable by the DNA.

1.0 INTRODUCTION

1.1 Objective

The Monte Carlo Adjoint Shielding Code System - MASH 1.0[1] was used to analyze two series of nuclear radiation shielding experiments performed in the Fall of 1989 and Spring of 1990 at the Army Pulse Radiation Facility (APRF) in Aberdeen Proving Grounds, Maryland. The objective of these efforts was to "benchmark" MASH 1.0 against the experiments performed at the APRF and determine the capability of MASH in reproducing the measured neutron and gamma-ray integral and spectral data. The results of these analyses[2,3] were used in the recommendations to the North Atlantic Treaty Organization (NATO) Panel VII Ad Hoc Group of Shielding Experts for replacing the Vehicle Code System (VCS)[4,5] with MASH 1.0 as the reference code of choice for future armored vehicle nuclear vulnerability calculations.

This report summarizes the results of MASH 1.0 calculations designed to model the next set of measurements in this series of nuclear radiation shielding experiments. These experiments were performed in the Spring of 1991 at the APRF and involved measurements obtained by experimentalists from APRF, the Armed Forces Radiobiological Research Institute (AFRRI), Harry Diamond Laboratories (HDL), and the Establissement Technique Central de l'Armement, France (ETCA). As in the case of the Spring 1990 experiments, the experimentalists utilized two passive integral detectors including the BD-100R Bubble Dosimeters for neutron measurements and Thermoluminescent Dosimeters (TLDs) for gamma-ray measurements.

The analysis of the Fall 1989 measurements involved calculating free-field environments at distances of 170 and 400 meters from the APRF reactor along with measurements made using the "NATO standard test bed" (i.e. a two-meter box) at the "NATO standard reference point" at 400 meters. The analysis of the Spring 1990 measurements involved calculating free-field environments at a distance of 400 meters from the APRF reactor along with measurements made using the RT-200 humanoid phantom standing in the free-field and inside the two-meter box test bed at 400 meters. The specific objective of the effort described in this report was to further "benchmark" MASH 1.0 against experiments involving a humanoid phantom and the two-meter box lined with two inches of 5% borated polyethylene, and determine the capability of MASH of reproducing the measured neutron and gamma-ray integral data. In particular, free-field environments at 400 meters were to be calculated along with measurements made using the two-meter box with the 5% borated polyethylene liner and the RT-200 humanoid phantom standing in the free-field and inside the lined two-meter box.

MASH is currently being appraised as the "code-of-choice" to replace VCS. However, before it can be fully adopted for use in armored vehicle nuclear vulnerability calculations, the code system must first be verified and validated through comparisons with experimental data. This effort is one of the primary objectives of the Oak Ridge National Laboratory (ORNL) MASH Verification and Validation Subtask of the Defense Nuclear Agency (DNA) Radiation Environments Program (REP).

2.0 THE TWO-METER BOX TEST BED EXPERIMENTS

One of the purposes of the two-meter box test bed experiments was to provide spectral and integral data for use in the verification and validation of MASH. The experimental measurements were conducted at the Army Pulse Radiation Facility (APRF) bare fast reactor at Aberdeen Proving Grounds, Maryland. The verification and validation of MASH is being performed by ORNL and Science Applications International Corporation (SAIC).

2.1 The APRF Reactor Source

The APRF reactor is a bare critical assembly in the form of a right circular cylinder 22.6 cm in diameter and 19.8 cm in height. The reactor is mounted on a transporter and positioned outdoors at a height of 12.7 meters above a borated concrete experiment pad and approximately 14 meters (on the average) above the surrounding terrain to simulate the (low intensity) neutron and gamma-ray radiation environment typical of a tactical nuclear weapon. The neutron emission from the reactor is anisotropic, with the angular distribution peaked in the horizontal (forward) direction.

2.2 The Two-Meter Box Test Bed

The "Nato Standard Test Bed" is a large cubical steel walled box having interior dimensions of 200 cm x 200 cm x 200 cm and wall thicknesses (top and sides) of 5.08 cm. The bottom plate is 10.16 cm thick. The top and side wall thicknesses can be increased to 10.16 cm by the addition of 5.08 cm thick steel plates. The box contains lift tabs (for movement by crane), drainage holes at the base, a cable access hole at the base on the back side of the box, and two hatches. The hatches are located in the center of the top and back faces of the box and the hatch diameters in the interior box and outside plates are staggered to mitigate radiation streaming paths into the box. The hatches are included for loading and unloading experimental equipment (e.g. detectors, phantoms, etc.) and for simulating open-hatch vehicle experiments. The interior air space with dimensions of 200 cm x 200 cm x 200 cm gives the test bed the common name - "the two-meter box."

In this set of experiments, a 5.08-cm-thick 5% borated polyethylene liner was placed on the interior walls and ceiling of the box. The liner was fabricated in blocks and held in place using an aluminum frame. No liner material was placed on the floor of the box or immediately adjacent to the hook attached to the top hatch. Furthermore, to allow access into the box, no liner material was placed on the interior of the hatch on the back face of the box. The additional thickness of liner material yielded an interior air space with dimensions of approximately 190 cm x 190 cm x 195 cm.

2.3 The RT-200 Anthropomorphic Phantom

The RT-200 anthropomorphic phantom supplied by the Defence Research Establishment Ottawa, Canada (DREO), approximates a typical U. S. armored vehicle crewman. The RT-200 stands 175.0 cm tall, and weighs 74.0 kg. The chest depth and width are 21.4 cm and 33.8 cm respectively, and the head depth and width are 20.8 cm and 14.8 cm. The RT-200 is comprised of a head, neck, and torso (which contains a set of lungs). The phantom has non-articulating arms and legs as separate solid members and a physical appearance that resembles the male human form. The phantom is constructed from a numbered series of one-inch thick slices held together with plastic rods. Four of the slices, two in the mid-head and two in the mid-gut regions, have removable cut-outs to allow for "in-phantom" dosimetry measurements. External dosimetry measurements are made by taping the dosimeters directly to the phantom in the desired location(s), e.g., wrist, chest, belt, etc.

2.4 Details of the Measurements

The reactor was operated in the steady state mode for all of the experiments reported in this document. Power levels and run durations were determined for each experiment by the requirements of the detector system being used to assure sufficient statistical accuracy in the measured results. Meteorological data (air temperature, barometric pressure, and relative humidity) were recorded during the course of the experiments by the Aberdeen Proving Grounds Meteorological Observation Station at Poverty Island and provided to the APRF staff. In addition, the APRF staff made several ground moisture measurements throughout the course of the experiments to record the water content of the soil.

All measurements using the two-meter box test bed and RT-200 phantom were made at a distance of 400 meters from the APRF reactor. The 400 meter test site is referred to as the "NATO standard reference point" and is a sufficient distance for the neutron and gamma-ray spectra to reach equilibrium shapes due to modifications of the reactor source spectrum from interactions in the air and ground. The box was oriented with one face normal to the axis from the reactor to the test site and with the side hatch away from the APRF reactor. In all of the measurements both hatches were closed. The box was always present at the 400 meter test site. The measurements involving the RT-200 phantom were made with the phantom standing in the free-field or inside the two-meter box, either facing the APRF reactor or with the left side towards the reactor. Free-field measurements were obtained by placing the detectors or RT-200 phantom at a distance of 400 meters from the reactor and at a distance from the two-meter box of approximately 10 meters. The in-box measurements were obtained by placing the detectors or RT-200 phantom inside the box with the signal and high voltage cables (if required) passing through the cable port to data acquisition equipment inside the APRF building or to mobile counting laboratories located near the 400 meter site.

2.5 Experimental Equipment

Two different detectors were used by the experimentalists to measure the radiation environments in the free-field and inside the two-meter box test bed, including the BD-100R Bubble Dosimeters for neutron measurements and Thermoluminescent Dosimeters (TLDs) for gamma-ray measurements. Both of these detector systems measure integral quantities, and consequently, no spectral measurements were performed.

The BD-100R Bubble Dosimeter is ideally suited for these measurements because it is capable of measuring very low neutron dose (less than one mrem) and is tissue equivalent for neutron energies between 100 keV and 20 MeV. Furthermore, the BD-100R maintains an isotropic response over its active range, and is capable of immediate on-site data analysis. The experimentalists from APRF and ETCA were the only two teams performing neutron dose measurements for this series of experiments.

The Thermoluminescent Dosimeter (TLD) measures gamma-ray dose between 10 keV and 20 MeV. The TLD is sensitive to gamma rays but also moderately sensitive to thermal neutrons. Several varieties of TLDs with different shapes, sizes, and shields were used by the experimentalists. All experimentalists participated in the gamma-ray dose measurements and reported results in units of dose (tissue) except HDL which reported results in units of dose (CaF_2:Mn). Consequently, HDL provided ORNL analysts with the CaF_2:Mn gamma-ray energy sensitive response function (relative to air) for the MASH analysis of the HDL measurements.

The sequence of free-field and in-box neutron and gamma-ray measurements was carefully planned and coordinated by the APRF staff to ensure minimum interference between the different experimentalists and to achieve optimum reactor-detector-box dispositions. The integral power required for the BD-100R neutron dosimeter measurements is significantly less than that required for the TLD measurements. Consequently, the neutron measurements were performed separately from the gamma-ray measurements. The TLD measurements required full day runs (approximately 50 kWh of integrated power) due to the low sensitivity of the TLDs. Therefore, all experimentalists performed the TLD measurements simultaneously to allow for completion of the full experimental schedule.

Kerma values were reported for free-field measurements, free-in-air measurements inside the lined two-meter box, and measurements external and internal to the RT-200 humanoid phantom standing in the free-field and inside the lined two-meter box. The experimental data summarized in this report were taken from presentation charts and other documents provided by the different experimentalists.

3.0 MASH CALCULATIONAL TECHNIQUES

The MASH calculational technique employs a GRTUNCL-DORT[6] forward discrete ordinates calculation to determine the neutron and gamma-ray fluence on a coupling surface surrounding the armored vehicle or shielded structure and a MORSE[7] adjoint Monte Carlo calculation to determine the dose importance of the surface fluence. MASH then utilizes the Detector Response Code (DRC)[1] to fold the fluence together with the dose importance to yield the desired detector response(s). MASH was specifically designed to calculate the neutron and gamma-ray radiation environments and shielding protection factors of vehicles, structures, trenches, and other shield configurations. Consequently, the two-meter box experiments represent a realistic test problem for verifying the MASH code system.

3.1 Definition of Protection and Reduction Factors

Two quantities that are indicative of the ability of a ground combat vehicle to protect its crew members from penetrating nuclear radiation are protection factors (PFs) and reduction factors (RFs). The protection factors are more useful in the characterization of the vehicle shielding, whereas the reduction factors are more useful for comparisons with experimental data.

The neutron protection factor considers only the incident radiation field due to scattered and unscattered neutrons and secondary gamma radiation arising from (n,γ) reactions with the vehicle. Similarly, the gamma protection factor treats only that incident radiation resulting from gamma rays produced by prompt fission and extra-vehicle (n,γ) reactions (air and ground). Because detector systems are unable to discern the origin of the gamma rays (i.e. source, air secondary gamma ray, vehicle secondary gamma ray, etc.) contributing to the in-vehicle dose, the calculated reduction factors are more easily compared with experimental measurements than the protection factors. The definitions of the parameters and protection factors used in DRC to characterize the effectiveness of the vehicle shields are given in Table 1. It should be noted that the definitions of the protection factors and reduction factors are independent of the response function (i.e. tissue dose, silicon dose, etc.) used in the analysis.

3.2 Air-Over-Ground Environment

The APRF radiation environment was modeled in the GRTUNCL and DORT codes to determine the air-over-ground environment from which the fluence on the coupling surface could be obtained. GRTUNCL calculates the uncollided component of the fluence and DORT calculates the scalar and directional fluences of the collided component. All three components of the fluence are processed through VISTA[1] to obtain the fluence on the coupling surface to be folded in DRC.

Table 1. Definitions of Radiation Protection Factors and Reduction Factors.

TPF = TOTAL PROTECTION FACTOR

$$TPF = \frac{Free\text{-}Field\ Dose}{Inside\text{-}Vehicle\ Dose} = \frac{D_n^{FF} + D_{n\gamma,air}^{FF} + D_{n\gamma,grnd}^{FF} + D_\gamma^{FF}}{D_n^{iv} + D_{n\gamma,veh}^{iv} + D_{n\gamma,air}^{iv} + D_{n\gamma,grnd}^{iv} + D_\gamma^{iv}}$$

NPF = NEUTRON PROTECTION FACTOR

$$NPF = \frac{Free\text{-}Field\ Neutron\ Dose}{Target\ Dose\ Summing\ Direct\ Neutrons + Vehicle(n,\gamma)} = \frac{D_n^{FF}}{D_n^{iv} + D_{n\gamma,veh}^{iv}}$$

PF = GAMMA PROTECTION FACTOR

$$GPF = \frac{Free\text{-}Field\ Gamma\ Dose,\ (Direct\ \gamma\ +\ Air\ and\ Grnd(n,\gamma))}{Target\ Dose\ Caused\ By\ All\ Gamma\ Sources} = \frac{D_{n\gamma,air}^{FF} + D_{n\gamma,grnd}^{FF} + D_\gamma^{FF}}{D_{n\gamma,air}^{iv} + D_{n\gamma,grnd}^{iv} + D_\gamma^{iv}}$$

TRF = TOTAL REDUCTION FACTOR

$$TRF = \frac{Free\text{-}Field\ Dose}{Inside\text{-}Vehicle\ Dose} = \frac{D_n^{FF} + D_{n\gamma,air}^{FF} + D_{n\gamma,grnd}^{FF} + D_\gamma^{FF}}{D_n^{iv} + D_{n\gamma,veh}^{iv} + D_{n\gamma,air}^{iv} + D_{n\gamma,grnd}^{iv} + D_\gamma^{iv}}$$

NRF = NEUTRON REDUCTION FACTOR

$$NRF = \frac{Free\text{-}Field\ Neutron\ Dose}{Target\ Dose\ Caused\ By\ Direct\ Neutrons} = \frac{D_n^{FF}}{D_n^{iv}}$$

GRF = GAMMA REDUCTION FACTOR

$$GRF = \frac{Free\text{-}Field\ Gamma\ Dose,\ (Direct\ \gamma\ +\ Air\ and\ Ground(n,\gamma))}{Target\ Dose\ Caused\ By\ All\ Gamma\ Sources} = \frac{D_{n\gamma,air}^{FF} + D_{n\gamma,grnd}^{FF} + D_\gamma^{FF}}{D_{n\gamma,veh}^{iv} + D_{n\gamma,air}^{iv} + D_{n\gamma,grnd}^{iv} + D_\gamma^{iv}}$$

where

D_n^{FF} - *Direct neutron Free-Field Dose*	$D_{n\gamma,air}^{FF}$ - *Air (n,γ) Free-Field Dose*
$D_{n\gamma,grnd}^{FF}$ - *Ground (n,γ) Free-Field Dose*	D_γ^{FF} - *Direct Gamma Free-Field Dose*
D_n^{iv} - *Direct neutron Inside-Vehicle Dose*	$D_{n\gamma,veh}^{iv}$ - *Vehicle (n,γ) Inside-Vehicle Dose*
$D_{n\gamma,air}^{iv}$ - *Air (n,γ) Inside-Vehicle Dose*	$D_{n\gamma,grnd}^{iv}$ - *Ground (n,γ) Inside-Vehicle Dose*
D_γ^{iv} - *Direct Gamma Inside-Vehicle Dose*	

In early 1989, SAIC performed a detailed analysis of the APRF reactor and produced the energy- and angle-differential leakage spectrum to be used as the source for all transport calculations.[8] SAIC calculated the neutron leakage from the APRF reactor, integrated over all angles, to yield 1.293 x 10^{17} neutrons per kWh. Table 2 lists the APRF reactor neutron leakage spectrum (normalized to unity). The APRF gamma-ray leakage spectrum is divided into two components, prompt plus secondary gamma-ray leakage, and delayed gamma-ray leakage. The prompt and secondary gamma-ray leakage spectrum is a function of the reactor model used in the source analysis and is constant in both number of gamma rays per source neutron and spectral shape. The delayed gamma-ray leakage spectrum changes as a function of time after a fission event and therefore varies in both number and spectral shape. SAIC calculated delayed gamma-ray spectra for three different durations of operation; fifteen minutes, one hour, and four hours. For the purposes of the two-meter box test bed experiments, the one hour delayed gamma spectrum was utilized in the MASH analysis. The number of gamma rays per source neutron for the prompt plus secondary, one hour delayed, and total gamma-ray leakage spectra are 0.276, 0.112, and 0.388 respectively. The combined prompt plus secondary and one-hour delayed gamma-ray leakage spectrum (normalized to unity) for the APRF reactor is given in Table 3.

Table 2. APRF Reactor Neutron Leakage Spectrum (number of neutrons per energy bin) and DABL69 Free-In-Air Tissue Kerma Response Function (Gy-cm^2/n) Used in the MASH Analysis.

Group No.	Upper Energy (eV)	APRF Reactor Leakage	DABL69 Free-In-Air Tissue	Group No.	Upper Energy (eV)	APRF Reactor Leakage	DABL69 Free-In-Air Tissue
1	1.9640+07[a]	2.78-06	7.365-11	24	8.2085+05	3.50-02	2.059-11
2	1.6905+07	1.09-05	7.046-11	25	7.4274+05	5.35-02	1.937-11
3	1.4918+07	1.26-05	6.859-11	26	6.3927+05	5.04-02	1.791-11
4	1.4191+07	9.28-06	6.745-11	27	5.5023+05	1.05-01	1.638-11
5	1.3840+07	7.15-05	6.616-11	28	3.6883+05	7.33-02	1.301-11
6	1.2523+07	2.88-05	6.381-11	29	2.4724+05	4.78-02	1.026-11
7	1.2214+07	2.16-04	6.355-11	30	1.5764+05	2.18-02	8.065-12
8	1.1052+07	4.68-04	5.988-11	31	1.1109+05	1.86-02	5.634-12
9	1.0000+07	9.04-04	5.763-11	32	5.2475+04	4.38-03	3.592-12
10	9.0484+06	1.63-03	5.515-11	33	3.4307+04	1.55-03	2.592-12
11	8.1873+06	2.67-03	5.464-11	34	2.4788+04	4.48-04	2.130-12
12	7.4082+06	6.83-03	5.127-11	35	2.1875+04	9.36-04	1.476-12
13	6.3763+06	2.13-02	4.709-11	36	1.0595+04	2.53-04	6.284-13
14	4.9658+06	6.07-03	5.578-11	37	3.3546+03	3.84-05	2.199-13
15	4.7237+06	2.24-02	4.436-11	38	1.2341+03	3.46-06	9.259-14
16	4.0657+06	6.40-02	4.194-11	39	5.8495+02	4.90-07	4.481-14
17	3.0119+06	6.70-02	3.573-11	40	2.7536+02	1.17-07	2.073-14
18	2.3852+06	1.07-02	3.325-11	41	1.0130+02	1.94-08	1.037-14
19	2.3096+06	7.85-02	3.211-11	42	2.9023+01	2.51-09	9.324-15
20	1.8268+06	9.20-02	2.912-11	43	1.0677+01	4.74-10	1.359-14
21	1.4227+06	9.83-02	2.634-11	44	3.0590+00	6.92-11	2.285-14
22	1.1080+06	5.42-02	2.525-11	45	1.1253+00	1.21-11	3.727-14
23	9.6164+05	6.00-02	2.225-11	46	4.1399-01	1.94-12	1.291-13
					1.0000-05		

[a]Read as 1.9640 x 10^7

Table 3. APRF Reactor Gamma-Ray Leakage Spectrum (number of gamma-rays per energy bin) and DABL69 Free-In-Air Tissue Kerma Response Function (Gy-cm^2/γ) Used in the MASH Analysis.

Group No.	Upper Energy (eV)	APRF Reactor Leakage	DABL69 Free-In-Air Tissue	Group No.	Upper Energy (eV)	APRF Reactor Leakage	DABL69 Free-In-Air Tissue
1	2.000+07[a]	4.51-08	4.011-11	13	1.500+06	2.05-01	5.853-12
2	1.400+07	2.23-07	3.176-11	14	1.000+06	1.90-01	4.272-12
3	1.200+07	1.01-05	2.761-11	15	7.000+06	1.73-01	2.964-12
4	1.000+07	3.20-04	2.352-11	16	4.550+05	7.90-02	1.930-12
5	8.000+06	4.67-04	2.051-11	17	3.000+05	6.40-02	1.054-12
6	7.000+06	1.17-03	1.851-11	18	1.500+05	1.17-02	5.296-13
7	6.000+06	4.55-03	1.644-11	19	1.000+05	1.42-03	3.482-13
8	5.000+06	1.17-02	1.433-11	20	7.000+04	5.93-05	3.132-13
9	4.000+06	3.76-02	1.213-11	21	4.500+04	1.57-06	4.846-13
10	3.000+06	3.98-02	1.036-11	22	3.000+04	1.75-07	1.050-12
11	2.500+06	6.76-02	9.027-12	23	2.000+04	6.30-07	3.396-12
12	2.000+06	1.13-01	7.556-12	24	1.000+04		

[a]Read as 2.000 x 10^7

The air-over-ground model utilized 123 radial intervals and 146 axial intervals in a flat topographical r-z model. This mesh modeled a 2000 meter by 2000 meter air environment. Approximately one meter of ground was included in the air-over-ground calculations to model ground scattering. The source height was set at 16.143 meters above the air/ground interface and at the center of the radial mesh (r=0.0). The air-over-ground model utilized a 240 direction forward biased quadrature, a P_5 Legendre expansion of the cross sections, the reference DNA Defense Applications Broad-group Library (DABL69) 69 group (46n/23γ) cross-section library,[9] and three different materials - air, ground, and borated concrete (the reactor pad). Two ground moisture and six air moisture contents were utilized to encompass the full spectrum of ground moisture and meteorological data recorded by APRF. To model the ground moisture conditions, 24%, and 37% water (by weight) was utilized in the APRF soil compositions. The meteorological data and number densities for the various air compositions used in this analysis are given in Table 4. Six air-over-ground fluence files at the coupling surface were calculated using the GRTUNCL-DORT-VISTA code sequence. Utilizing these six fluence files enabled the ORNL analysts to choose an air-over-ground environment which closely approximated the environmental conditions for a given experimental measurement.

Table 4. Meteorological Data and Air Number Densities Used in the MASH Analysis of the APRF Spring 1991 Two-Meter Box Test Bed Experiments.

Meteorological Data					
Date	Experiment Number	Pressure (mm Hg)	Temperature (K)	Relative Humidity (%)	Density (gm/cm^3)
4/30/91	ss91-116	760.2	295.6	92.0	1.183-03[a]
5/1/91	ss91-118	760.1	296.9	48.0	1.182-03
5/2/91	ss91-121	758.7	292.5	42.0	1.200-03
5/7/91	ss91-126	766.9	289.3	58.0	1.226-03
5/8/91	ss91-131	768.5	297.7	42.0	1.193-03
5/9/91	ss91-136	770.0	292.2	71.0	1.216-03
Air Number Densities					
Date	Experiment Number	Hydrogen (atoms/barn · cm)	Nitrogen (atoms/barn · cm)	Oxygen (atoms/barn · cm)	Argon (atoms/barn · cm)
4/30/91	ss91-116	1.225-06	3.781-05	1.076-05	2.261-07
5/1/91	ss91-118	6.885-07	3.805-05	1.055-05	2.276-07
5/2/91	ss91-121	4.672-07	3.873-05	1.062-05	2.316-07
5/7/91	ss91-126	5.332-07	3.954-05	1.087-05	2.365-07
5/8/91	ss91-131	6.304-07	3.842-05	1.062-05	2.298-07
5/9/91	ss91-136	7.759-07	3.911-05	1.088-05	2.339-07

[a]Read as 1.183×10^{-3}.

3.3 The Two-Meter Box and Phantom Geometry Models

An isometric view of the two-meter box test bed with the 5% borated polyethylene liner described in Section 2.0 is shown in Figure 1. The two-meter box test bed was chosen for the "NATO standard test bed" because the geometry provides a simplistic vehicle for experimental and analytical (MASH) comparisons of radiation transmission through material types and thicknesses indicative of modern armored vehicles.

The RT-200 anthropomorphic phantom (also described in Section 2.0) is a complex form which does not lend itself easily to modeling using standard combinatorial geometry input currently available in the MASH code system. Consequently, a modified combinatorial geometry phantom model, developed from the original Snyder phantom model,[10] was used in the MASH analysis. An isometric view of the combinatorial geometry phantom model is shown in Figure 2. The combinatorial geometry model represents a simplified form of the RT-200 phantom and does not have all the detailed contours which characterize the anthropomorphic RT-200 phantom actually used in the measurements. The simplified phantom model is 174.4 cm tall and weighs approximately 70.0 kg. The chest contains a set of lungs and has a depth and width of 20.0 cm and 34.4 cm, respectively.

Likewise, the head depth and width are 20.0 cm and 15.1 cm. Since the gross features, i.e., size, height, weight, physical dimensions, etc., of the combinatorial geometry phantom are similar to those of the RT-200 phantom, it is believed that the differences in the calculational model and the humanoid phantom used in the measurements will not cause significant errors in the MASH analysis of the experiments.

The two-meter box and 5% borated polyethylene liner (Figure 1) and combinatorial geometry phantom (Figure 2) were modeled in the MORSE component of the MASH code system using the GIFT[11,12] geometry package. Figure 3 depicts an isometric view of the GIFT geometry model of the phantom standing in the lined two-meter box (facing the reactor). The material compositions for the air, ground, steel, 5% borated polyethylene liner, BD-100R neutron dosimeters, and phantom (soft tissue, bone, and lung) are given in Table 5.

There were multiple detector positions utilized in the Spring 1991 experiments. Table 6 lists the positions of the BD-100R bubble dosimeters. The same general locations were used for the TLD measurements. There were multiple dosimeters used at each position in the measurements on and inside the phantom as evidenced in Table 6. A set of preliminary scoping calculations determined significant differences in the calculated neutron doses as a result of including (or excluding) the BD-100R dosimeters in the geometry model. Differences within statistical deviations were generally seen in the calculated gamma-ray doses. However, the BD-100R buddle dosimeter is a volumetric detector and MASH utilizes a point detector for computing the dose. Consequently, the BD-100R detectors were not modeled in the MASH clculations even thought they are included in the geometry models. At each detector location (left wrist, front belt, etc.) the MASH analyses utilized a point central to the location of the multiple BD-100R detectors. There are two positions not associated with the phantom relating to measurements made inside the box. The "Center of Box" location corresponds to the location used in the Fall 1989 measurements and was used when the phantom was outside the box. The "Detector on Shelf" location is situated off to one side on a small aluminum table and was used when the phantom was standing inside the box. The Kerr neutron and gamma-ray Free-In-Air (FIA) tissue kerma response functions in the DABL69 cross-section library were utilized in DRC to obtain the dose responses in the free-field and in the two-meter box. Listings of the neutron and gamma-ray FIA tissue kerma response functions are given in Tables 2 and 3 respectively.

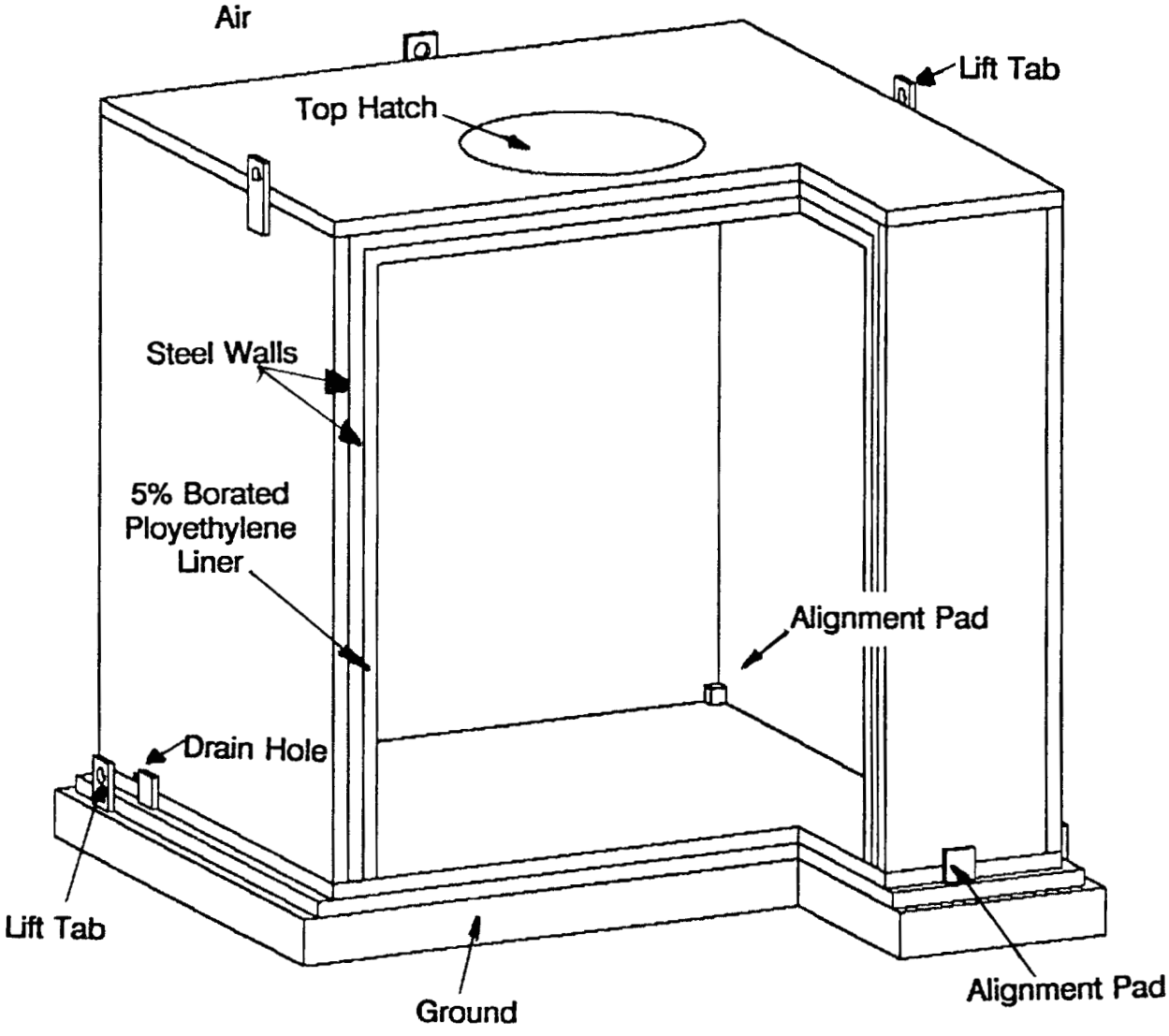

Figure 1. Isometric View of the Two-Meter Box Test Bed with a 5% Borated Polyethylene Liner.

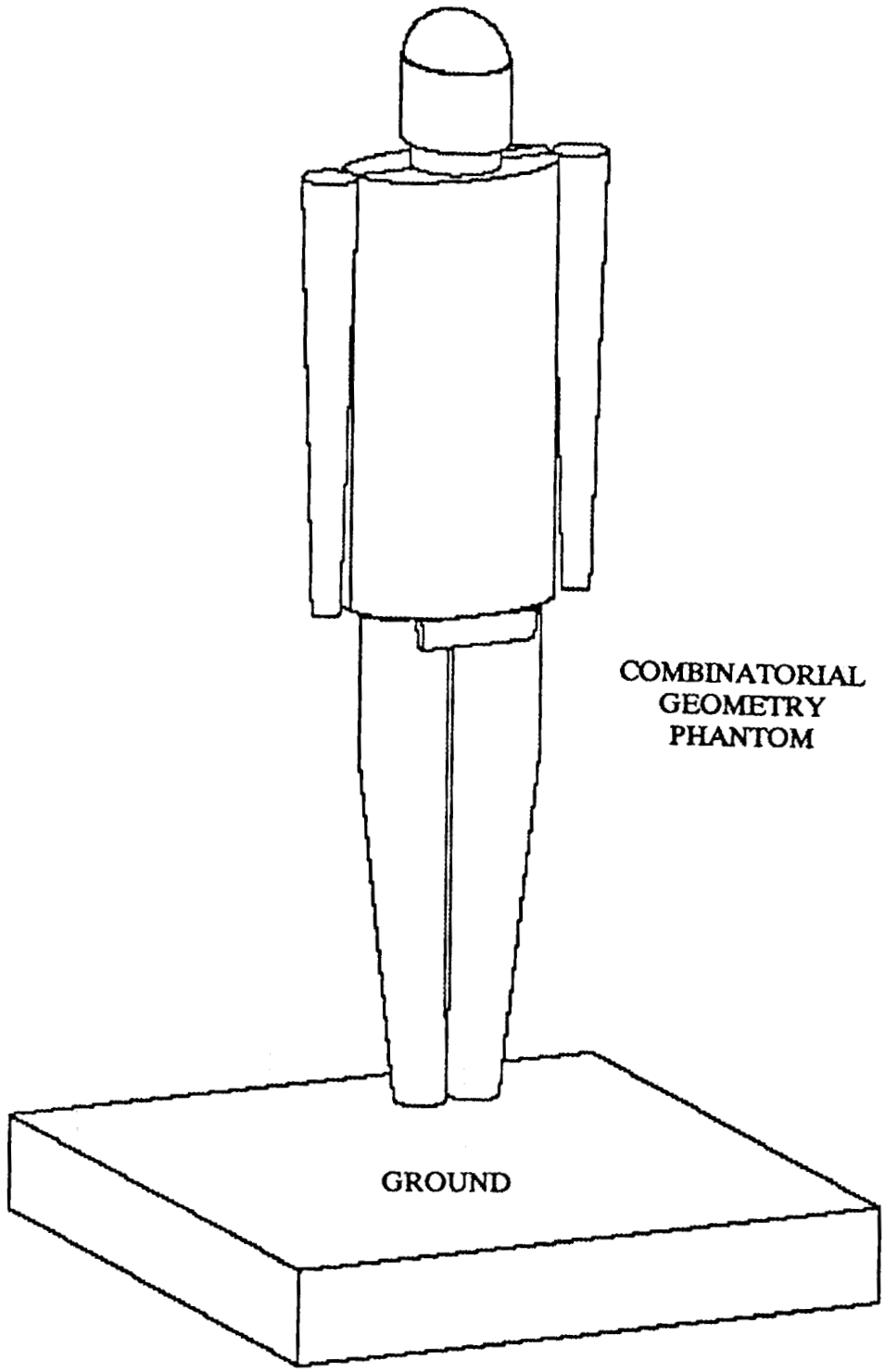

Figure 2. Isometric View of the Combinatorial Geometry Phantom Model Used in the MASH Analysis.

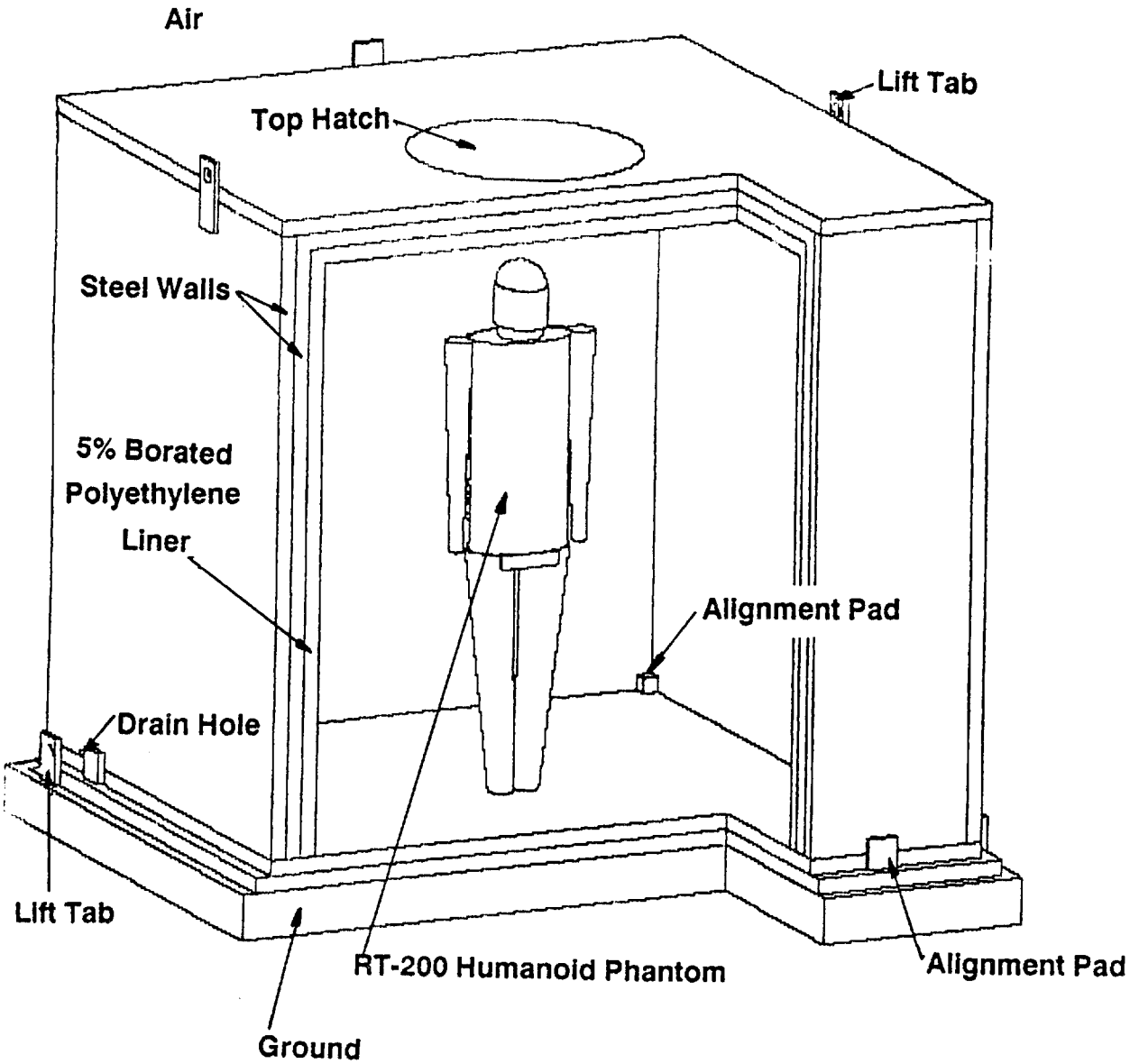

Figure 3. Isometric View of the MASH Geometry Model of the Combinatorial Geometry Phantom Standing Inside the Lined (5% Borated Polyethylene) Two-Meter Box Test Bed.

Table 5. Compositions of the Materials Used in the MASH Analysis of the APRF Spring 1991 Two-Meter Box Test Bed Experiments.

		Material Composition (atoms/(barn·cm))								
Atomic Number	Element	APRF Ground	Air	1020 Steel	Plastic Lung	Soft Tissue	Bone	Water	Lexan	5% Borated Polyethylene
1	Hydrogen	4.80-02[a]	7.01-07		1.65-02	5.88-02	6.14-02	6.69-02	3.98-02	7.13-02
5	Boron-10	8.86-09								4.87-04
5	Boron-11	3.24-08								1.97-03
6	Carbon	3.49-04		8.08-04	1.18-02	3.36-02	1.79-02		4.54-02	3.41-02
7	Nitrogen	4.39-05	3.83-05		1.02-03	1.99-03	1.84-03			
8	Oxygen	4.30-02	1.06-05		3.82-03	7.72-03	2.52-02	3.34-02	8.52-03	3.64-03
11	Sodium	1.32-04				2.32-07	1.20-04			
12	Magnesium	8.43-05					3.88-05			
13	Aluminum	1.27-03			1.31-09	2.29-09				
14	Silicon	8.79-03		4.21-04			6.00-07			
15	Phosphorus			6.11-05			1.39-03			
16	Sulfur	3.34-06		7.38-05			4.55-05			
17	Chlorine	3.27-06			7.13-08	2.35-08	3.40-05			
18	Argon		2.29-07							
19	Potassium	1.89-04					3.30-05			
20	Calcium	2.40-05					2.14-03			
25	Manganese	6.65-06		3.88-04						
26	Iron	2.97-04		8.39-02			1.21-06			
27	Cobolt	2.57-07								
28	Nickel	2.58-07								
29	Copper	4.49-07								
50	Tin	6.76-08								
ρ(gm/cm^3)		1.75+00	1.19-03	7.86+00	3.90-01	1.03+00	1.40+00	1.00+00	1.20+00	9.40-01

[a]Read as 4.80×10^{-2}

Table 6. MASH Coordinate Positions for the Analysis of the APRF Spring 1991 Two-Meter Box Test Bed Experiments BD-100R Bubble Dosimeter Locations on the RT-200 Humanoid Phantom and Inside the Two-Meter Box.

Detector Position	Coordinate Positions (cm)		
	X-Coordinate	Y-Coordinate	Z-Coordinate
Mid Head	0.0	0.0	177.15
Left Chest (r)	-10.82	-5.88	149.06
Left Chest (m)	-10.82	-7.49	149.06
Left Chest (l)	-10.82	-9.10	149.06
Front Belt (r)	-10.82	1.61	116.04
Front Belt (m)	-10.82	0.0	116.04
Front Belt (l)	-10.82	-1.61	116.04
Back Belt (r)	10.82	1.61	116.04
Back Belt (m)	10.82	0.0	116.04
Back Belt (l)	10.82	-1.61	116.04
Mid-Gut	0.0	0.0	116.04
Right Arm, Front (o)	-2.97	22.34	95.30
Right Arm, Front (i)	-2.97	20.27	95.30
Left Arm, Side (b)	0.81	-24.51	95.30
Left Arm, Side (f)	-0.81	-24.51	95.30
Detector on Shelf (i)	-23.00	-58.39	87.46
Detector on Shelf (m)	-23.00	-60.00	87.46
Detector on Shelf (o)	-23.00	-61.61	87.46
Right Arm, Side (b)	0.81	24.51	95.30
Right Arm, Side (f)	-0.81	24.51	95.30
Left Arm, Front (i)	-2.97	-20.27	95.30
Left Arm, Front (o)	-2.97	-22.34	95.30
Center of Box	0.0	0.0	110.16

(b=back, c=center, f=front, i-inner, l=left, m=middle, r=right, and o=outer)

3.4 The Two-Meter Box Calculations

The MASH calculations also utilized the reference DNA DABL69 69 group (46n/23γ) cross-section library. The Monte Carlo (MORSE) calculations for the phantom standing in the free-field generated and tracked 200,000 primary source particles for the external detector locations (belt, wrist, chest, etc.), and 400,000 primary source particles for the internal detector locations (mid-head, and mid-gut), sampled over the 69 energy groups. The Monte Carlo (MORSE) calculations for the phantom standing in the two-meter box with the 5% borated liner, generated and tracked 500,000 primary source particles for the left chest (LC) and front belt (FB) positions, 750,000 primary source particles for the left wrist (LW), right wrist (RW), back belt (BB), and detector on shelf (DS) positions, and 1,000,000 primary source particles for the mid-gut (MG), mid-head (MH), and center of box (COB) positions. At all positions, the primary source particles were sampled over the 69 energy groups. An energy dependent relative importance factor was utilized over the 69 groups to increase the frequency of sampling the adjoint source particles from energy groups which have a significant effect on the dose response function. The secondary particle production probability was set to 1.0 for all regions and energy groups in the Monte Carlo calculations, and the in-group energy biasing option in MORSE was switched on. Region dependent and energy independent splitting and Russian Roulette parameters were utilized in the two-meter box steel and 5% borated polyethylene liner regions to improve the efficiency of the Monte Carlo calculations. This was accomplished by subdividing the 10.16-cm-thickness of steel into two equally thick concentric regions and assigning each of the steel regions and the liner region different splitting and Russian Roulette parameters which would allow a sufficient number of source particles (and secondary particles) to escape to obtain acceptable statistics. Only one biasing region was used in the phantom model due to the complexity of segmenting the geometry in a cost efficient manner. The average air and ground moisture conditions for this series of experiments (APRF air for run ss91-121 given in Table 4, and 37 wt% H_2O given in Table 5) were chosen for the adjoint MORSE calculations. The elemental compositions given in Table 5 were mixed to give the MORSE materials listed in Table 7. It should be noted that in this analysis, the MORSE materials and GIFT geometry model materials are equivalent.

As presently configured, DRC assumes the DORT fluence on the "coupling surface" is dependent on energy and elevation only, and not on azimuth. Consequently, DRC only uses the fluence at the 400 meter radius in the DORT mesh and does not use the radii encompassing the box. This assumption is valid for small objects at a great distance from the source. Since the size of the box and/or phantom is small relative to the distance from the source, it was felt this assumption was valid for this analysis and would produce an uncertainty within the statistical deviations of the calculated results.

For documentation purposes, sample input data streams (decks) for the two-meter box and phantom analyses (MORSE), along with the GIFT geometry models for the two-meter box with the 5% borated polyethylene liner, the phantom, and the phantom in the lined two-meter box, are included in the appendices. This will enable future versions of MASH to be "benchmarked" to the analysis reported in this document. Sample input data streams (decks) for the air-over-ground analysis (GIP, GRTUNCL, DORT, and VISTA), and DRC are given in the Spring 1990 report[3] and are not repeated here.

Table 7. MASH Geometry Regions and Cross-Section Materials Used in the Analysis of the APRF Spring 1991 Two-Meter Box Test Bed Experiments.

MORSE Material Number	Material Description	MORSE Material Number	Material Description
1	APRF Ground	6	Bone, Skeleton
2	Air	7	Water
3	SAE 1020 Steel	8	Lexan
4	Plastic Lung	9	5% Borated Polyethylene
5	Soft Tissue		

4.0 DISCUSSION OF RESULTS

4.1 Neutron Dose and Reduction Factors

There is a considerable amount of data generated in the MASH analysis of a series of experiments when multiple detector locations, teams of experimentalists, and geometry configurations and orientations are considered. For documentation purposes and completeness, the bulk of this data is included in the appendices along with the majority of the data comparisons to the experimental data. Data averaged over the different experimental parameters (detector location, ground range, and vehicle orientation) will be presented in the main text.

Comparisons of the calculated (MASH) and measured (APRF and ETCA) neutron Free-in-Air (FIA) tissue dose and reduction factors are given in Appendix A. Tables A-1 and A-4 present the data for the phantom standing in the free-field (facing the reactor) at 400 meters from the APRF reactor. Tables A-2 and A-5 present the measured and calculated dose data for the phantom standing in the lined two-meter box (facing and left side towards reactor) at 400 meters. The comparisons of measured and calculated neutron reduction factors (NRFs) for the dose data presented in Tables A-2 and A-5 are presented in Tables A-3 and A-6, respectively. Comparisons of the measured and calculated neutron doses and reduction factors, averaged over internal, external, and all detector locations on or inside the phantom, are presented in Tables 8 and 9 for the APRF data, and Tables 10 and 11 for the ETCA data. Finally, in Tables 12 and 13, the measured data, again averaged over internal, external, and all detector locations on or inside the phantom, and for both teams of experimentalists (APRF and ETCA)), are averaged together and compared to the MASH calculations. Calculation to experiment (C/E) ratios are included in each table to help quantify the comparisons.

The C/E ratios for the FIA dose to the phantom standing in the free-field indicate marginal agreement with the APRF data (Table A-1), and excellent agreement with the ETCA data (Table A-4). A similar comparison of the two sets of measured dose data in Tables A-1 and A-4 indicate differences up to ±30% at a given detector location. Consequently, the calculation to experiment (C/E) ratios, even though some are greater than the ±20% DNA mandate, are typically within the experiment to experiment (E/E) ratios. The worst comparison with APRF data, for a detector on the phantom, occurred at the back belt location with a C/E ratio of 1.36 (Table A-1). Reasons as to why the comparisons to the APRF results at the external detectors are poorer than the comparisons to the results at the internal detectors are unknown at this time. The spread of the experimental data indicate the C/E ratios are within the uncertainties associated with the measurements. One interesting point worth noting in the dose data comparisons for the phantom standing in the free-field is the agreement at the two internal detector locations (mid-head and mid-gut). In the Spring 1990 comparisons,[3] the internal detector locations (especially the mid-gut) yielded the worst C/E ratios. In this analysis, the C/E ratios for both sets of experimental data are within ±10%.

The C/E ratios for the FIA dose to the phantom standing in the lined two-meter box (Tables A-2 and A-5) indicate excellent agreement with the measured dose external and internal to the phantom for almost all of the detector locations and both phantom orientations. The agreement between the MASH calculations and measured dose is typically ±10% for the various detector locations external and internal to the phantom. Unlike the experimental results for the phantom standing in the free-field, the APRF and ETCA measured results for the phantom standing in the lined two-meter box show excellent agreement, typically within ±5%. It should be noted that some of the differences associated with the internal detector locations may be statistical due to the very low doses measured and calculated at these two positions.

One final result worth mentioning in Tables A-1, A-2, A-4, and A-5 are the C/E's for the free-field (FF) dose comparisons. As in case with the Fall 1989 comparisons[2] and Spring 1990 comparisons[3], MASH calculates approximately 20% more dose than is measured. The spread on the measured free-field dose data results is significant, ranging from 3.51 mrad/kWh (ETCA, Table A-5) to 4.78 mrad/kWh (ETCA, Table A-4). This range in measured free-field results is 20%-25% larger than the maximum range calculated using MASH for the most extreme changes in meteorological conditions and ground moisture at the APRF test site at 400 meters. Despite this range in experimental data, the overall indication from the free-field dose results indicates a consistency in both the measured and calculated free-field dose between the three sets of experiments (Fall 1989, Spring 1990, and Spring 1991).

There is no apparent reason for the discrepancies in the results shown in the dose data tables given in Appendix A. Possible causes include modeling differences (MASH combinatorial geometry phantom vs. the RT-200 humanoid phantom), detector placement on/in the MASH model versus actual position on the RT-200 phantom, temperature corrections for the BD-100R dosimeters, insufficient/inaccurate bubble counts, cross sections, Legendre expansion of the cross sections, quadrature, etc. Some of the differences exhibited in the result of this study are contrary to the results shown in the Spring 1990 study[3]. Other comparison results between the two analyses are consistent. Typically, the MASH results are consistent with respect to dose magnitude and phantom orientation. The experimental results exhibit significant differences; considerably larger than what changes in environmental conditions would dictate.

The neutron reduction factor (NRF) comparisons presented in Tables A-3 and A-6 amplify the free-field dose discrepancies noted in Tables A-2 and A-5. In particular, at the detector locations where MASH underestimates the measured dose (i.e., C/E < 1.0), the C/E ratios for the corresponding neutron reduction factors will be large. This is due to the consistent over-estimation of the free-field dose in MASH. Those detector locations where the dose C/E ratios (Tables A-2 and A-5) are less than one have large NRF C/E ratios exhibited in Tables A-3 and A-6, ranging from a factor of approximately 1.30 to 1.80. Obviously, these results indicate poor agreement between MASH and the measurements and are significantly greater than the ±20% DNA mandate for acceptable comparisons.

Understanding the differences associated with each individual comparison for each team of experimentalists is important in understanding the physics and/or mechanics of the processes involved. Often, however, the quantity and diversity of the C/E ratios tend to "muddy the picture" as to the overall quality of the comparison. Consequently, averaging the

experimental and analytical results over external, internal, and all detector locations on or inside the phantom yields a summary indication of the agreement between MASH and the measurements for the dose comparisons (Tables 8, 10, and 12), and the reduction factor comparisons (Tables 9, 11, and 13). The results presented in these tables smooth out the anomalies and inconsistencies associated with each individual comparison and give a clearer indication of the overall quality of the comparisons. As one would expect, the results and trends discussed above are still prevalent in the summary results presented in Tables 8 through 13 and do not yield all C/E ratios within ±20%. In particular, the C/E ratios for the phantom standing in the free-field indicate marginal agreement between calculation and experiment, and for the phantom standing in the two-meter box, the C/E ratios indicate MASH estimates the measured dose to within approximately 10%. The over-estimation of the free-field dose by MASH, coupled with an underestimation of the measured on/in phantom dose, yields corresponding discrepancies in calculated and measured NRFs of 30% to 80%.

4.2 Gamma-Ray Dose and Reduction Factors

Comparisons of the calculated (MASH) and measured gamma-ray dose and reduction factors are given in Appendix B for the different organizations participating in the Spring 1991 experiments at APRF. The tables of dose and reduction factor data have been grouped by organization (not all organizations participated in the full series of measurements). Tables B-1 through B-3 present the comparisons to the HDL data, Tables B-4 through B-8 present the comparisons to the APRF data, Tables B-9 through B-11 present the comparisons to the ETCA data, and Tables B-12 and B-13 present the comparisons to the AFRRI data. In each set of data, the gamma-ray dose and reduction factor comparisons are presented for the phantom standing in the free-field, followed by the gamma-ray dose comparisons then reduction factor (GRF) comparisons for the phantom standing in the two-meter box. The comparisons to the APRF data (Tables B-4 through B-8) are given for two different sizes of TLDs. The APRF team performed measurements on the phantom standing in the free-field and inside the two-meter box using large (.250" x .250" x .070") CaF_2:Mn TLDs [Tables B-4, B-7, and B-8], and small (.125" x .125" x .035") CaF_2:Mn TLDs [Tables B-5 and B-6]. The small TLDs were only used for the phantom standing inside the two-meter box. The MASH calculations were compared to both sets of TLD measurements for completeness.

Due to the considerable amount of data presented in the tables of Appendix B, the comparisons of the measured and calculated gamma-ray doses and reduction factors, averaged over internal, external, and all detector locations on or inside the phantom, are presented in Tables 14 through 23 for all the different teams of experimentalists. Furthermore, in Tables 24 and 25, the measured data, again averaged over internal, external, and all detector locations on or inside the phantom, and for all the teams of experimentalists reporting dose in unit of mrad(Tissue), are averaged together and compared to the MASH calculations. Calculation to experiment (C/E) ratios are included in each table of gamma-ray data (Appendix B and Tables 14 through 25) to help quantify the comparisons.

The experimentalists measured the gamma-ray data using two types of Thermoluminescent Dosimeters (TLDs); calcium fluoride (CaF_2:Mn), and aluminum oxide (Al_2O_3:C). The TLDs were of different sizes and shapes and with different types of shields

(i.e., Sn, Al, CH_2, etc.). All experimentalists (except HDL) reported gamma-ray results in units of dose(Tissue), i.e. mrad(Tissue). To obtain results in units of dose(Tissue), the experimentalists had to apply conversion factor(s) to the response function to convert the response from dose(CaF_2:Mn) or dose(Al_2O_3:C) (referred to as dose(TLD)) to dose(Tissue). The HDL data is reported in units of dose(CaF_2:Mn). HDL supplied ORNL analysts with the CaF_2:Mn response function for direct comparisons to the HDL experimental data. None of the experimentalists corrected the data to account for the differences in the gamma-ray spectrum of the APRF radiation field and the radiation field of the calibration facility. Furthermore, it should be noted that CaF_2:Mn is moderately sensitive to thermal neutrons. Again, none of the experimental data were corrected for the contribution due to the thermal neutron fluence. This should not be a big factor for measurements inside the two-meter box without the phantom present. However, for the free-field measurements outside the two-meter box and all phantom measurements, the thermal neutrons may contribute 5-10% of the total thermoluminescence signal. The MASH results in Appendix B and Tables 14 through 25 are reported in units of dose(Tissue) using the DABL69[9] Free-In-Air tissue kerma response function or dose(CaF_2:Mn) using the response function provided by HDL. The MASH results do not contain any contribution from thermal neutrons and are not corrected back to the gamma-ray spectrum of the calibration field used for the different TLDs. The composite effect of the differences in the way the measured and calculated data are reported is difficult to ascertain. It is conceivable that the uncertainties associated with these differences are greater than the ±20% mandate of DNA for acceptable comparisons without regard to the actual comparisons of the calculations and measurements themselves.

Analyzing the comparisons of the calculational and experimental gamma-ray dose and reduction factor results presented in Appendix B show the C/E ratios are typically between 0.80 and 1.20. Within the comparisons to any individual organization, there are detector locations and geometry configurations (i.e. phantom free-field, phantom in the two-meter box, etc.) which have marginal agreement and a corresponding C/E ratio outside the ±20% acceptable range. However, this same detector location may exhibit excellent agreement when the phantom orientation is changed relative to the reactor. Furthermore, that same detector location, when compared to the results for a different organization, may exhibit excellent agreement between MASH and experiment. This situation lends credence to the comparisons of the "averaged" data presented in Tables 14 through 25. Once again, the comparisons of the average values yield a clear picture of the quality of the overall comparison of MASH to the measurements. It should be noted that as in the case of the Fall 1989 comparison[2], the calculation to experiment C/E) ratios are within the range of ratios obtained when two different sets of experimental data (E/E ratios) are compared. Without going into explicit detail on the comparisons between MASH and each set of experimental data, the more significant trends associated with the comparisons presented in Appendix B will be discussed.

The comparisons of the free-field (FF) dose showed differences of approximately 15% to 20% for dose(Tissue) between the different teams of experimentalists. The APRF and ETCA teams measured gamma-ray doses of approximately 1.45 mrad(Tissue)/kWh and the AFRRI team measured gamma-ray doses of approximately 1.23 mrad(Tissue)/kWh. Although TLDs were not used in the Fall 1989 comparison, these results are approximately 10% lower for the APRF and ETCA teams and approximately 30% lower for the AFRRI team when compared to the published results of the Fall 1989 study. The MASH calculations exhibited

an increase of approximately 10% in the reported free-field dose (compared to the Fall 1989 study). Similar comparisons with the Spring 1990 data[2] show the APRF and ETCA Spring 1991 data are approximately 20% lower in integral free-field dose(tissue), whereas the MASH calculations remained virtually the same (approximately 1.35 mrad(Tissue)/kWh). With respect to the MASH calculations, the differences between Fall 1989, Spring 1990, and Spring 1991 free-field results can be attributed to meteorological conditions, detector energy range, and an updated APRF leakage source. The extended range of measured free-field doses yielded a corresponding range in C/E values from 0.91 to 1.11, which is within the DNA mandated ±20% acceptance limit.

An interesting result shown in Tables B-5 through B-8 indicate the large TLDs [(.250" x .250" x .070") CaF_2:Mn TLDs] used by the APRF team give better agreement than the small TLDs [(.125" x .125" x .035") CaF_2:Mn TLDs]. In particular, the typical integral dose C/E results with the large TLDs ranged from approximately 0.95 to 1.09 (Table B-7), whereas the integral dose C/E results with the small TLDs ranged from approximately 1.00 to 1.16 (Table B-5). This appears to indicate the larger TLD (with more thermoluminescent material) yields better agreement with the calculation. It would be reasonable to expect the larger TLD to yield more consistent results than the smaller TLD for the same integrated reactor power since there would be more signal to read. The corresponding C/E ratios for the gamma-ray reduction factor comparisons (Tables B-6 and B-8) indicate the same trend as the dose data.

The spread of the dose C/E ratios within a given set of comparisons to a particular experimentalists data typically included values both greater than and less than unity for any given phantom orientation/geometry configuration. The APRF comparisons, however, exhibited a trend of all dose C/E ratios less than unity (except one TLD location) for the phantom standing in the free-field and all dose C/E ratios greater than unity (except one TLD location) for the phantom standing in the two-meter box when compared to the small TLDs. As a general trend, the MASH calculations calculated 5% to 15% more dose than was measured.

In the Spring 1990 study[3], there were consistent discrepancies between calculation and measurement at the mid-gut location for the phantom standing in the two-meter box and at the detector location on the shelf in the two-meter box (DS) when the phantom was standing in the free-field. These detector locations usually exhibited the largest dose C/E ratios with MASH calculating more dose than was measured. These results suggests a possible difference between calculated and measured angular distributions of the gamma-ray fluence spectrum inside the "unlined" two-meter box. In this study, there is no consistent pattern exhibited by the C/E ratios at any given detector location. The 5% borated polyethylene liner softens the spectrum and possibly reduces the dose contribution from the portion of the energy spectrum the measurements and MASH calculations disagree. A full spectral analysis would be required to assess this hypothesis.

The comparisons of the calculated and measured reduction factors showed almost all of the C/E ratios to be within ±20%. As in the case with the dose data comparisons, there are a few detector locations that exhibited inconsistent GRF C/E comparisons with respect to a given set of measured data, i.e. APRF, ETCA, etc.). However, the comparisons at the same detector location would exhibit excellent agreement when compared to a different set

of measured data. One difference between the Spring 1991 study and Spring 1990 study[3] is that the more consistent agreement in the free-field dose (Spring 1991) did not cause large discrepancies in the gamma-ray reduction factor comparisons. Consequently most of the GRF C/E ratios are within the ±20% mandate of DNA.

Averaging the calculational and experimental data over external, internal, and overall detector location on or inside the phantom yielded a clear indication of how well the MASH calculations compare to the measurements. These results (Tables 14 through 23) indicate good agreement between MASH and the measurements as a function of detector position (external vs. internal), geometry configuration, and phantom orientation. The comparison to the HDL data (Table 14) shows good agreement in the dose results for the phantom standing in the free-field and standing inside the lined two-meter box. The reduction factor comparisons (Table 15) also shows good agreement for both geometry configurations (phantom standing in the free-field and inside the two-meter box). The comparisons to the APRF data (Tables 16 through 19) show excellent agreement in the dose results (Tables 16 and 18) and good agreement in the reduction factor results (Tables 17 and 19) for the phantom standing in the two-meter box. The better agreement again appears to be with the large (.250" x .250" x .070") CaF_2:Mn TLDs. The comparisons to the ETCA results (Tables 20 and 21), and AFRRI results (Tables 22 and 23) all show excellent agreement between MASH and experiment for both dose and reduction factor data. With respect to all of the comparisons in Tables 14 through 23), the internal detector locations (predominantly the mid-head position) yielded the largest discrepancy between calculation and experiment. Differences in calculational model and measured phantom, absolute detector location in relation to the model or phantom, quality of measurement, and convergence of the calculation are the most probable causes for the larger discrepancies associated with the internal detector locations. This averaged discrepancy, however, was still within the DNA ±20% mandate in every case except one (HDL GRF comparison, Table 15).

To further summarize the quantity of measured gamma-ray data reported in units of dose(Tissue), the measured results from APRF, ETCA, and AFRRI were again averaged over external, internal, and overall detector location on or inside the phantom and compared to the MASH results in Tables 24 and 25. The HDL data was not included in this table due to the differences in reported dose units. In viewing the comparisons in Tables 24 and 25, all of the C/E ratios indicate excellent agreement and are well within ±20%. This suggests consistent agreement between MASH and measurement for the gamma-ray data taken in this experiment.

Table 8

Comparisons of Calculated and APRF Measured Neutron Dose Averaged Over External, Internal, and All Detector Locations On or Inside the RT-200 Humanoid Phantom at the 400 Meter Test Site at the APRF.			
Neutron Dose (mrad(Tissue)/kWh)	MASH	APRF	C/E
Phantom Free-Field - Front Toward Reactor			
External Detector Average	3.88	3.11	1.25
Internal Detector Average	0.98	0.91	1.08
Overall Detector Average	3.05	2.37	1.29
Phantom Inside Two-Meter Box - Front Toward Reactor			
External Detector Average	0.32	0.34	0.93
Internal Detector Average	0.08	0.10	0.80
Overall Detector Average	0.25	0.26	0.96
Phantom Inside Two-Meter Box - Left-Side Toward Reactor			
External Detector Average	0.32	0.33	0.97
Internal Detector Average	0.07	0.08	0.88
Overall Detector Average	0.25	0.24	1.04

Table 9

Comparisons of Calculated and APRF Measured Neutron Reduction Factors Averaged Over External, Internal, and All Detector Locations On or Inside the RT-200 Humanoid Phantom at the 400 Meter Test Site at the APRF.			
Neutron Reduction Factor (Tissue)	MASH	APRF	C/E
Phantom Free-Field - Front Toward Reactor			
External Detector Average	1.28	1.37	0.93
Internal Detector Average	5.10	4.70	1.09
Overall Detector Average	1.63	1.80	0.90
Phantom Inside Two-Meter Box - Front Toward Reactor			
External Detector Average	14.8	11.5	1.29
Internal Detector Average	58.6	40.9	1.43
Overall Detector Average	18.9	15.1	1.25
Phantom Inside Two-Meter Box - Left-Side Toward Reactor			
External Detector Average	15.5	11.9	1.30
Internal Detector Average	75.7	51.7	1.46
Overall Detector Average	20.0	16.1	1.24

Table 10

Comparisons of Calculated and ETCA Measured Neutron Dose Averaged Over External, Internal, and All Detector Locations On or Inside the RT-200 Humanoid Phantom at the 400 Meter Test Site at the APRF.			
Neutron Dose (mrad(Tissue)/kWh)	MASH	ETCA	C/E
Phantom Free-Field - Front Toward Reactor			
External Detector Average	3.88	3.51	1.11
Internal Detector Average	0.98	1.01	0.97
Overall Detector Average	3.05	2.68	1.14
Phantom Inside Two-Meter Box - Front Toward Reactor			
External Detector Average	0.32	0.32	1.00
Internal Detector Average	0.08	0.09	0.89
Overall Detector Average	0.25	0.25	1.00
Phantom Inside Two-Meter Box - Left-Side Toward Reactor			
External Detector Average	0.32	0.31	1.03
Internal Detector Average	0.07	0.10	0.70
Overall Detector Average	0.25	0.24	1.04

Table 11

Comparisons of Calculated and ETCA Measured Neutron Reduction Factors Averaged Over External, Internal, and All Detector Locations On or Inside the RT-200 Humanoid Phantom at the 400 Meter Test Site at the APRF.			
Neutron Reduction Factor (Tissue)	MASH	ETCA	C/E
Phantom Free-Field - Front Toward Reactor			
External Detector Average	1.28	1.36	0.94
Internal Detector Average	5.10	4.74	1.08
Overall Detector Average	1.63	1.79	0.91
Phantom Inside Two-Meter Box - Front Toward Reactor			
External Detector Average	14.8	10.9	1.36
Internal Detector Average	58.6	39.0	1.50
Overall Detector Average	18.9	14.3	1.32
Phantom Inside Two-Meter Box - Left-Side Toward Reactor			
External Detector Average	15.5	13.4	1.16
Internal Detector Average	75.7	43.7	1.73
Overall Detector Average	20.0	17.4	1.15

Table 12

Comparisons of Calculated and Average Experimentally Measured Neutron Dose Averaged Over External, Internal, and All Detector Locations On or Inside the RT-200 Humanoid Phantom at the 400 Meter Test Site at the APRF.			
Neutron Dose (mrad(Tissue)/kWh)	MASH	Avg. Expt.	C/E
Phantom Free-Field - Front Toward Reactor			
External Detector Average	3.88	3.31	1.17
Internal Detector Average	0.98	0.96	1.02
Overall Detector Average	3.05	2.53	1.21
Phantom Inside Two-Meter Box - Front Toward Reactor			
External Detector Average	0.32	0.33	0.97
Internal Detector Average	0.08	0.10	0.80
Overall Detector Average	0.25	0.26	0.96
Phantom Inside Two-Meter Box - Left-Side Toward Reactor			
External Detector Average	0.32	0.32	1.00
Internal Detector Average	0.07	0.09	0.78
Overall Detector Average	0.25	0.24	1.04

Table 13

Comparisons of Calculated and Average Experimentally Measured Neutron Reduction Factors Averaged Over External, Internal, and All Detector Locations On or Inside the RT-200 Humanoid Phantom at the 400 Meter Test Site at the APRF.			
Neutron Reduction Factor (Tissue)	MASH	Avg. Expt.	C/E
Phantom Free-Field - Front Toward Reactor			
External Detector Average	1.28	1.36	0.94
Internal Detector Average	5.10	4.71	1.08
Overall Detector Average	1.63	1.79	0.91
Phantom Inside Two-Meter Box - Front Toward Reactor			
External Detector Average	14.8	11.2	1.32
Internal Detector Average	58.6	39.9	1.47
Overall Detector Average	18.9	14.7	1.29
Phantom Inside Two-Meter Box - Left-Side Toward Reactor			
External Detector Average	15.5	12.6	1.23
Internal Detector Average	75.7	47.4	1.60
Overall Detector Average	20.0	16.7	1.20

Table 14

Comparisons of Calculated and HDL Measured Gamma-Ray Dose Averaged Over External, Internal, and All Detector Locations On or Inside the RT-200 Humanoid Phantom at the 400 Meter Test Site at the APRF.			
Gamma Dose (mrad(CaF_2:Mn)/kWh)	MASH	HDL	C/E
Phantom Free-Field - Front Toward Reactor			
External Detector Average	1.68	1.51	1.11
Internal Detector Average	2.08	1.74	1.20
Overall Detector Average	1.79	1.58	1.13
Phantom Inside Two-Meter Box - Front Toward Reactor			
External Detector Average	0.39	0.37	1.05
Internal Detector Average	0.41	0.46	0.89
Overall Detector Average	0.40	0.40	1.00
Phantom Inside Two-Meter Box - Left-Side Toward Reactor			
External Detector Average	0.38	0.35	1.09
Internal Detector Average	0.40	0.35	1.14
Overall Detector Average	0.39	0.35	1.11

Table 15

Comparisons of Calculated and HDL Measured Gamma-Ray Reduction Factors Averaged Over External, Internal, and All Detector Locations On or Inside the RT-200 Humanoid Phantom at the 400 Meter Test Site at the APRF.			
Gamma Reduction Factor (CaF_2:Mn)	MASH	HDL	C/E
Phantom Free-Field - Front Toward Reactor			
External Detector Average	0.82	0.81	1.01
Internal Detector Average	0.66	0.71	0.93
Overall Detector Average	0.77	0.78	0.99
Phantom Inside Two-Meter Box - Front Toward Reactor			
External Detector Average	3.51	3.33	1.05
Internal Detector Average	3.34	2.67	1.25
Overall Detector Average	3.46	3.11	1.11
Phantom Inside Two-Meter Box - Left-Side Toward Reactor			
External Detector Average	3.61	3.53	1.02
Internal Detector Average	3.43	3.56	0.96
Overall Detector Average	3.55	3.54	1.00

Table 16

Comparisons of Calculated and APRF Measured Gamma-Ray Dose Averaged Over External, Internal and All Detector Locations On or Inside the RT-200 Humanoid Phantom at the 400 Meter Test Site at the APRF. (Small TLD)			
Gamma Dose (mrad(Tissue)/kWh)	MASH	APRF	C/E
Phantom Free-Field - Front Toward Reactor			
External Detector Average	1.61	NM*	-
Internal Detector Average	1.96	NM	-
Overall Detector Average	1.71	NM	-
Phantom Inside Two-Meter Box - Front Toward Reactor			
External Detector Average	0.38	0.31	1.23
Internal Detector Average	0.37	0.33	1.12
Overall Detector Average	0.37	0.32	1.16
Phantom Inside Two-Meter Box - Left-Side Toward Reactor			
External Detector Average	0.37	0.31	1.19
Internal Detector Average	0.36	0.32	1.13
Overall Detector Average	0.37	0.31	1.19

*Not Measured

Table 17

Comparisons of Calculated and APRF Measured Gamma-Ray Reduction Factors Averaged Over External, Internal, and All Detector Locations On or Inside the RT-200 Humanoid Phantom at the 400 Meter Test Site at the APRF. (Small TLD)			
Gamma Reduction Factor (Tissue)	MASH	APRF	C/E
Phantom Free-Field - Front Toward Reactor			
External Detector Average	0.84	NM*	-
Internal Detector Average	0.69	NM	-
Overall Detector Average	0.79	NM	-
Phantom Inside Two-Meter Box - Front Toward Reactor			
External Detector Average	3.59	4.49	0.80
Internal Detector Average	3.65	4.45	0.82
Overall Detector Average	3.61	4.48	0.81
Phantom Inside Two-Meter Box - Left-Side Toward Reactor			
External Detector Average	3.67	4.23	0.87
Internal Detector Average	3.75	3.68	1.02
Overall Detector Average	3.69	4.06	0.91

*Not Measured

Table 18

Comparisons of Calculated and APRF Measured Gamma-Ray Dose Averaged Over External, Internal, and All Detector Locations On or Inside the RT-200 Humanoid Phantom at the 400 Meter Test Site at the APRF. (Large TLD)			
Gamma Dose (mrad(Tissue)/kWh)	MASH	APRF	C/E
Phantom Free-Field - Front Toward Reactor			
External Detector Average	1.61	1.83	0.88
Internal Detector Average	1.96	2.04	0.96
Overall Detector Average	1.71	1.89	0.90
Phantom Inside Two-Meter Box - Front Toward Reactor			
External Detector Average	0.38	0.36	1.06
Internal Detector Average	0.37	0.39	0.95
Overall Detector Average	0.37	0.37	1.00
Phantom Inside Two-Meter Box - Left-Side Toward Reactor			
External Detector Average	0.37	0.35	1.06
Internal Detector Average	0.36	0.39	0.92
Overall Detector Average	0.37	0.36	1.03

Table 19

Comparisons of Calculated and APRF Measured Gamma-Ray Reduction Factors Averaged Over External, Internal, and All Detector Locations On or Inside the RT-200 Humanoid Phantom at the 400 Meter Test Site at APRF. (Large TLD)			
Gamma Reduction Factor (Tissue)	MASH	APRF	C/E
Phantom Free-Field - Front Toward Reactor			
External Detector Average	0.84	0.82	1.02
Internal Detector Average	0.69	0.73	0.95
Overall Detector Average	0.79	0.79	1.00
Phantom Inside Two-Meter Box - Front Toward Reactor			
External Detector Average	3.59	4.16	0.86
Internal Detector Average	3.65	3.80	0.96
Overall Detector Average	3.61	4.05	0.89
Phantom Inside Two-Meter Box - Left-Side Toward Reactor			
External Detector Average	3.67	4.25	0.86
Internal Detector Average	3.75	3.82	0.98
Overall Detector Average	3.69	4.12	0.90

Table 20

Comparisons of Calculated and ETCA Measured Gamma-Ray Dose Averaged Over External, Internal, and All Detector Locations On or Inside the RT-200 Humanoid Phantom at the 400 Meter Test Site at the APRF.			
Gamma Dose (mrad(Tissue)/kWh)	MASH	ETCA	C/E
Phantom Free-Field - Front Toward Reactor			
External Detector Average	1.61	1.61	1.00
Internal Detector Average	1.96	1.84	1.07
Overall Detector Average	1.71	1.67	1.02
Phantom Inside Two-Meter Box - Front Toward Reactor			
External Detector Average	0.38	0.37	1.03
Internal Detector Average	0.37	0.39	0.95
Overall Detector Average	0.37	0.38	0.97
Phantom Inside Two-Meter Box - Left-Side Toward Reactor			
External Detector Average	0.37	0.35	1.06
Internal Detector Average	0.36	0.39	0.92
Overall Detector Average	0.37	0.36	1.03

Table 21

Comparisons of Calculated and ETCA Measured Gamma-Ray Reduction Factors Averaged Over External, Internal, and All Detector Locations On or Inside the RT-200 Humanoid Phantom at the 400 Meter Test Site at the APRF.			
Gamma Reduction Factor (Tissue)	MASH	ETCA	C/E
Phantom Free-Field - Front Toward Reactor			
External Detector Average	0.84	0.86	0.98
Internal Detector Average	0.69	0.76	0.91
Overall Detector Average	0.79	0.83	0.95
Phantom Inside Two-Meter Box - Front Toward Reactor			
External Detector Average	3.59	3.75	0.96
Internal Detector Average	3.65	3.54	1.03
Overall Detector Average	3.61	3.68	0.98
Phantom Inside Two-Meter Box - Left-Side Toward Reactor			
External Detector Average	3.67	3.71	0.99
Internal Detector Average	3.75	3.38	1.11
Overall Detector Average	3.69	3.59	1.03

Table 22

Comparisons of Calculated and AFRRI Measured Gamma-Ray Dose Averaged Over External, Internal, and All Detector Locations On or Inside the RT-200 Humanoid Phantom at the 400 Meter Test Site at the APRF.			
Gamma Dose (mrad(Tissue)/kWh)	MASH	AFRRI	C/E
Phantom Free-Field - Front Toward Reactor			
External Detector Average	1.61	NM*	-
Internal Detector Average	1.96	NM	-
Overall Detector Average	1.71	NM	-
Phantom Inside Two-Meter Box - Front Toward Reactor			
External Detector Average	0.38	0.31	1.23
Internal Detector Average	0.37	0.33	1.12
Overall Detector Average	0.37	0.32	1.16
Phantom Inside Two-Meter Box - Left-Side Toward Reactor			
External Detector Average	0.37	0.31	1.19
Internal Detector Average	0.36	0.32	1.13
Overall Detector Average	0.37	0.31	1.19

*Not Measured

Table 23

Comparisons of Calculated and AFRRI Measured Gamma-Ray Reduction Factors Averaged Over External, Internal, and All Detector Locations On or Inside the RT-200 Humanoid Phantom at the 400 Meter Test Site at the APRF.			
Gamma Reduction Factor (Tissue)	MASH	AFRRI	C/E
Phantom Free-Field - Front Toward Reactor			
External Detector Average	0.84	NM*	-
Internal Detector Average	0.69	NM	-
Overall Detector Average	0.79	NM	-
Phantom Inside Two-Meter Box - Front Toward Reactor			
External Detector Average	3.59	3.97	0.90
Internal Detector Average	3.65	3.73	0.98
Overall Detector Average	3.61	3.90	0.93
Phantom Inside Two-Meter Box - Left-Side Toward Reactor			
External Detector Average	3.67	3.98	0.92
Internal Detector Average	3.75	3.94	0.95
Overall Detector Average	3.69	3.97	0.93

*Not Measured

Table 24

Comparisons of Calculated and Average Experimentally Measured Gamma-Ray Dose (Tissue) Averaged Over External, Internal, and All Detector Locations On or Inside the RT-200 Humanoid Phantom at the 400 Meter Test Site at the APRF.			
Gamma Dose (mad(Tissue)/kWh)	MASH	Avg. Expt.	C/E
Phantom Free-Field - Front Toward Reactor			
External Detector Average	1.61	1.72	0.94
Internal Detector Average	1.96	1.94	1.01
Overall Detector Average	1.71	1.78	0.96
Phantom Inside Two-Meter Box - Front Toward Reactor			
External Detector Average	0.38	0.34	1.12
Internal Detector Average	0.37	0.36	1.03
Overall Detector Average	0.37	0.35	1.06
Phantom Inside Two-Meter Box - Left-Side Toward Reactor			
External Detector Average	0.37	0.34	1.09
Internal Detector Average	0.36	0.37	0.97
Overall Detector Average	0.37	0.34	1.09

Table 25

Comparisons of Calculated and Average Experimentally Measured Gamma-Ray Reduction Factors (Tissue) Averaged Over External, Internal, and All Detector Locations On or Inside the RT-200 Humanoid Phantom at the 400 Meter Test Site at the APRF.			
Gamma Reduction Factor (Tissue)	MASH	Avg. Expt.	C/E
Phantom Free-Field - Front Toward Reactor			
External Detector Average	0.84	0.84	1.00
Internal Detector Average	0.69	0.74	0.93
Overall Detector Average	0.79	0.81	0.98
Phantom Inside Two-Meter Box - Front Toward Reactor			
External Detector Average	3.59	4.07	0.88
Internal Detector Average	3.65	3.85	0.95
Overall Detector Average	3.61	4.01	0.90
Phantom Inside Two-Meter Box - Left-Side Toward Reactor			
External Detector Average	3.67	4.03	0.91
Internal Detector Average	3.75	3.69	1.02
Overall Detector Average	3.69	3.92	0.94

5.0 MONTE CARLO STATISTICAL UNCERTAINTY

Analysis of the MORSE escape history tapes in DRC for all of the detector positions on or inside the phantom (except the mid-gut position) and inside the two-meter box test bed yielded statistical uncertainties on the order of ±4% for integral neutron fluence(dose) and ±2% for total gamma-ray fluence(dose). The mid-gut position yielded statistical uncertainties on the order of ±5% to ±7% for integral neutron fluence(dose) and ±2% for total gamma-ray fluence(dose). The statistical uncertainties for the vehicle secondary particle production, i.e. vehicle (n,γ), the direct gamma-ray plus air secondary gamma production, i.e. source γ's + air (n,γ), and all contributions from the ground secondary particle production, i.e. ground (n,γ), are typically ±2%, ±4%, and ±25 to ±35% respectively. It should be noted that the large statistical uncertainties associated with the ground secondary particle production are not critical to the quality of the calculated results since this contribution to the total dose is insignificant. Spectral fluence(dose) results exhibited statistical uncertainties typically between ±5% and ±15% for neutron energies between 10 MeV and thermal, and between ±3% and ±10% for gamma energies between 10 MeV and 100 keV for all detector locations except the mid-gut location and the mid-head location for the phantom standing in the two-meter box. These two locations (mid-head inside box and mid-gut) exhibited spectral fluence(dose) results with statistical uncertainties typically between ±10% and ±30% for neutron energies between 10 MeV and thermal, and between ±5% and ±12% for gamma-ray energies between 10 MeV and 100 keV. These energy ranges contain the energy groups in the DABL69 group structure which make a significant contribution to the response.

Unfortunately, there was limited detailed information on uncertainties reported with the experimental data utilized in this report. Based on uncertainties reported in numerous previous documents, the accuracy of the detector systems used in this set of experiments ranges from approximately ±5% to ±10%, and the reproducibility of the detector system results on a day-to-day basis is approximately ±5% to ±10%.

As stated earlier, the composite effect of the differences in the way the measured and calculated gamma-ray data are reported is difficult to ascertain and is not considered in this report.

6.0 CONCLUSIONS

The multiple air-over-ground environments yielded an accurate representation of the ground moisture and meteorological data supplied by APRF. Plotting the dose response as a function of hydrogen content in the air, ground moisture, and detector energy range, and correlating the different measurements with the ground moisture and meteorological data, allowed the ORNL analysts to extrapolate between the different air-over-ground environments to obtain results consistent with the environmental data present at the time of a given measurement. This appears to be the most viable option for representing changing environmental data over a series of measurements. Calculating the fluence on the coupling surface for each air-over-ground environment during of a series of measurements would be prohibitive.

Analyzing 500,000 to 1,000,000 adjoint source particles was sufficient to obtain integral data statistics within ±5% for almost all of the detector locations. The mid-gut locations for the phantom standing inside the two-meter box could have utilized more adjoint source particles to obtain a statistical convergence within ±5%. Convergence on the spectral data would be marginal for the number of adjoint source particles used in this analysis since most of the neutron group data was only converged to approximately 10% to 15%.

Should comparisons of spectral data for this type of experiment become a requirement in the future, the MASH analysis will have to be rerun to obtain acceptable statistical convergence on the spectral data. For spectral data comparisons inside the 5% borated polyethylene lined two-meter box, as many as 1,000,000 to 2,000,000 adjoint source particles might be required to obtain tight (within ±5% to ±8%) statistical convergence on the energy groups (neutron and gamma-ray) contributing to the response of interest.

Analyzing the calculated dose responses over the energy range of the measured results yielded consistent comparisons between the calculated and measured responses in almost all cases. This point almost goes without saying but is important in this work since one of the purposes is to validate the MASH code system.

The differences in the computational combinatorial geometry phantom model used in the MASH analysis and the RT-200 Humanoid Phantom used in the measurements was not deemed a significant contributor to the discrepancies seen in the comparisons of the results. Absolute detector locations (especially mid-head and mid-gut) relative to the phantom geometry could contribute to some of the differences seen in the results at these locations.

In general, the calculational results show mixed agreement with the measured data. The neutron dose results indicate good agreement (typically ±20%) for the phantom standing in the free-field and excellent agreement (typically ±10%) for the phantom standing inside the two-meter box. The neutron reduction factors however, agreed for the phantom standing in the free-field but exhibited significant differences for the phantom standing inside the box. With respect to the gamma-ray data, there were individual discrepancies between calculations and measurements however, typical agreement was within ±20%. The C/E comparisons for

the gamma-ray free-field environment at 400 meters showed improved agreement between calculation and experiment relative to the same comparisons in the Fall 1989 and Spring 1990 studies.

To determine the overall quality of the comparisons between MASH and the measurements, both calculational and experimental data were averaged over detector position (internal and external), response function (tissue and CaF_2:Mn), radiation type (neutron and gamma-ray), and phantom orientation (front facing and left side toward reactor). This averaging procedure produced one set of data for the phantom standing in the free-field, and one set of data for the phantom standing inside the lined two-meter box. The results presented in Table 26, show overall, that the calculations agreed quite well with most of the measured data supplied by the experimental teams. The principal "trouble spot" is the neutron data comparisons (reduction factor) for the phantom standing inside the lined two-meter box. Generally, the overall agreement was within the ±20% limit deemed as acceptable by the DNA.

Table 26. Overall Comparisons of Calculated and Average Experimentally Measured Neutron and Gamma-Ray Dose and Reduction Factors Averaged Over External, Internal, and All Detector Locations On or Inside the RT-200 Humanoid Phantom, and Phantom Orientation Free-Field or Inside the Two-Meter Box, at the 400 Meter Test Site at the APRF.

	Phantom Free-Field			Phantom Inside Two Meter Box		
Response	MASH	Expt	C/E	MASH	Expt	C/E
Neutron Dose (mrad(Tissue)/kWh)						
External Detector Average	3.88	3.31	1.17	0.32	0.33	0.97
Internal Detector Average	0.98	0.96	1.02	0.07	0.09	0.78
Overall Detector Average	3.05	2.53	1.21	0.25	0.25	1.00
Gamma Dose (mrad(Tissue)/kWh)						
External Detector Average	1.61	1.72	0.94	0.38	0.34	1.12
Internal Detector Average	1.96	1.94	1.01	0.37	0.37	1.00
Overall Detector Average	1.71	1.78	0.96	0.37	0.35	1.06
Gamma Dose (mrad(CaF_2:Mn)/kWh)						
External Detector Average	1.68	1.51	1.11	0.39	0.36	1.08
Internal Detector Average	2.08	1.74	1.20	0.41	0.41	1.00
Overall Detector Average	1.79	1.58	1.13	0.40	0.38	1.05
Neutron Reduction Factor						
External Detector Average	1.28	1.36	0.94	15.1	11.9	1.27
Internal Detector Average	5.10	4.71	1.08	66.1	43.3	1.53
Overall Detector Average	1.63	1.79	0.91	19.4	15.6	1.24
Gamma Reduction Factor (Tissue)						
External Detector Average	0.84	0.84	1.00	3.63	4.05	0.90
Internal Detector Average	0.69	0.74	0.93	3.70	3.77	0.98
Ovrall Detector Average	0.79	0.81	0.98	3.65	3.96	0.92
Gamma Reduction Factor (CaF_2:Mn)						
External Detector Average	0.82	0.81	1.01	3.56	3.43	1.04
Internal Detector Average	0.66	0.71	0.93	3.38	3.05	1.11
Overall Detector Average	0.77	0.78	0.99	3.50	3.31	1.06

7.0 RECOMMENDATIONS

This was the third concerted effort aimed at benchmarking the MASH code against measurements, and again there were some glitches in the effort. The most significant problem occurred in the reporting of the gamma-ray dose data. This series of experiments was performed before the analysis of the Spring 1990 experiments was completed. Consequently, the problems associated with data reporting which surfaced in the Spring 1990 comparisons were repeated in this comparison. The calculational and experimental results must report the same data for a meaningful comparison to be made. For TLD data, all corrections to the data for spectral effects (calibration field versus radiation field), response functions [dose(tissue) or dose(TLD)], and contributions due to thermal neutrons must be accounted for or removed from both sets of data. This will allow a true "benchmark" comparison of the MASH code system and reduce the possible sources of discrepancy to be considered.

The comparisons again indicate multiple teams of experimentalists performing the same set of measurements yield a better indication of the quality of the comparison. By averaging the different sets of experimental data together, the anomalies and inconsistencies associated with any one measurement will not manifest themselves in the overall comparison, yet the trends and results consistent in all of the sets of experimental data will remain. Consequently, future efforts in this series of experiments, should continue to have as a minimum two different teams of experimentalists performing the same measurement using the same type detector system. Also, cross checking experimental results with different detector systems is still considered favorable for determining consistency in the experimental results.

The consistent discrepancy associated with the calculated and measured free-field gamma-ray data (from the Fall 1989 and Spring 1990 studies) was less significant in this effort, but still must be addressed before the overall quality of the gamma-ray data comparisons can be improved. To resolve the discrepancy, the differences in the spectral data (Fall 1989 comparison) must be successfully addressed and reconciled. To resolve discrepancies with the comparisons on or inside the phantom, future experiments should consider including the use of a simplified phantom model of known dimensions, simple geometric shapes, and known materials, e.g. a cylindrical water-filled lucite phantom.

With adequate resolution of the concerns alluded to in this report, the Spring 1990 report, and the Fall 1989 report, and with better communication and understanding between the analysts and experimentalists as to the needs of the other, agreement is achievable for all comparisons within the DNA mandated acceptance limit of ±20%.

8.0 REFERENCES

1. J. O. Johnson ed., "A User's Manual for MASH 1.0 - A Monte Carlo Adjoint Shielding Code System," ORNL/TM-11778, Oak Ridge National Laboratory, (March 1992).

2. J. O. Johnson, J. D. Drischler, and J. M. Barnes, "Analysis of the Fall-1989 Two-Meter Box Test Bed Experiments Performed at the Army Pulse Radiation Facility (APRF)," ORNL/TM-11777, Oak Ridge National Laboratory, (May 1991).

3. J. O. Johnson, J. D. Drischler, and J. M. Barnes, "Analysis of the Spring-1990 Two-Meter Box Test Bed Experiments Performed at the Army Pulse Radiation Facility (APRF)," ORNL/TM-11917, Oak Ridge National Laboratory, (August 1992).

4. W. A. Rhoades and M. B. Emmett et al., "Vehicle Code System (VCS) User's Manual," ORNL/TM-4648, Oak Ridge National Laboratory, (August 1974).

5. W. A. Rhoades et al., "Development of a Code System for Determining Radiation Protection of Armored Vehicles (The VCS Code)," ORNL/TM-4664, Oak Ridge National Laboratory, (October 1974).

6. W. A. Rhoades and R. L. Childs, "The DORT Two-Dimensional Discrete Ordinates Transport Code," Nuclear Science & Engineering 99, 1, 88-89 (May 1988).

7. M. B. Emmett, "The MORSE Monte Carlo Radiation Transport Code System," ORNL-4972(1975), ORNL-4972/R1(1983), ORNL-4972/R2(1984) Oak Ridge National Laboratory.

8. D. C. Kaul and S. D. Egbert, "Radiation Leakage From The Army Pulse Radiation Facility (APRF) Fast Reactor," SAIC-89/1423, Science Applications International Corporation, San Diego, California, (May 1989).

9. D. T. Ingersoll, R. W. Roussin, C. Y. Fu, and J. E. White, "DABL69: A Broad-Group Neutron/Photon Cross-Section Library for Defense Nuclear Applications," ORNL/TM-10568, Oak Ridge National Laboratory, (June 1989).

10. W. S. Snyder, M. R. Ford, and G. G. Warner, "Estimates of Specific Absorbed Fractions for Photon Sources Uniformly Distributed in Various Organs of a Heterogeneous Phantom," MIRD Pamphlet No. 5, New York: Society for Nuclear Medicine, (1978).

11. L. W. Bain, Jr. and M. J. Reisinger, "The GIFT Code Users Manual; Volume I, Introduction and Input Requirements," BRL Report No. 1802, AD B006037l, Ballistic Research Laboratory, (July 1975).

12. G. G. Kuehl, L. W. Bain, Jr., and M. J. Reisinger, "The GIFT Code Users Manual; Volume II, The Output Options," ARBRL-TR-02189, AD A078364, Ballistic Research Laboratory, (September 1979).

APPENDIX A

Comparisons of the Calculated (MASH) and Measured Neutron Dose Reduction Factors for the Spring 1991 Two-Meter Box Test Bed Experiments Performed at the APRF.

Table A-1

MASH VS. APRF						
Phantom Free-Field Neutron Dose and Reduction Factors(mrad(Tissue)/kWh)						
Detector Position	Neutron Dose Phantom Facing Reactor			Neutron Reduction Factors Phantom Facing Reactor		
	MASH	APRF	C/E	MASH	APRF	C/E
FF[1]	4.97	4.26	1.17	-	-	-
DS[2]	0.38 (.033)*	NM+	-	13.08	NM	-
FB[3]	4.49 (.018)	NM	-	1.11	NM	-
BB[4]	1.63 (.012)	1.20	1.36	3.05	3.55	0.86
LC[5]	4.54 (.017)	3.72	1.22	1.09	1.15	0.95
LW[6]	4.33 (.018)	3.60	1.20	1.15	1.18	0.97
RW[7]	4.42 (.018)	3.91	1.13	1.12	1.09	1.03
MH[8]	1.23 (.021)	1.16	1.06	4.04	3.67	1.10
MG[9]	0.72 (.034)	0.65	1.11	6.90	6.55	1.05

*Fractional Standard Deviation
+Not Measured
[1]Free-Field
[2]Detector on Shelf in 2m Box
[3]Front Belt
[4]Back Belt
[5]Left Chest
[6]Left Wrist
[7]Right Wrist
[8]Mid-Head
[9]Mid-Gut

Table A-2

MASH VS. APRF						
Phantom In 2m Box Neutron Dose(mrad(Tissue)/kWh)						
Detector Position	Phantom Facing Reactor			Phantom Left Side Toward Reactor		
	MASH	APRF	C/E	MASH	APRF	C/E
FF[1]	4.69	3.88	1.21	4.92	3.88	1.27
DS[2]	0.37 (.035)*	0.37	1.00	0.37 (.035)	0.36	1.03
FB[3]	0.36 (.044)	NM+	-	0.29 (.057)	NM	-
BB[4]	0.17 (.043)	0.25	0.68	0.31 (.049)	0.35	0.89
LC[5]	0.37 (.051)	0.37	1.00	0.33 (.066)	0.32	1.03
LW[6]	0.32 (.038)	0.35	0.91	0.40 (.041)	0.36	1.11
RW[7]	0.36 (.040)	0.38	0.95	0.26 (.043)	0.27	0.96
MH[8]	0.10 (.052)	0.13	0.77	0.10 (.045)	0.12	0.83
MG[9]	0.06 (.072)	0.06	1.00	0.03 (.080)	0.03	1.00

*Fractional Standard Deviation
+Not Measured
[1]Free-Field
[2]Detector on Shelf in 2m Box
[3]Front Belt
[4]Back Belt
[5]Left Chest
[6]Left Wrist
[7]Right Wrist
[8]Mid-Head
[9]Mid-Gut

Table A-3

MASH VS. APRF						
Phantom In 2m Box Neutron Reduction Factors(mrad(Tissue)/kWh)						
Detector Position	Phantom Facing Reactor			Phantom Left Side Toward Reactor		
	MASH	APRF	C/E	MASH	APRF	C/E
FF[1]						
DS[2]	12.68	10.49	1.21	13.30	10.78	1.23
FB[3]	13.03	NM*	-	16.97	NM	-
BB[4]	27.59	15.52	1.78	15.87	11.09	1.43
LC[5]	12.68	10.49	1.21	14.91	12.13	1.23
LW[6]	14.66	11.09	1.32	12.30	10.78	1.14
RW[7]	13.03	10.21	1.28	18.92	14.37	1.32
MH[8]	46.90	29.85	1.57	49.20	32.33	1.52
MG[9]	78.17	64.67	1.21	164.00	129.33	1.27

*Not Measured

[1]Free-Field
[2]Detector on Shelf in 2m Box
[3]Front Belt
[4]Back Belt
[5]Left Chest
[6]Left Wrist
[7]Right Wrist
[8]Mid-Head
[9]Mid-Gut

Table A-4

MASH VS. ETCA						
Phantom Free-Field Neutron Dose and Reduction Factors(mrad(Tissue)/kWh)						
Detector Position	Neutron Dose Phantom Facing Reactor			Neutron Reduction Factors Phantom Facing Reactor		
	MASH	ETCA	C/E	MASH	ETCA	C/E
FF[1]	4.97	4.78	1.04	-	-	-
DS[2]	0.38 (.033)*	0.37+	1.03	13.08	12.92	1.01
FB[3]	4.49 (.018)	4.46	1.01	1.11	1.07	1.04
BB[4]	1.63 (.012)	1.55	1.05	3.05	3.08	0.99
LC[5]	4.54 (.017)	4.24	1.07	1.09	1.13	0.96
LW[6]	4.33 (.018)	4.74	0.91	1.15	1.01	1.14
RW[7]	4.42 (.018)	3.52	1.26	1.12	1.36	0.82
MH[8]	1.23 (.021)	1.22	1.01	4.04	3.92	1.03
MG[9]	0.72 (.034)	0.80	0.90	6.90	5.98	1.15

*Fractional Standard Deviation
+Average Value
[1]Free-Field
[2]Detector on Shelf in 2m Box
[3]Front Belt
[4]Back Belt
[5]Left Chest
[6]Left Wrist
[7]Right Wrist
[8]Mid-Head
[9]Mid-Gut

Table A-5

MASH VS. ETCA						
Phantom In 2m Box Neutron Dose (mrad(Tissue)/kWh)						
Detector Position	Phantom Facing Reactor			Phantom Left Side Toward Reactor		
	MASH	ETCA	C/E	MASH	ETCA	C/E
FF[1]	4.69	3.51	1.34	4.92	4.15[+]	1.19
DS[2]	0.37 (.035)[*]	0.41	0.90	0.37 (.035)	0.33	1.12
FB[3]	0.36 (.044)	NM[†]	-	0.29 (.057)	NM	-
BB[4]	0.17 (.043)	0.16	1.06	0.31 (.049)	0.29	1.07
LC[5]	0.37 (.051)	0.39	0.95	0.33 (.066)	0.32	1.03
LW[6]	0.32 (.038)	0.37	0.86	0.40 (.041)	0.38	1.05
RW[7]	0.36 (.040)	0.37	0.97	0.26 (.034)	0.25	1.04
MH[8]	0.10 (.052)	0.12	0.83	0.10 (.045)	0.15	0.67
MG[9]	0.06 (.072)	0.06	1.00	0.03 (.080)	0.04	0.75

[*]Fractional Standard Deviation
[+]Average Value
[†]Not Measured
[1]Free-Field
[2]Detector on Shelf in 2m Box
[3]Front Belt
[4]Back Belt
[5]Left Chest
[6]Left Wrist
[7]Right Wrist
[8]Mid-Head
[9]Mid-Gut

Table A-6

MASH VS. ETCA						
Phantom In 2m Box Neutron Reduction Factors(mrad(Tissue)/kWh)						
Detector Position	Phantom Facing Reactor			Phantom Left Side Toward Reactor		
	MASH	ETCA	C/E	MASH	ETCA	C/E
FF[1]						
DS[2]	12.68	8.56	1.48	13.30	12.58	1.06
FB[3]	13.03	NM*	-	16.97	NM	-
BB[4]	27.59	21.94	1.26	15.87	14.31	1.11
LC[5]	12.68	9.00	1.41	14.91	12.97	1.15
LW[6]	14.66	9.49	1.54	12.30	10.92	1.13
RW[7]	13.03	9.49	1.37	18.92	16.60	1.14
MH[8]	46.90	29.25	1.60	49.20	27.67	1.78
MG[9]	78.17	58.50	1.34	164.00	103.75	1.58

*Not Measured

[1]Free-Field
[2]Detector on Shelf in 2m Box
[3]Front Belt
[4]Back Belt
[5]Left Chest
[6]Left Wrist
[7]Right Wrist
[8]Mid-Head
[9]Mid-Gut

APPENDIX B

Comparisons of the Calculated (MASH) and Measured Gamma-Ray Dose and Reduction Factors for the Spring 1991 Two-Meter Box Test Bed Experiments Performed at the APRF.

Table B-1

MASH VS. HDL						
Phantom Free-Feld Gamma-Ray Dose and Reduction Factors(mrad(CaF_2:Mn)/kWh)						
Detector Position	Gamma-Ray Dose Phantom Facing Reactor			Gamma-Ray Reduction Factors Phantom Facing Reactor		
	MASH	HDL	C/E	MASH	HDL	C/E
FF[1]	1.37	1.23	1.11			
DS[2]	0.38 (.013)*	0.41	0.93	3.61	3.00	1.20
FB[3]	1.91 (.016)	1.65	1.16	0.72	0.75	0.96
BB[4]	1.48 (.016)	1.30	1.14	0.93	0.95	0.98
LC[5]	1.84 (.016)	1.61	1.14	0.74	0.76	0.97
LW[6]	1.52 (.013)	1.58	0.96	0.90	0.78	1.15
RW[7]	1.63 (.013)	1.43	1.14	0.84	0.86	0.98
MH[8]	2.04 (.013)	1.72	1.19	0.67	0.72	0.93
MG[9]	2.11 (.012)	1.75	1.21	0.65	0.70	0.93

*Fractional Standard Deviation

[1]Free-Field
[2]Detector on Shelf in 2m Box
[3]Front Belt
[4]Back Belt
[5]Left Chest
[6]Left Wrist
[7]Right Wrist
[8]Mid-Head
[9]Mid-Gut

Table B-2

MASH VS. HDL						
Phantom In 2m Box Gamma-Ray Dose(mrad(CaF_2:Mn)/kWh)						
Detector Position	Phantom Facing Reactor			Phantom Left Side Toward Reactor		
	MASH	HDL	C/E	MASH	HDL	C/E
FF[1]	1.37	1.23	1.11	1.37	1.23	1.11
DS[2]	0.36 (.013)*	0.32	1.13	0.36 (.013)	0.31	1.16
FB[3]	0.41 (.017)	0.40	1.03	0.38 (.016)	0.30	1.27
BB[4]	0.36 (.013)	0.34	1.06	0.38 (.012)	0.37	1.03
LC[5]	0.42 (.014)	0.43	0.98	0.41 (.014)	0.34	1.21
LW[6]	0.38 (.013)	0.36	1.06	0.40 (.014)	0.38	1.05
RW[7]	0.38 (.013)	0.32	1.19	0.33 (.014)	0.35	0.94
MH[8]	0.42 (.011)	0.51	0.82	0.42 (.011)	0.35	1.20
MG[9]	0.40 (.013)	0.41	0.98	0.38 (.012)	0.34	1.12

*Fractional Standard Deviation

[1]Free-Field
[2]Detector on Shelf in 2m Box
[3]Front Belt
[4]Back Belt
[5]Left Chest
[6]Left Wrist
[7]Right Wrist
[8]Mid-Head
[9]Mid-Gut

Table B-3

MASH VS. HDL						
Phantom In 2m Box Gamma-Ray Reduction Factors(mrad(CaF_2:Mn)/kWh)						
Detector Position	Phantom Facing Reactor			Phantom Left Side Toward Reactor		
	MASH	HDL	C/E	MASH	HDL	C/E
FF[1]						
DS[2]	3.81	3.84	0.99	3.81	3.97	0.96
FB[3]	3.34	3.08	1.08	3.61	4.10	0.88
BB[4]	3.81	3.62	1.05	3.61	3.32	1.09
LC[5]	3.26	2.86	1.14	3.34	3.62	0.92
LW[6]	3.61	3.42	1.06	3.43	3.24	1.06
RW[7]	3.61	3.84	0.94	4.15	3.51	1.18
MH[8]	3.26	2.41	1.35	3.26	3.51	0.93
MG[9]	3.43	3.00	1.14	3.61	3.62	1.00

[1]Free-Field
[2]Detector on Shelf in 2m Box
[3]Front Belt
[4]Back Belt
[5]Left Chest
[6]Left Wrist
[7]Right Wrist
[8]Mid-Head
[9]Mid-Gut

Table B-4

MASH VS. APRF (Large TLD)						
Phantom Free-Field Gamma-Ray Dose and Reduction Factors(mrad(Tissue)/kWh)						
Detector Position	Gamma-Ray Dose Phantom Facing Reactor			Gamma-Ray Reduction Factors Phantom Facing Reactor		
	MASH	APRF	C/E	MASH	APRF	C/E
FF[1]	1.35	1.49	0.91			
DS[2]	0.40 (.013)*	0.35	1.14	3.38	4.26	0.79
FB[3]	1.81 (.017)	2.02	0.90	0.75	0.74	1.01
BB[4]	1.43 (.018)	1.45	0.99	0.94	1.03	0.91
LC[5]	1.78 (.018)	2.05	0.87	0.76	0.73	1.04
LW[6]	1.47 (.015)	1.82	0.81	0.92	0.82	1.12
RW[7]	1.57 (.015)	1.82	0.86	0.86	0.82	1.05
MH[8]	1.96 (.015)	2.03	0.97	0.69	0.73	0.95
MG[9]	1.95 (.013)	2.04	0.96	0.69	0.73	0.95

*Fractional Standard Deviation

[1]Free-Field
[2]Detector on Shelf in 2m Box
[3]Front Belt
[4]Back Belt
[5]Left Chest
[6]Left Wrist
[7]Right Wrist
[8]Mid-Head
[9]Mid-Gut

Table B-5

MASH VS. APRF (Small TLD)						
Phantom In 2m Box Gamma-Ray Dose(mrad(Tissue)/kWh)						
Detector Position	Phantom Facing Reactor			Phantom Left Side Toward Reactor		
	MASH	APRF	C/E	MASH	APRF	C/E
FF[1]	1.35	1.49	0.91	1.35	1.38	0.98
DS[2]	0.38 (.013)*	0.33	1.15	0.38 (.013)	0.34	1.12
FB[3]	0.40 (.018)	0.35	1.14	0.37 (.016)	0.34	1.09
BB[4]	0.34 (.013)	0.31	1.10	0.37 (.013)	0.31	1.19
LC[5]	0.40 (.015)	0.35	1.14	0.39 (.015)	0.35	1.11
LW[6]	0.37 (.013)	0.32	1.16	0.39 (.014)	0.34	1.15
RW[7]	0.37 (.013)	0.33	1.12	0.32 (.014)	0.29	1.10
MH[8]	0.39 (.012)	0.31	1.26	0.39 (.012)	0.42	0.93
MG[9]	0.35 (.015)	0.36	0.97	0.33 (.013)	0.33	1.00

*Fractional Standard Deviation

[1]Free-Field
[2]Detector on Shelf in 2m Box
[3]Front Belt
[4]Back Belt
[5]Left Chest
[6]Left Wrist
[7]Right Wrist
[8]Mid-Head
[9]Mid-Gut

Table B-6

MASH VS. APRF (Small TLD)						
Phantom In 2m Box Gamma-Ray Reduction Factors(mrad(Tissue)/kWh)						
Detector Position	Phantom Facing Reactor			Phantom Left Side Toward Reactor		
	MASH	APRF	C/E	MASH	APRF	C/E
FF[1]						
DS[2]	3.55	4.52	0.79	3.55	4.06	0.87
FB[3]	3.38	4.26	0.79	3.65	4.06	0.90
BB[4]	3.97	4.81	0.83	3.65	4.45	0.82
LC[5]	3.38	4.26	0.79	3.46	3.94	0.88
LW[6]	3.65	4.66	0.78	3.46	4.06	0.85
RW[7]	3.65	4.52	0.81	4.22	4.76	0.89
MH[8]	3.46	4.81	0.72	3.46	3.29	1.05
MG[9]	3.86	4.14	0.93	4.09	4.18	0.98

[1]Free-Field
[2]Detector on Shelf in 2m Box
[3]Front Belt
[4]Back Belt
[5]Left Chest
[6]Left Wrist
[7]Right Wrist
[8]Mid-Head
[9]Mid-Gut

Table B-7

MASH VS. APRF (Large TLD)						
Phantom In 2m Box Gamma-Ray Dose(mrad(Tissue)/kWh)						
Detector Position	Phantom Facing Reactor			Phantom Left Side Toward Reactor		
	MASH	APRF	C/E	MASH	APRF	C/E
FF[1]	1.35	1.48	0.91	1.35	1.47	0.92
DS[2]	0.38 (.013)*	0.34	1.12	0.38 (.013)	0.34	1.12
FB[3]	0.40 (.018)	0.38	1.05	0.37 (.016)	0.35	1.06
BB[4]	0.34 (.013)	0.30	1.13	0.37 (.013)	0.34	1.09
LC[5]	0.40 (.015)	0.41	0.98	0.39 (.015)	0.38	1.03
LW[6]	0.37 (.013)	0.34	1.09	0.39 (.014)	0.36	1.08
RW[7]	0.37 (.013)	0.35	1.06	0.32 (.014)	0.30	1.07
MH[8]	0.39 (.012)	0.41	0.95	0.39 (.012)	0.41	0.95
MG[9]	0.35 (.015)	0.37	0.95	0.33 (.013)	0.36	0.92

*Fractional Standard Deviation

[1]Free-Field
[2]Detector on Shelf in 2m Box
[3]Front Belt
[4]Back Belt
[5]Left Chest
[6]Left Wrist
[7]Right Wrist
[8]Mid-Head
[9]Mid-Gut

Table B-8

MASH VS. APRF (Large TLD)						
Phantom In 2m Box Gamma-Ray Reduction Factors(mrad(Tissue)/kWh)						
Detector Position	Phantom Facing Reactor			Phantom Left Side Toward Reactor		
	MASH	APRF	C/E	MASH	APRF	C/E
FF[1]						
DS[2]	3.55	4.35	0.82	3.55	4.32	0.82
FB[3]	3.38	3.89	0.87	3.65	4.20	0.87
BB[4]	3.97	4.93	0.81	3.65	4.32	0.84
LC[5]	3.38	3.61	0.94	3.46	3.87	0.89
LW[6]	3.65	4.35	0.84	3.46	4.08	0.85
RW[7]	3.65	4.23	0.86	4.22	4.90	0.86
MH[8]	3.46	3.61	0.96	3.46	3.59	0.96
MG[9]	3.86	4.00	0.97	4.09	4.08	1.00

[1]Free-Field
[2]Detector on Shelf in 2m Box
[3]Front Belt
[4]Back Belt
[5]Left Chest
[6]Left Wrist
[7]Right Wrist
[8]Mid-Head
[9]Mid-Gut

Table B-9

MASH VS. ETCA						
Phantom Free-Field Gamma-Ray Dose and Reduction Factors(mrad(Tissue/kWh)						
Detector Position	Gamma-Ray Dose Phantom Facing Reactor			Gamma-Ray Reduction Factors Phantom Facing Reactor		
	MASH	ETCA	C/E	MASH	ETCA	C/E
FF[1]	1.35	1.39	0.97	-	-	-
DS[2]	0.40 (.013)*	0.32	1.25	3.38	4.34	0.78
FB[3]	1.81 (.017)	1.82	0.99	0.75	0.76	0.99
BB[4]	1.43 (.018)	1.43	1.00	0.94	0.97	0.97
LC[5]	1.78 (.018)	1.77	1.01	0.76	0.79	0.96
LW[6]	1.47 (.015)	1.52	0.97	0.92	0.91	1.01
RW[7]	1.57 (.015)	1.50	1.05	0.86	0.93	0.92
MH[8]	1.96 (.015)	1.86	1.05	0.69	0.75	0.92
MG[9]	1.95 (.013)	1.81	1.08	0.69	0.77	0.90

*Fractional Standard Deviation

[1]Free-Field
[2]Detector on Shelf in 2m Box
[3]Front Belt
[4]Back Belt
[5]Left Chest
[6]Left Wrist
[7]Right Wrist
[8]Mid-Head
[9]Mid-Gut

Table B-10

MASH VS. ETCA						
Phantom In 2m Box Gamma-Ray Dose(mrad(Tissue)/kWh)						
Detector Position	Phantom Facing Reactor			Phantom Left Side Toward Reactor		
	MASH	ETCA	C/E	MASH	ETCA	C/E
FF[1]	1.35	1.38	0.98	1.35	1.30	1.04
DS[2]	0.38 (.013)*	0.38	1.00	0.38 (.013)	0.36	1.06
FB[3]	0.40 (.018)	NM+	-	0.37 (.016)	-	-
BB[4]	0.34 (.013)	0.35	0.97	0.37 (.013)	0.32	1.16
LC[5]	0.40 (.015)	0.40	1.00	0.39 (.015)	0.35	1.11
LW[6]	0.37 (.013)	0.38	0.97	0.39 (.014)	0.36	1.08
RW[7]	0.37 (.013)	0.34	1.09	0.32 (.014)	0.37	0.86
MH[8]	0.39 (.012)	0.44	0.89	0.39 (.012)	0.41	0.95
MG[9]	0.35 (.015)	0.34	1.03	0.33 (.013)	0.36	0.92

*Fractional Standard Deviation
+Not Measured
[1]Free-Field
[2]Detector on Shelf in 2m Box
[3]Front Belt
[4]Back Belt
[5]Left Chest
[6]Left Wrist
[7]Right Wrist
[8]Mid-Head
[9]Mid-Gut

Table B-11

MASH VS. ETCA						
Phantom In 2m Box Gamma-Ray Reduction Factors(mrad(Tissue)/kWh)						
Detector Position	Phantom Facing Reactor			Phantom Left Side Toward Reactor		
	MASH	ETCA	C/E	MASH	ETCA	C/E
FF[1]						
DS[2]	3.55	3.63	0.98	3.55	3.61	0.98
FB[3]	3.38	NM*	-	3.65	NM	-
BB[4]	3.97	3.94	1.01	3.65	4.06	0.90
LC[5]	3.38	3.45	0.98	3.46	3.71	0.93
LW[6]	3.65	3.63	1.01	3.46	3.61	0.96
RW[7]	3.65	4.06	0.90	4.22	3.51	1.20
MH[8]	3.46	3.14	1.10	3.46	3.17	1.09
MG[9]	3.86	4.06	0.95	4.09	3.61	1.13

*Not Measured

[1]Free-Field
[2]Detector on Shelf in 2m Box
[3]Front Belt
[4]Back Belt
[5]Left Chest
[6]Left Wrist
[7]Right Wrist
[8]Mid-Head
[9]Mid-Gut

Table B-12

MASH VS. AFRRI						
Phantom In 2m Box Gamma-Ray Dose(mrad(Tissue)/kWh)						
Detector Position	Phantom Facing Reactor			Phantom Left Side Toward Reactor		
	MASH	AFRRI	C/E	MASH	AFRRI	C/E
FF[1]	1.35	1.23	1.10	1.35	1.24	1.09
DS[2]	0.38 (.013)*	0.30	1.27	0.38 (.013)	0.29	1.31
FB[3]	0.40 (.018)	0.33	1.21	0.37 (.016)	0.33	1.12
BB[4]	0.34 (.013)	0.28	1.21	0.37 (.013)	0.32	1.16
LC[5]	0.40 (.015)	0.33	1.21	0.39 (.015)	0.34	1.15
LW[6]	0.37 (.013)	0.30	1.23	0.39 (.014)	0.31	1.26
RW[7]	0.37 (.013)	0.31	1.19	0.32 (.014)	0.26	1.23
MH[8]	0.39 (.012)	0.35	1.11	0.39 (.012)	0.34	1.15
MG[9]	0.35 (.015)	0.31	1.13	0.33 (.013)	0.29	1.14

*Fractional Standard Deviation

[1]Free-Field
[2]Detector on Shelf in 2m Box
[3]Front Belt
[4]Back Belt
[5]Left Chest
[6]Left Wrist
[7]Right Wrist
[8]Mid-Head
[9]Mid-Gut

Table B-13

MASH VS. AFRRI						
Phantom In 2m Box Gamma-Ray Reduction Factors(mrad(Tissue)/kWh)						
Detector Position	Phantom Facing Reactor			Phantom Left Side Toward Reactor		
	MASH	AFRRI	C/E	MASH	AFRRI	C/E
FF[1]						
DS[2]	3.55	4.10	0.87	3.55	4.28	0.83
FB[3]	3.38	3.73	0.91	3.65	3.76	0.97
BB[4]	3.97	4.39	0.90	3.65	3.88	0.94
LC[5]	3.38	3.73	0.91	3.46	3.65	0.95
LW[6]	3.65	4.10	0.89	3.46	4.00	0.87
RW[7]	3.65	3.97	0.92	4.22	4.77	0.88
MH[8]	3.46	3.51	0.99	3.46	3.65	0.95
MG[9]	3.86	3.97	0.97	4.09	4.28	0.96

[1]Free-Field
[2]Detector on Shelf in 2m Box
[3]Front Belt
[4]Back Belt
[5]Left Chest
[6]Left Wrist
[7]Right Wrist
[8]Mid-Head
[9]Mid-Gut

APPENDIX C

Sample Input Decks for MORSE Used in the MASH Analysis of the Spring 1991 Two-Meter Box Test Bed Experiments Performed at the APRF.

```
aprf aog/400m/16.14m ss91-121-37 s90e5 5/91 exp. 2m box + liner  COB
 $$ 1000 1500 1000    1   46   23   46   69    0    1  650    9    0
 $$   0   69    1    0
 ** 1.0   1.0-05   1.0+04   0.0   2.2+05
 ** 0.0   0.0   110.16   0.0   0.0   0.0   0.0
 ** 69r1.0
 ** 8r1.0 13r2.0 10r3.0 5r2.0 10r1.0 4r3.0 15r5.0 4r3.0
 ** 1.9640+7  1.6905+7  1.4918+7  1.4191+7  1.3840+7  1.2523+7  1.2214+7
    1.1052+7  1.0000+7  9.0484+6  8.1873+6  7.4082+6  6.3763+6  4.9658+6
    4.7237+6  4.0657+6  3.0119+6  2.3852+6  2.3069+6  1.8268+6  1.4227+6
    1.1080+6  9.6164+5  8.2085+5  7.4274+5  6.3927+5  5.5023+5  3.6883+5
    2.4724+5  1.5764+5  1.1109+5  5.2475+4  3.4307+4  2.4788+4  2.1875+4
    1.0595+4  3.3546+3  1.2341+3  5.8295+2  2.7536+2  1.0130+2  2.9023+1
    1.0677+1  3.0590+0  1.12535+0 4.1399-1  2.0000+7  1.4000+7  1.2000+7
    1.0000+7  8.0000+6  7.0000+6  6.0000+6  5.0000+6  4.0000+6  3.0000+6
    2.5000+6  2.0000+6  1.5000+6  1.0.00+6  7.0000+5  4.5500+5  3.0000+5
    1.5000+5  1.0000+5  7.0000+4  4.5000+4  3.0000+4  2.0000+4
    0000444245555555
 $$   1    1    0    0    0    8   69    1
 $$   1    1   46    1    1    1  **   5.0+00   5.0-02   5.0-01   0.0
 $$   1    1   46    2    1    2  **   5.0+00   5.0-02   5.0-01   0.0
 $$   1    1   46    3    1    3  **   5.0+00   5.0-02   5.0-01   0.0
 $$   1    1   46    4    1    4  **   4.0+00   4.0-02   4.0-01   0.0
 $$   1    1   46    5    1    5  **   3.0+00   3.0-02   3.0-01   0.0
 $$   1    1   46    6    1    6  **   2.0+00   2.0-02   2.0-01   0.0
 $$   1    1   46    7    1    7  **   3.0+00   3.0-02   3.0-01   0.0
 $$   1    1   46    8    1    8  **   3.0+00   3.0-02   3.0-01   0.0
 $$   47    1   69    1    1    1  **   5.0+00   5.0-02   5.0-01   0.0
 $$   47    1   69    2    1    2  **   5.0+00   5.0-02   5.0-01   0.0
 $$   47    1   69    3    1    3  **   5.0+00   5.0-02   5.0-01   0.0
 $$   47    1   69    4    1    4  **   4.0+00   4.0-02   4.0-01   0.0
 $$   47    1   69    5    1    5  **   3.0+00   3.0-02   3.0-01   0.0
 $$   47    1   69    6    1    6  **   2.0+00   2.0-02   2.0-01   0.0
 $$   47    1   69    7    1    7  **   3.0+00   3.0-02   3.0-01   0.0
 $$   47    1   69    8    1    8  **   3.0+00   3.0-02   3.0-01   0.0
 $$  -1   9r0
 $$   0    0    0    0
 ** 23r1.0
 ** 23r1.0
 ** 23r1.0
 ** 23r1.0
 ** 23r1.0
 ** 23r1.0
 ** 23r1.0
 ** 23r1.0
```

Figure C-1. Sample MORSE Input for the MASH Analysis of the Empty Lined (5% Borated Polyethylene) Two-Meter Box Used in the APRF Spring 1991 Two-Meter Box Test Bed Experiments.

```
0000000000     0.001    0.0001    0    0    0
    1    1
   23
    2    6
    1    6    9   12   19   20
    3   16
    2    3    4    5    7    8   10   11   13   14   15   16   17   18
   21   22
    9    1
   25
    0    1
   24
    8    6    4    4    4    1    6    6    8    4    4    8    6    6
    6    6    6    6    8    8    6    6    7    8    1
2m box exp/aprf 5/91 exp. ss91-121-37 s90e5, 1020 steel + phantom n.d.
 $$  46   46   23   23   69   72    4    9   24   67    6    3    0    3
 $$  7z   -2   3z
2m box + liner  COB
 **   8r1.0
 $$   1    2
```

Figure C-1. (cont.)

```
cm   2.0 meter cubic box geometry (4 inches of steel) and 2 inch liner
   50   25
    1rpp   -120.0000  120.0000 -120.0000  120.0000  -15.0000  230.0000
    2rpp   -115.2398  115.2398 -115.2398  115.2398    0.0000    5.0800
    3rpp   -110.1598  110.1598 -110.1598  110.1598    5.0800   10.1600
    4rpp    -99.9998  -89.8398  -99.9998  -89.8398   10.1600   15.2400
    5rpp     89.8398   99.9998  -99.9998  -89.8398   10.1600   15.2400
    6rpp     89.8398   99.9998   89.8398   99.9998   10.1600   15.2400
    7rpp    -99.9998  -89.8398   89.8398   99.9998   10.1600   15.2400
    8rpp   -105.0798  105.0798 -105.0798  105.0798   10.1600  215.2396
    9rpp    -94.9198   94.9198  -94.9198   94.9198   10.1600  205.0796
   10rpp    -79.6798  -69.5198 -112.0598 -110.1598    5.0800   15.2400
   11rpp     69.5198   79.6798 -112.0598 -110.1598    5.0800   15.2400
   12rpp    110.1598  112.0598  -79.6798  -69.5298    5.0800   15.2400
   13rpp    110.1598  112.0598   69.5298   79.6798    5.0800   15.2400
   14rpp     69.5198   79.6798  110.1598  112.0598    5.0800   15.2400
   15rpp    -79.6798  -69.5198  110.1598  112.0598    5.0800   15.2400
   16rpp   -112.0598 -110.1598   69.5198   79.6798    5.0800   15.2400
   17rpp   -112.0598 -110.1598  -79.6798  -69.5198    5.0800   15.2400
   18rpp    -99.9998  -89.8398 -117.1398 -115.2398    0.0000   15.2400
   19rpp     89.8398   99.9998 -117.1398 -115.2398    0.0000   15.2400
   20rpp     89.8398   99.9998  115.2398  117.1398    0.0000   15.2400
   21rpp    -99.9998  -89.8398  115.2398  117.1398    0.0000   15.2400
   22rcc    -94.9198 -117.1398   10.1600    0.0000    1.9000    0.0000
             2.5400
   23rcc     94.9198 -117.1398   10.1600    0.0000    1.9000    0.0000
             2.5400
   24rcc     94.9198  115.2398   10.1600    0.0000    1.9000    0.0000
             2.5400
   25rcc    -94.9198  115.2398   10.1600    0.0000    1.9000    0.0000
             2.5400
   26rcc      0.0000    0.0000  210.1596    0.0000    0.0000    5.0800
            25.4000
   27rcc     99.9998    0.0000  110.1598    5.0800    0.0000    0.0000
            25.4000
   28rcc     99.9998  -49.1998   10.1600   10.1600    0.0000    0.0000
             5.0800
   29rpp   -110.1598  110.1598 -110.1598 -105.0798   10.1600  215.2396
   30rpp    105.0798  110.1598 -105.0798  105.0798   10.1600  215.2396
   31rpp   -110.1598  110.1598  105.0798  110.1598   10.1600  215.2396
   32rpp   -110.1598 -105.0798 -105.0798  105.0798   10.1600  215.2396
   33rpp   -110.1598  110.1598 -110.1598  110.1598  215.2396  220.3196
   34rcc      0.0000    0.0000  215.2396    0.0000    0.0000    5.0800
            37.4650
   35rcc    105.0798    0.0000  110.1598    5.0800    0.0000    0.0000
            37.4650
```

Figure C-2. Sample Geometry Input for the MASH Analysis of the Empty Lined (5% Borated Polyethylene) Two-Meter Box Used in the APRF Spring 1991 Two-Meter Box Test Bed Experiments.

```
36rpp     -5.0800    5.0800 -112.0598 -110.1598  205.1596  228.0196
37rpp    110.1598  112.0598   -5.0800    5.0800  205.1596  228.0196
38rpp     -5.0800    5.0800  110.1598  112.0598  205.1596  228.0196
39rpp   -112.0598 -110.1598   -5.0800    5.0800  205.1596  228.0196
40rcc      0.0000 -112.0598  222.9396    0.0000    1.9000    0.0000
           2.5400
41rcc    110.1598    0.0000  222.9396    1.9000    0.0000    0.0000
           2.5400
42rcc      0.0000  110.1598  222.9396    0.0000    1.9000    0.0000
           2.5400
43rcc   -112.0598    0.0000  222.9396    1.9000    0.0000    0.0000
           2.5400
44rcc    -85.0000 -110.1598   11.4300    0.0000   10.1600    0.0000
           1.2700
45rcc     85.0000 -110.1598   11.4300    0.0000   10.1600    0.0000
           1.2700
46rcc     85.0000   99.9998   11.4300    0.0000   10.1600    0.0000
           1.2700
47rcc    -85.0000   99.9998   11.4300    0.0000   10.1600    0.0000
           1.2700
48rpp   -120.0000  120.0000 -120.0000  120.0000  -15.0000    0.0000
49rpp     -125.0   125.0000   -125.0   125.0000   -16.00   235.0000
50rpp    -99.9998   99.9998  -99.9998   99.9998   10.1600  210.1596
 1        1     -2     -3     -8    -10    -11    -12    -13    -14    z1001
        -15    -16    -17    -18    -19    -20    -21    -22    -23    air
        -24    -25    -28    -29    -30    -31    -32    -33    -34
        -35    -36    -37    -38    -39    -40    -41    -42    -43
        -44    -45    -46    -47    -48
 2        2     -3    -10    -11    -12    -13    -14    -15    -16    z1002
        -17    -18    -19    -20    -21                              base
 3        3     -4     -5     -6     -7     -8     -9    -10    -11    z1003
        -12    -13    -14    -15    -16    -17    -29    -30    -31    base
        -32
 4 or    4or    5or    6or    7                                       z1004
 5        8    -50    -26    -27    -28    -44    -45    -46    -47    z1005
 6        9     -4     -5     -6     -7                               z1006
 7 or   10or   11or   12or   13or   14or   15or   16or   17          z1007
 8 or   18    -22or   19    -23or   20    -24or   21    -25          z1008
 9 or   22or   23or   24or   25                                       z1009
10      26                                                            z1010
11      27                                                            z1011
12      28     -3                                                     z1012
13      29     -8    -30    -32    -33    -36    -44    -45           z1013
14      30     -8    -33    -35    -37    -28                         z1014
15      31     -8    -30    -32    -33    -38    -46    -47           z1015
16      32     -8    -33    -39                                       z1016
```

Figure C-2. (cont.)

```
17        33      -8     -34     -36     -37     -38     -39                     z1017
18 or     36     -40or    37     -41or    38     -42or    39     -43             z1018
19 or     40or    41or   42or     43                                             z1019
20 or     44or    45or   46or     47                                             z1020
21        34     -26                                                             z1021
22        35     -27                                                             z1022
23        48      -2                                                             z1023
24        49      -1                                                             z1024
25        50      -4      -5      -6      -7     -26     -27     -28     -44     z1025
         -45     -46     -47      -9                                             air
-1
 1 1001    0    2    0    /box/z1001/surounding/air
 2 1002    0    3    0    /box/z1002/bottom/base/pad
 3 1003    0    3    0    /box/z1003/upper/base/pad
 4 1004    0    3    0    /box/z1004/inner/alignment/pad
 5 1005    0    3    0    /box/z1005/inner/box
 6 1006    0    2    0    /box/z1006/inner/box/air-void
 7 1007    0    3    0    /box/z1007/outer/wall/alignment/pad
 8 1008    0    3    0    /box/z1008/base/pad/lift/eyelets
 9 1009    0    2    0    /box/z1009/eyelets/voids-air
10 1010    0    3    0    /box/z1010/inner/box/top/hatch
11 1011    0    3    0    /box/z1011/inner/box/side/hatch
12 1012    0    2    0    /box/z1012/inner/outer/cable/run/void-air
13 1013    0    3    0    /box/z1013/outer/wall/negative/y-axis
14 1014    0    3    0    /box/z1014/outer/wall/positive/x-axis
15 1015    0    3    0    /box/z1015/outer/wall/positive/y-axis
16 1016    0    3    0    /box/z1016/outer/wall/negative/x-axis
17 1017    0    3    0    /box/z1017/outer/top
18 1018    0    3    0    /box/z1018/outer/wall/lift/eyelets
19 1019    0    2    0    /box/z1019/outer/wall/lift/eyelets/void-air
20 1020    0    2    0    /box/z1020/inner/outer/drain/holes
21 1021    0    3    0    /box/z1021/outer/top/hatch
22 1022    0    3    0    /box/z1022/outer/wall/side/hatch
23 1023    0    1    0    /box/z1023/ground
24 1024    0    0    0    /box/z1024/external/void
25 1025    0    9    0    /box/z1025/2-inch/borated poly
```

Figure C-2. (cont.)

```
aprf aog/400m/16.14m ss91-121-37 s90e5 5/91 exp. ph+det  LAV(i)
 $$ 1000 1500  200    1   46   23   46   69    0    1  650    9    0
 $$   0   69    1    0
 ** 1.0   1.0-05   1.0+04   0.0   2.2+05
 ** -2.9719   -20.2738   95.3   0.0   0.0   0.0   0.0
 ** 69r1.0
 ** 8r1.0 13r2.0 10r3.0 5r2.0 10r1.0 4r3.0 15r5.0 4r3.0
 ** 1.9640+7  1.6905+7  1.4918+7  1.4191+7  1.3840+7  1.2523+7  1.2214+7
    1.1052+7  1.0000+7  9.0484+6  8.1873+6  7.4082+6  6.3763+6  4.9658+6
    4.7237+6  4.0657+6  3.0119+6  2.3852+6  2.3069+6  1.8268+6  1.4227+6
    1.1080+6  9.6164+5  8.2085+5  7.4274+5  6.3927+5  5.5023+5  3.6883+5
    2.4724+5  1.5764+5  1.1109+5  5.2475+4  3.4307+4  2.4788+4  2.1875+4
    1.0595+4  3.3546+3  1.2341+3  5.8295+2  2.7536+2  1.0130+2  2.9023+1
    1.0677+1  3.0590+0  1.12535+0 4.1399-1  2.0000+7  1.4000+7  1.2000+7
    1.0000+7  8.0000+6  7.0000+6  6.0000+6  5.0000+6  4.0000+6  3.0000+6
    2.5000+6  2.0000+6  1.5000+6  1.0.00+6  7.0000+5  4.5500+5  3.0000+5
    1.5000+5  1.0000+5  7.0000+4  4.5000+4  3.0000+4  2.0000+4
    0000444244555555
 $$   1    1    0    0    0    8   69    1
 $$   1    1   46    1    1    1  **   5.0+00   5.0-02   5.0-01   0.0
 $$   1    1   46    2    1    2  **   5.0+00   5.0-02   5.0-01   0.0
 $$   1    1   46    3    1    3  **   5.0+00   5.0-02   5.0-01   0.0
 $$   1    1   46    4    1    4  **   4.0+00   4.0-02   4.0-01   0.0
 $$   1    1   46    5    1    5  **   3.0+00   3.0-02   3.0-01   0.0
 $$   1    1   46    6    1    6  **   2.0+00   2.0-02   2.0-01   0.0
 $$   1    1   46    7    1    7  **   3.0+00   3.0-02   3.0-01   0.0
 $$   1    1   46    8    1    8  **   3.0+00   3.0-02   3.0-01   0.0
 $$   47    1   69    1    1    1  **   5.0+00   5.0-02   5.0-01   0.0
 $$   47    1   69    2    1    2  **   5.0+00   5.0-02   5.0-01   0.0
 $$   47    1   69    3    1    3  **   5.0+00   5.0-02   5.0-01   0.0
 $$   47    1   69    4    1    4  **   4.0+00   4.0-02   4.0-01   0.0
 $$   47    1   69    5    1    5  **   3.0+00   3.0-02   3.0-01   0.0
 $$   47    1   69    6    1    6  **   2.0+00   2.0-02   2.0-01   0.0
 $$   47    1   69    7    1    7  **   3.0+00   3.0-02   3.0-01   0.0
 $$   47    1   69    8    1    8  **   3.0+00   3.0-02   3.0-01   0.0
 $$  -1   9r0
 $$   0    0    0    0
 ** 23r1.0
 ** 23r1.0
 ** 23r1.0
 ** 23r1.0
 ** 23r1.0
 ** 23r1.0
 ** 23r1.0
 ** 23r1.0
```

Figure C-3. Sample MORSE Input for the MASH Analysis of the Combinatorial Geometry Phantom (with BD-100R Detectors) Used in the APRF Spring 1991 Two-Meter Box Test Bed Experiments.

```
0000000000      0.001     0.0001     0     0     0
    1     1
   15
    2     1
   14
    4     2
    5     6
    5     7
    1     2     3     4    16    17    18
    6     7
    7     8     9    10    11    12    13
    7    19
   20    21    22    23    24    25    26    27    28    29    30    31    32    34
   35    36    37    38    39
    8     1
   19
    0     1
   33
    1     1     1     1     1     1     1     1     1     1     1     1     1     1
    1     1     1     1     1     1     1     1     1     1     1     1     1     1
    1     1     1     1     1     1     1     1     1     1     1
2m box exp/aprf 5/91 exp. ss91-121-37 s90e5, 1020 steel + phantom n.d.
 $$  46    46    23    23    69    72     4     9    24    67     6     3     0     3
 $$  7z    -2    3z
2m ph+det  LAV(i)
 **   8r1.0
 $$   1     2
```

Figure C-3. (cont.)

```
cm   70kg-91-phantom with arms and detectors
   97   39
    1ell        .0000      .0000  177.1500    10.000      .0000      .0000
    1          7.5650
    2rec        .0000      .0000  164.3000     .0000      .0000    12.8500
    2         10.0000      .0000     .0000     .0000    -8.0000      .0000
    3rec        .0000      .0000   90.3000     .0000      .0000    70.0000
    3           .0000    19.2000     .0000   -10.0000      .0000      .0000
    4tec        .0000     4.6000   10.3000     .0000     5.0000    80.0000
    4           .0000     4.0000     .0000    -4.0000      .0000      .0000
    4          2.0000
    5tec        .0000    -4.6000   10.3000     .0000    -5.0000    80.0000
    5           .0000     4.0000     .0000    -4.0000      .0000      .0000
    5          2.0000
    6rcc        .0000      .0000  160.3000     .0000      .0000     4.0000
    6          7.0000
    7arb     -10.0000   -10.0000   90.3000    -9.5200    -9.5200    85.5000
    7         -9.5200     9.5200   85.5000   -10.0000    10.0000    90.3000
    7           .0000     9.5200   85.5000     .0000    10.0000    90.3000
    7           .0000   -10.0000   90.3000     .0000    -9.5200    85.5000
    7      1234 4356 6587 7821 7146 2358
    8rpp     -50.0000    50.0000  -50.0000    50.0000   -15.0000   230.0000
    9rpp     -50.0000    50.0000  -50.0000    50.0000   -15.0000     0.0000
   10ell        .0000     8.5000  133.8000     .0000      .0000    24.0000
   10          6.1070
   11rpp      -6.1237     1.5000     .0000     5.4000   136.3000   144.3000
   12rec        .0000      .0000   91.3000     .0000      .0000    42.5000
   12           .0000    16.4900     .0000    -9.2900      .0000      .0000
   13ell        .0000    -8.5000  133.8000     .0000      .0000    24.0000
   13          6.1070
   14rpp      -6.1237     1.0000    -8.0000     .0000   133.8000   145.3000
   15ell        .0000      .0000  177.1500     9.5000      .0000      .0000
   15          7.0660
   16ell       0.0000      .0000  177.1500     6.0000      .0000      .0000
   16          6.1610
   17rec       5.5000      .0000  112.3000     .0000      .0000    48.0000
   17         -2.5000      .0000     .0000     .0000     2.0000      .0000
   18tec        .0000    21.5338   90.3000     .0000     -.7000    69.0000
   18           .0000     2.0000     .0000    -1.0370      .0000      .0000
   18          1.3500
   19tec        .0000   -21.5338   90.3000     .0000      .7000    69.0000
   19           .0000     2.0000     .0000    -1.0370      .0000      .0000
   19          1.3500
   20tec        .0000     4.6000   10.5000     .0000     5.0000    79.8000
   20           .0000     2.2727     .0000    -2.2727      .0000      .0000
   20          1.1000
```

Figure C-4. Sample Geometry Input for the MASH Analysis of the Combinatorial Geometry Phantom (with BD-100R Detectors) Used in the APRF Spring 1991 Two-Meter Box Test Bed Experiments.

21tec	.0000	-4.6000	10.5000	.0000	-5.0000	79.8000
21	.0000	2.2727	.0000	-2.2727	.0000	.0000
21	1.1000					
22rec	-3.0000	.0000	90.3000	.0000	.0000	22.0000
22	.0000	12.0000	.0000	-12.0000	.0000	.0000
23rec	-3.8000	.0000	90.3000	.0000	.0000	22.0000
23	.0000	11.3000	.0000	-11.3000	.0000	.0000
24rpp	-15.5000	-3.0000	-12.0000	12.0000	90.3000	112.3000
25rpp	5.0000	10.0000	-10.0000	10.0000	90.3000	104.3000
26rec	.0000	.0000	125.4000	.0000	.0000	32.2000
26	.0000	17.0000	.0000	-9.8000	.0000	.0000
27rec	.0000	.0000	125.4000	.0000	.0000	32.2000
27	.0000	16.5000	.0000	-9.3000	.0000	.0000
28rec	.0000	.0000	126.8000	.0000	.0000	1.4000
28	.0000	17.0000	.0000	-9.8000	.0000	.0000
29rec	.0000	.0000	129.6000	.0000	.0000	1.4000
29	.0000	17.0000	.0000	-9.8000	.0000	.0000
30rec	.0000	.0000	132.4000	.0000	.0000	1.4000
30	.0000	17.0000	.0000	-9.8000	.0000	.0000
31rec	.0000	.0000	135.2000	.0000	.0000	1.4000
31	.0000	17.0000	.0000	-9.8000	.0000	.0000
32rec	.0000	.0000	138.0000	.0000	.0000	1.4000
32	.0000	17.0000	.0000	-9.8000	.0000	.0000
33rec	.0000	.0000	140.8000	.0000	.0000	1.4000
33	.0000	17.0000	.0000	-9.8000	.0000	.0000
34rec	.0000	.0000	143.6000	.0000	.0000	1.4000
34	.0000	17.0000	.0000	-9.8000	.0000	.0000
35rec	.0000	.0000	146.4000	.0000	.0000	1.4000
35	.0000	17.0000	.0000	-9.8000	.0000	.0000
36rec	.0000	.0000	149.2000	.0000	.0000	1.4000
36	.0000	17.0000	.0000	-9.8000	.0000	.0000
37rec	.0000	.0000	152.0000	.0000	.0000	1.4000
37	.0000	17.0000	.0000	-9.8000	.0000	.0000
38rec	.0000	.0000	154.8000	.0000	.0000	1.4000
38	.0000	17.0000	.0000	-9.8000	.0000	.0000
39rec	.0000	.0000	160.3000	.0000	.0000	9.2700
39	-2.5000	.0000	.0000	.0000	2.0000	.0000
40rcc	11.1000	.0000	157.8514	.0000	.0000	1.3972
40	20.6986					
41rcc	11.1000	.0000	157.8514	.0000	.0000	1.3972
41	19.3014					
42raw	-15.7245	-30.0000	157.8514	26.8245	30.0000	.0000
42	-25.2690	22.5943	.0000	.0000	.0000	1.3972
43raw	-15.7245	30.0000	157.8514	26.8245	-30.0000	.0000
43	-25.2690	-22.5943	.0000	.0000	.0000	1.3972
44rec	.0000	.0000	141.2000	.0000	.0000	16.4000
44	.0000	19.0000	.0000	-9.8000	.0000	.0000

Figure C-4. (cont.)

45rec	.0000	.0000	141.2000	.0000	.0000	16.4000
45	.0000	17.0000	.0000	-9.8000	.0000	.0000
46sph	.0000	.0000	90.3000	1.0000		
47raw	7.5000	-30.0000	141.2000	-7.5000	30.0000	.0000
47	13.7500	3.4375	.0000	.0000	.0000	16.4000
48sph	.0000	.0000	90.3000	1.0000		
49raw	7.5000	30.0000	141.2000	-7.5000	-30.0000	.0000
49	13.7500	-3.4375	.0000	.0000	.0000	16.4000
50rec	.0000	.0000	164.3000	.0000	.0000	10.7300
50	9.0000	.0000	.0000	.0000	-7.0000	.0000
51rec	.0000	.0000	164.3000	.0000	.0000	10.7300
51	7.6000	.0000	.0000	.0000	-5.6000	.0000
52rpp	-15.0000	.0000	-15.0000	15.0000	164.3000	175.0300
53sph	.0000	10.0000	142.3000	0.3600		
54sph	.0000	-10.0000	142.3000	0.3600		
55rec	.0000	.0000	90.3000	.0000	.0000	70.0000
55	.0000	17.2000	.0000	-10.0000	.0000	.0000
56rpp	.0000	15.0000	-17.2000	17.2000	90.3000	160.3000
57trc	.0000	21.5338	160.3000	.0000	.0000	-70.0000
57	4.3238	2.1619				
58trc	.0000	-21.5338	160.3000	.0000	.0000	-70.0000
58	4.3238	2.1619				
59rcc	-4.0	0.0	177.1500	8.0	0.0	0.0
59	0.8					
60rcc	-3.9843	0.0	177.1500	7.9746	0.0	0.0
60	0.7873					
61rcc	-10.82	-5.88	145.06	0.0	0.0	8.0
61	0.8					
62rcc	-10.82	-5.88	145.0727	0.0	0.0	7.9746
62	0.7873					
63rcc	-10.82	-7.49	145.06	0.0	0.0	8.0
63	0.8					
64rcc	-10.82	-7.49	145.0727	0.0	0.0	7.9746
64	0.7873					
65rcc	-10.82	-9.10	145.06	0.0	0.0	8.0
65	0.8					
66rcc	-10.82	-9.10	145.0727	0.0	0.0	7.9746
66	0.7873					
67rcc	-10.82	1.61	112.04	0.0	0.0	8.0
67	0.8					
68rcc	-10.82	1.61	112.0527	0.0	0.0	7.9746
68	0.7873					
69rcc	-10.82	0.0	112.04	0.0	0.0	8.0
69	0.8					
70rcc	-10.82	0.0	112.0527	0.0	0.0	7.9746
70	0.7873					

Figure C-4. (cont.)

```
71rcc      -10.82     -1.61    112.04       0.0       0.0       8.0
71           0.8
72rcc      -10.82     -1.61  112.0527       0.0       0.0    7.9746
72         0.7873
73rcc       10.82      1.61    112.04       0.0       0.0       8.0
73           0.8
74rcc       10.82      1.61  112.0527       0.0       0.0    7.9746
74         0.7873
75rcc       10.82       0.0    112.04       0.0       0.0       8.0
75           0.8
76rcc       10.82       0.0  112.0527       0.0       0.0    7.9746
76         0.7873
77rcc       10.82     -1.61    112.04       0.0       0.0       8.0
77           0.8
78rcc       10.82     -1.61  112.0527       0.0       0.0    7.9746
78         0.7873
79rcc        -4.0       0.0    116.04       8.0       0.0       0.0
79           0.8
80rcc     -3.9873       0.0    116.04    7.9746       0.0       0.0
80         0.7873
81rcc     -2.9719   22.3438      91.3       0.0       0.0       8.0
81           0.8
82rcc     -2.9719   22.3438   91.3127       0.0       0.0    7.9746
82         0.7873
83rcc     -2.9719   20.7238      91.3       0.0       0.0       8.0
83           0.8
84rcc     -2.9719   20.7238   91.3127       0.0       0.0    7.9746
84         0.7873
85rpp    -60.0000   60.0000  -60.0000   60.0000  -16.5000  235.0000
86rcc        0.81  -24.5057      91.3       0.0       0.0       8.0
86           0.8
87rcc        0.81  -24.5057   91.3127       0.0       0.0    7.9746
87         0.7873
88rcc       -0.81  -24.5057      91.3       0.0       0.0       8.0
88           0.8
89rcc       -0.81  -24.5057   91.3127       0.0       0.0    7.9746
89         0.7873
90rcc        0.81   24.5057      91.3       0.0       0.0       8.0
90           0.8
91rcc        0.81   24.5057   91.3127       0.0       0.0    7.9746
91         0.7873
92rcc       -0.81   24.5057      91.3       0.0       0.0       8.0
92           0.8
93rcc       -0.81   24.5057   91.3127       0.0       0.0    7.9746
93         0.7873
94rcc     -2.9719  -20.7238      91.3       0.0       0.0       8.0
94           0.8
```

Figure C-4. (cont.)

```
95rcc      -2.9719  -20.7238   91.3127       0.0       0.0    7.9746
95          0.7873
96rcc      -2.9719  -22.3438      91.3       0.0       0.0       8.0
96             0.8
97rcc      -2.9719  -22.3438   91.3127       0.0       0.0    7.9746
97          0.7873
 1 or    1    -15    -39    -50    -59    -60
   or    2    -15    -39    -50    -59    -60
   or   16    -59    -60
   or    2    -15    -39    -52    -59    -60
   or    2    -15    -39     51    -59    -60
   or    6    -39
 2 or    3    -10    -13    -17    -18    -19    -22    -26    -40
       -44    -80     56    -79    -80    -53    -54
   or   55    -10    -13    -17    -18    -19    -22    -26    -40
       -44    -79    -80
   or   11    -17    -13
   or   14    -17    -10
   or   12    -22    -17    -79    -80
   or   23      3     56    -79    -80
   or   24     55    -79    -80
   or   25      3     56    -79    -80
   or   23     55
   or   27    -10    -13    -17or   28    -10    -13    -17
   or   29    -10    -13    -17or   30    -10    -13    -17
   or   31    -10    -13    -17or   32    -10    -13    -17
   or   33    -10    -13    -17or   34    -10    -13    -17
   or   35    -10    -13    -17or   36    -10    -13    -17
   or   37    -10    -13    -17or   38    -10    -13    -17
   or   41    -10    -13    -17    -18    -19      3     56
   or   41    -10    -13    -17    -18    -19     55
   or   40    -42    -43    -41    -18    -19      3     56
   or   40    -42    -43    -41    -18    -19     55
   or   44    -47    -49    -26     55
   or   44    -47    -49    -26     56
 3 or    4    -20or    5    -21
 4       7     -4     -5    -20    -21
 5      10    -11    -12
 6      13    -14    -12
 7 or   15    -16    -59or   17    -79or   39    -79
 8 or   18or   19
 9 or   20or   21
10      22    -23    -24    -25    -17
11      26    -27    -28    -29    -30    -31    -32    -33    -34
       -35    -36    -37    -38
12 or   40    -41     42    -20    -21
   or   40    -41     43    -20    -21
```

Figure C-4. (cont.)

```
13 or   44    -26     47or   44    -26     49
14 or    8     -1      -2     -3     -4     -5     -7    -53    -54
         -6    -57     -58    -61    -63    -65    -67    -69    -71
        -73    -75     -77    -79    -83    -86    -88     -9    -81
        -90    -92     -94    -96
   or    8     -1      -2    -55     -4     -5     -7    -53    -54
         -6    -57     -58    -56     -9    -61    -63    -65    -67
        -69    -71     -73    -75    -77    -79    -83    -86    -88
        -81    -90     -92    -94    -96
15       9
16      50     52     -51    -15
17 or   54    -55or    53    -55
18 or   57    -18     -81    -83    -90    -92or   58    -19    -86
        -88    -94     -96
19 or   59    -60or    61    -62or   63    -64or   65    -66
   or   67    -68or    69    -70or   71    -72or   73    -74
   or   75    -76or    77    -78or   79    -80or   81    -82
   or   83    -84or    86    -87or   88    -89or   90    -91
   or   92    -93or    94    -95or   96    -97
20      60
21      62
22      64
23      66
24      68
25      70
26      72
27      74
28      76
29      78
30      80
31      82
32      84
33      85     -8
34      87
35      89
36      91
37      93
38      95
39      97
-1
 1    1    0    5   100    /phantom/z1001/flesh/head-neck
 2    1    0    5   100    /phantom/1002/flesh/torso
 3    2    0    5    90    /phantom/1003/flesh/legs
 4    2    0    5    90    /phantom/z1004/sex/organ
 5    2    0    4    90    /phantom/z1005/internal/left/lung
 6    2    0    4    90    /phantom/z1006/internal/right/lung
 7    2    0    6    90    /phantom/z1007/skeletal/skull/neck/spinal
```

Figure C-4. (cont.)

8	2	0	6	90	/phantom/z1008/skeletal/arms
9	2	0	6	90	/phantom/z1009/skeletal/legs
10	2	0	6	90	/phantom/z1010/skeletal/hip
11	2	0	6	90	/phantom/z1011/skeletal/ribs
12	3	0	6	80	/phantom/z1012/skeletal/pelvis
13	13	0	6	80	/phantom/z1013/skeletal/shoulder/blades
14	3	0	2	100	/phantom/z1014/surrounding/air
15	3	0	1	100	/phantom/z1015/15-cm/ground
16	13	0	5	80	/phantom/z1016/flesh/throat
17	3	0	5	80	/phantom/z1017/flesh/breasts
18	3	0	5	80	/phantom/z1018/flesh/arms
19	1106	0	8	100	/detectors/z1019/containers
20	1107	0	7	100	/detector/z1020/mid-head
21	1109	0	7	100	/detector/z1021/left-chest 1
22	1111	0	7	100	/detector/z1022/left-chest 2
23	1113	0	7	100	/detector/z1023/left-chest 3
24	1115	0	7	100	/detector/z1024/front/mid-gut 1
25	1117	0	7	100	/detector/z1025/fornt/mid-gut 2
26	1119	0	7	100	/detector/z1026/front/mid-gut 3
27	1121	0	7	100	/detector/z1027/rear/mid-gut 1
28	1123	0	7	100	/detector/z1028/rear/mid-gut 2
29	1125	0	7	100	/detector/z1029/rear/mid-gut 3
30	1127	0	7	100	/detector/z1030/inner/mid-gut
31	1129	0	7	100	/detector/z1031/rt. arm/outer
32	1131	0	7	100	/detector/z1032/rt. arm/inner
33	0	0	0	0	/external void
34	1133	0	7	100	/detector/z1034/left/arm/rear
35	1135	0	7	100	/detector/z1035/left/arm/front
36	1160	0	7	100	/detector/z1036/right/arm/rear
37	1160	0	7	100	/detector/z1037/right/arm/front
38	1160	0	7	100	/detector/z1038/left/arm/inner
39	1160	0	7	100	/detector/z1039/left/arm/outer

Figure C-4. (cont.)

```
aprf aog/400m/16.14m ss91-121-37 s90e5 5/91 exp. box+ph+det+lin  DOS(m)
 $$ 1000 1500  750    1   46   23   46   69    0    1  650    9    0
 $$   0   69    1    0
 ** 1.0   1.0-05   1.0+04   0.0   2.2+05
 ** -23.00   -59.9998   87.46   0.0   0.0   0.0   0.0
 ** 69r1.0
 ** 8r1.0 13r2.0 10r3.0 5r2.0 10r1.0 4r3.0 15r5.0 4r3.0
 ** 1.9640+7  1.6905+7  1.4918+7  1.4191+7  1.3840+7  1.2523+7  1.2214+7
    1.1052+7  1.0000+7  9.0484+6  8.1873+6  7.4082+6  6.3763+6  4.9658+6
    4.7237+6  4.0657+6  3.0119+6  2.3852+6  2.3069+6  1.8268+6  1.4227+6
    1.1080+6  9.6164+5  8.2085+5  7.4274+5  6.3927+5  5.5023+5  3.6883+5
    2.4724+5  1.5764+5  1.1109+5  5.2475+4  3.4307+4  2.4788+4  2.1875+4
    1.0595+4  3.3546+3  1.2341+3  5.8295+2  2.7536+2  1.0130+2  2.9023+1
    1.0677+1  3.0590+0  1.12535+0 4.1399-1  2.0000+7  1.4000+7  1.2000+7
    1.0000+7  8.0000+6  7.0000+6  6.0000+6  5.0000+6  4.0000+6  3.0000+6
    2.5000+6  2.0000+6  1.5000+6  1.0.00+6  7.0000+5  4.5500+5  3.0000+5
    1.5000+5  1.0000+5  7.0000+4  4.5000+4  3.0000+4  2.0000+4
    0000444255555656
 $$   1    1    0    0    0    8   69    1
 $$   1    1   46    1    1    1  **   5.0+00   5.0-02   5.0-01   0.0
 $$   1    1   46    2    1    2  **   5.0+00   5.0-02   5.0-01   0.0
 $$   1    1   46    3    1    3  **   5.0+00   5.0-02   5.0-01   0.0
 $$   1    1   46    4    1    4  **   4.0+00   4.0-02   4.0-01   0.0
 $$   1    1   46    5    1    5  **   3.0+00   3.0-02   3.0-01   0.0
 $$   1    1   46    6    1    6  **   2.0+00   2.0-02   2.0-01   0.0
 $$   1    1   46    7    1    7  **   3.0+00   3.0-02   3.0-01   0.0
 $$   1    1   46    8    1    8  **   3.0+00   3.0-02   3.0-01   0.0
 $$   47    1   69    1    1    1  **   5.0+00   5.0-02   5.0-01   0.0
 $$   47    1   69    2    1    2  **   5.0+00   5.0-02   5.0-01   0.0
 $$   47    1   69    3    1    3  **   5.0+00   5.0-02   5.0-01   0.0
 $$   47    1   69    4    1    4  **   4.0+00   4.0-02   4.0-01   0.0
 $$   47    1   69    5    1    5  **   3.0+00   3.0-02   3.0-01   0.0
 $$   47    1   69    6    1    6  **   2.0+00   2.0-02   2.0-01   0.0
 $$   47    1   69    7    1    7  **   3.0+00   3.0-02   3.0-01   0.0
 $$   47    1   69    8    1    8  **   3.0+00   3.0-02   3.0-01   0.0
 $$  -1   9r0
 $$   0    0    0    0
 ** 23r1.0
 ** 23r1.0
 ** 23r1.0
 ** 23r1.0
 ** 23r1.0
 ** 23r1.0
 ** 23r1.0
 ** 23r1.0
```

Figure C-5. Sample MORSE Input for the MASH Analysis of the Combinatorial Geometry Phantom (with BD-100R Detectors) Standing in the Lined(5% Borated Polyethylene) Two-Meter Box Used in the APRF Spring 1991 Two-Meter Box Test Bed Experiments.

```
0000000000      0.001     0.0001     0     0     0
    1    1
   23
    2    6
    1    6    9   12   19   20
    3   16
    2    3    4    5    7    8   10   11   13   14   15   16   17   18
   21   22
    4    2
   29   30
    5    7
   25   26   27   28   38   39   40
    6    7
   31   32   33   34   35   36   37
    7   22
   42   43   44   45   46   47   48   49   50   51   52   53   54   55
   56   58   59   60   61   62   63   64
    8    1
   41
    9    1
   57
    0    1
   24
    8    6    5    5    5    3    6    6    8    5    5    8    6    6
    6    6    6    6    8    8    6    6    7    8    2    2    2    2
    2    2    2    2    2    2    2    2    2    2    2    2    1    1
    1    1    1    1    1    1    1    1    1    1    1    1    1    1
    4    1    1    1    1    1    1    1
2m box exp/aprf 5/91 exp. ss91-121-37 s90e5, 1020 steel + phantom n.d.
 $$  46   46   23   23   69   72    4    9   24   67    6    3    0    3
 $$  7z   -2   3z
2m box+ph+det+lin  DOS(m)
 **   8rl.0
 $$   1    2
```

Figure C-5. (cont.)

```
cm   2.0 m box geom. (4 in. of steel) with phanton, detectors and liner
  150   64
    1rpp   -120.0000  120.0000 -120.0000  120.0000  -15.0000  230.0000
    2rpp   -115.2398  115.2398 -115.2398  115.2398    0.0000    5.0800
    3rpp   -110.1598  110.1598 -110.1598  110.1598    5.0800   10.1600
    4rpp    -99.9998  -89.8398  -99.9998  -89.8398   10.1600   15.2400
    5rpp     89.8398   99.9998  -99.9998  -89.8398   10.1600   15.2400
    6rpp     89.8398   99.9998   89.8398   99.9998   10.1600   15.2400
    7rpp    -99.9998  -89.8398   89.8398   99.9998   10.1600   15.2400
    8rpp   -105.0798  105.0798 -105.0798  105.0798   10.1600  215.2396
    9rpp    -94.9198   94.9198  -94.9198   94.9198   10.1600  205.0796
   10rpp    -79.6798  -69.5198 -112.0598 -110.1598    5.0800   15.2400
   11rpp     69.5198   79.6798 -112.0598 -110.1598    5.0800   15.2400
   12rpp    110.1598  112.0598  -79.6798  -69.5298    5.0800   15.2400
   13rpp    110.1598  112.0598   69.5298   79.6798    5.0800   15.2400
   14rpp     69.5198   79.6798  110.1598  112.0598    5.0800   15.2400
   15rpp    -79.6798  -69.5198  110.1598  112.0598    5.0800   15.2400
   16rpp   -112.0598 -110.1598   69.5198   79.6798    5.0800   15.2400
   17rpp   -112.0598 -110.1598  -79.6798  -69.5198    5.0800   15.2400
   18rpp    -99.9998  -89.8398 -117.1398 -115.2398    0.0000   15.2400
   19rpp     89.8398   99.9998 -117.1398 -115.2398    0.0000   15.2400
   20rpp     89.8398   99.9998  115.2398  117.1398    0.0000   15.2400
   21rpp    -99.9998  -89.8398  115.2398  117.1398    0.0000   15.2400
   22rcc    -94.9198 -117.1398   10.1600    0.0000    1.9000    0.0000
             2.5400
   23rcc     94.9198 -117.1398   10.1600    0.0000    1.9000    0.0000
             2.5400
   24rcc     94.9198  115.2398   10.1600    0.0000    1.9000    0.0000
             2.5400
   25rcc    -94.9198  115.2398   10.1600    0.0000    1.9000    0.0000
             2.5400
   26rcc      0.0000    0.0000  210.1596    0.0000    0.0000    5.0800
            25.4000
   27rcc     99.9998    0.0000  110.1598    5.0800    0.0000    0.0000
            25.4000
   28rcc     99.9998  -49.1998   10.1600   10.1600    0.0000    0.0000
             5.0800
   29rpp   -110.1598  110.1598 -110.1598 -105.0798   10.1600  215.2396
   30rpp    105.0798  110.1598 -105.0798  105.0798   10.1600  215.2396
   31rpp   -110.1598  110.1598  105.0798  110.1598   10.1600  215.2396
   32rpp   -110.1598 -105.0798 -105.0798  105.0798   10.1600  215.2396
   33rpp   -110.1598  110.1598 -110.1598  110.1598  215.2396  220.3196
   34rcc      0.0000    0.0000  215.2396    0.0000    0.0000    5.0800
            37.4650
   35rcc    105.0798    0.0000  110.1598    5.0800    0.0000    0.0000
            37.4650
```

Figure C-6. Sample Geometry Input for the MASH Analysis of the Combinatorial Geometry Phantom (with BD-100R Detectors) Standing in the Lined (5% Borated Polyethylene) Two-Meter Box Used in the APRF Spring 1991 Two-Meter Box Test Bed Experiments.

```
36rpp      -5.0800     5.0800 -112.0598 -110.1598  205.1596  228.0196
37rpp     110.1598   112.0598   -5.0800    5.0800  205.1596  228.0196
38rpp      -5.0800     5.0800  110.1598  112.0598  205.1596  228.0196
39rpp    -112.0598  -110.1598   -5.0800    5.0800  205.1596  228.0196
40rcc       0.0000  -112.0598  222.9396    0.0000    1.9000    0.0000
           2.5400
41rcc     110.1598     0.0000  222.9396    1.9000    0.0000    0.0000
           2.5400
42rcc       0.0000   110.1598  222.9396    0.0000    1.9000    0.0000
           2.5400
43rcc    -112.0598     0.0000  222.9396    1.9000    0.0000    0.0000
           2.5400
44rcc     -85.0000  -110.1598   11.4300    0.0000   10.1600    0.0000
           1.2700
45rcc      85.0000  -110.1598   11.4300    0.0000   10.1600    0.0000
           1.2700
46rcc      85.0000    99.9998   11.4300    0.0000   10.1600    0.0000
           1.2700
47rcc     -85.0000    99.9998   11.4300    0.0000   10.1600    0.0000
           1.2700
48rpp    -120.0000   120.0000 -120.0000  120.0000  -15.0000    0.0000
49rpp      -125.0    125.0000   -125.0   125.0000   -16.00   235.0000
50ell       .0000      .0000  177.1500    10.000     .0000     .0000
50          7.5650
51rec       .0000      .0000  164.3000     .0000     .0000   12.8500
51         10.0000      .0000     .0000     .0000   -8.0000     .0000
52rec       .0000      .0000   90.3000     .0000     .0000   70.0000
52          .0000    19.2000     .0000  -10.0000     .0000     .0000
53tec       .0000     4.6000   10.3000     .0000    5.0000   80.0000
53          .0000     4.0000     .0000   -4.0000     .0000     .0000
53          2.0000
54tec       .0000    -4.6000   10.3000     .0000   -5.0000   80.0000
54          .0000     4.0000     .0000   -4.0000     .0000     .0000
54          2.0000
55rcc       .0000      .0000  160.3000     .0000     .0000    4.0000
55          7.0000
56arb     -10.0000   -10.0000   90.3000   -9.5200   -9.5200   85.5000
56         -9.5200     9.5200   85.5000  -10.0000   10.0000   90.3000
56          .0000     9.5200   85.5000     .0000   10.0000   90.3000
56          .0000   -10.0000   90.3000     .0000   -9.5200   85.5000
56     1234 4356 6587 7821 7146 2358
57ell       .0000     8.5000  133.8000     .0000     .0000   24.0000
57          6.1070
58rpp      -6.1237     1.5000     .0000    5.4000  136.3000  144.3000
59rec       .0000      .0000   91.3000     .0000     .0000   42.5000
59          .0000    16.4900     .0000   -9.2900     .0000     .0000
```

Figure C-6. (cont.)

60ell	.0000	-8.5000	133.8000	.0000	.0000	24.0000
60	6.1070					
61rpp	-6.1237	1.0000	-8.0000	.0000	133.8000	145.3000
62ell	.0000	.0000	177.1500	9.5000	.0000	.0000
62	7.0660					
63ell	0.0000	.0000	177.1500	6.0000	.0000	.0000
63	6.1610					
64rec	5.5000	.0000	112.3000	.0000	.0000	48.0000
64	-2.5000	.0000	.0000	.0000	2.0000	.0000
65tec	.0000	21.5338	90.3000	.0000	-.7000	69.0000
65	.0000	2.0000	.0000	-1.0370	.0000	.0000
65	1.3500					
66tec	.0000	-21.5338	90.3000	.0000	.7000	69.0000
66	.0000	2.0000	.0000	-1.0370	.0000	.0000
66	1.3500					
67tec	.0000	4.6000	10.5000	.0000	5.0000	79.8000
67	.0000	2.2727	.0000	-2.2727	.0000	.0000
67	1.1000					
68tec	.0000	-4.6000	10.5000	.0000	-5.0000	79.8000
68	.0000	2.2727	.0000	-2.2727	.0000	.0000
68	1.1000					
69rec	-3.0000	.0000	90.3000	.0000	.0000	22.0000
69	.0000	12.0000	.0000	-12.0000	.0000	.0000
70rec	-3.8000	.0000	90.3000	.0000	.0000	22.0000
70	.0000	11.3000	.0000	-11.3000	.0000	.0000
71rpp	-15.5000	-3.0000	-12.0000	12.0000	90.3000	112.3000
72rpp	5.0000	10.0000	-10.0000	10.0000	90.3000	104.3000
73rec	.0000	.0000	125.4000	.0000	.0000	32.2000
73	.0000	17.0000	.0000	-9.8000	.0000	.0000
74rec	.0000	.0000	125.4000	.0000	.0000	32.2000
74	.0000	16.5000	.0000	-9.3000	.0000	.0000
75rec	.0000	.0000	126.8000	.0000	.0000	1.4000
75	.0000	17.0000	.0000	-9.8000	.0000	.0000
76rec	.0000	.0000	129.6000	.0000	.0000	1.4000
76	.0000	17.0000	.0000	-9.8000	.0000	.0000
77rec	.0000	.0000	132.4000	.0000	.0000	1.4000
77	.0000	17.0000	.0000	-9.8000	.0000	.0000
78rec	.0000	.0000	135.2000	.0000	.0000	1.4000
78	.0000	17.0000	.0000	-9.8000	.0000	.0000
79rec	.0000	.0000	138.0000	.0000	.0000	1.4000
79	.0000	17.0000	.0000	-9.8000	.0000	.0000
80rec	.0000	.0000	140.8000	.0000	.0000	1.4000
80	.0000	17.0000	.0000	-9.8000	.0000	.0000
81rec	.0000	.0000	143.6000	.0000	.0000	1.4000
81	.0000	17.0000	.0000	-9.8000	.0000	.0000
82rec	.0000	.0000	146.4000	.0000	.0000	1.4000
82	.0000	17.0000	.0000	-9.8000	.0000	.0000

Figure C-6. (cont.)

83rec	.0000	.0000	149.2000	.0000	.0000	1.4000
83	.0000	17.0000	.0000	-9.8000	.0000	.0000
84rec	.0000	.0000	152.0000	.0000	.0000	1.4000
84	.0000	17.0000	.0000	-9.8000	.0000	.0000
85rec	.0000	.0000	154.8000	.0000	.0000	1.4000
85	.0000	17.0000	.0000	-9.8000	.0000	.0000
86rec	.0000	.0000	160.3000	.0000	.0000	9.2700
86	-2.5000	.0000	.0000	.0000	2.0000	.0000
87rcc	11.1000	.0000	157.8514	.0000	.0000	1.3972
87	20.6986					
88rcc	11.1000	.0000	157.8514	.0000	.0000	1.3972
88	19.3014					
89raw	-15.7245	-30.0000	157.8514	26.8245	30.0000	.0000
89	-25.2690	22.5943	.0000	.0000	.0000	1.3972
90raw	-15.7245	30.0000	157.8514	26.8245	-30.0000	.0000
90	-25.2690	-22.5943	.0000	.0000	.0000	1.3972
91rec	.0000	.0000	141.2000	.0000	.0000	16.4000
91	.0000	19.0000	.0000	-9.8000	.0000	.0000
92rec	.0000	.0000	141.2000	.0000	.0000	16.4000
92	.0000	17.0000	.0000	-9.8000	.0000	.0000
93sph	.0000	.0000	90.3000	1.0000		
94raw	7.5000	-30.0000	141.2000	-7.5000	30.0000	.0000
94	13.7500	3.4375	.0000	.0000	.0000	16.4000
95sph	.0000	.0000	90.3000	1.0000		
96raw	7.5000	30.0000	141.2000	-7.5000	-30.0000	.0000
96	13.7500	-3.4375	.0000	.0000	.0000	16.4000
97rec	.0000	.0000	164.3000	.0000	.0000	10.7300
97	9.0000	.0000	.0000	.0000	-7.0000	.0000
98rec	.0000	.0000	164.3000	.0000	.0000	10.7300
98	7.6000	.0000	.0000	.0000	-5.6000	.0000
99rpp	-15.0000	.0000	-15.0000	15.0000	164.3000	175.0300
100sph	.0000	10.0000	142.3000	0.3600		
101sph	.0000	-10.0000	142.3000	0.3600		
102rec	.0000	.0000	90.3000	.0000	.0000	70.0000
102	.0000	17.2000	.0000	-10.0000	.0000	.0000
103rpp	.0000	15.0000	-17.2000	17.2000	90.3000	160.3000
104trc	.0000	21.5338	160.3000	.0000	.0000	-70.0000
104	4.3238	2.1619				
105trc	.0000	-21.5338	160.3000	.0000	.0000	-70.0000
105	4.3238	2.1619				
106rcc	-4.0	0.0	177.1500	8.0	0.0	0.0
106	0.8					
107rcc	-3.9843	0.0	177.1500	7.9746	0.0	0.0
107	0.7873					
108rcc	-10.82	-5.88	145.06	0.0	0.0	8.0
108	0.8					

Figure C-6. (cont.)

```
109rcc      -10.82     -5.88  145.0727       0.0       0.0    7.9746
109         0.7873
110rcc      -10.82     -7.49    145.06       0.0       0.0       8.0
110            0.8
111rcc      -10.82     -7.49  145.0727       0.0       0.0    7.9746
111         0.7873
112rcc      -10.82     -9.10    145.06       0.0       0.0       8.0
112            0.8
113rcc      -10.82     -9.10  145.0727       0.0       0.0    7.9746
113         0.7873
114rcc      -10.82      1.61    112.04       0.0       0.0       8.0
114            0.8
115rcc      -10.82      1.61  112.0527       0.0       0.0    7.9746
115         0.7873
116rcc      -10.82       0.0    112.04       0.0       0.0       8.0
116            0.8
117rcc      -10.82       0.0  112.0527       0.0       0.0    7.9746
117         0.7873
118rcc      -10.82     -1.61    112.04       0.0       0.0       8.0
118            0.8
119rcc      -10.82     -1.61  112.0527       0.0       0.0    7.9746
119         0.7873
120rcc       10.82      1.61    112.04       0.0       0.0       8.0
120            0.8
121rcc       10.82      1.61  112.0527       0.0       0.0    7.9746
121         0.7873
122rcc       10.82       0.0    112.04       0.0       0.0       8.0
122            0.8
123rcc       10.82       0.0  112.0527       0.0       0.0    7.9746
123         0.7873
124rcc       10.82     -1.61    112.04       0.0       0.0       8.0
124            0.8
125rcc       10.82     -1.61  112.0527       0.0       0.0    7.9746
125         0.7873
126rcc        -4.0       0.0    116.04       8.0       0.0       0.0
126            0.8
127rcc     -3.9873       0.0    116.04    7.9746       0.0       0.0
127         0.7873
128rcc     -2.9719   22.3438      91.3       0.0       0.0       8.0
128            0.8
129rcc     -2.9719   22.3438   91.3127       0.0       0.0    7.9746
129         0.7873
130rcc     -2.9719   20.7238      91.3       0.0       0.0       8.0
130            0.8
131rcc     -2.9719   20.7238   91.3127       0.0       0.0    7.9746
131         0.7873
```

Figure C-6. (cont.)

```
132rcc        0.81  -24.5057      91.3       0.0       0.0       8.0
132            0.8
133rcc        0.81  -24.5057   91.3127       0.0       0.0    7.9746
133         0.7873
134rcc       -0.81  -24.5057      91.3       0.0       0.0       8.0
134            0.8
135rcc       -0.81  -24.5057   91.3127       0.0       0.0    7.9746
135         0.7873
136rpp    -99.9998   99.9998  -99.9998   99.9998   10.1600  210.1596
137rcc      -23.00  -58.3898     83.46       0.0       0.0       8.0
137            0.8
138rcc      -23.00  -58.3898   83.4727       0.0       0.0    7.9746
138         0.7873
139rcc      -23.00  -59.9998     83.46       0.0       0.0       8.0
139            0.8
140rcc      -23.00  -59.9998   83.4727       0.0       0.0    7.9746
140         0.7873
141rcc      -23.00  -61.6098     83.46       0.0       0.0       8.0
141            0.8
142rcc      -23.00  -61.6098   83.4727       0.0       0.0    7.9746
142         0.7873
143rcc        0.81   24.5057      91.3       0.0       0.0       8.0
143            0.8
144rcc        0.81   24.5057   91.3127       0.0       0.0    7.9746
144         0.7873
145rcc       -0.81   24.5057      91.3       0.0       0.0       8.0
145            0.8
146rcc       -0.81   24.5057   91.3127       0.0       0.0    7.9746
146         0.7873
147rcc      -2.9719  -20.7238      91.3       0.0       0.0       8.0
147            0.8
148rcc      -2.9719  -20.7238   91.3127       0.0       0.0    7.9746
148         0.7873
149rcc      -2.9719  -22.3438      91.3       0.0       0.0       8.0
149            0.8
150rcc      -2.9719  -22.3438   91.3127       0.0       0.0    7.9746
150         0.7873
 1        1     -2     -3     -8    -10    -11    -12    -13    -14
        -15    -16    -17    -18    -19    -20    -21    -22    -23
        -24    -25    -28    -29    -30    -31    -32    -33    -34
        -35    -36    -37    -38    -39    -40    -41    -42    -43
        -44    -45    -46    -47    -48
  2      2     -3    -10    -11    -12    -13    -14    -15    -16
        -17    -18    -19    -20    -21
  3      3     -4     -5     -6     -7     -8     -9    -10    -11
        -12    -13    -14    -15    -16    -17    -29    -30    -31
        -32
```

Figure C-6. (cont.)

4	or	4or	5or	6or	7					
5		8	-136	-26	-27	-28	-44	-45	-46	-47
6		9	-4	-5	-6	-7	-50	-51	-52	-53
		-54	-55	-56	-100	-101	-102	-103	-104	-105
		-108	-110	-112	-114	-116	-118	-120	-122	-124
		-128	-130	-132	-134	-137	-139	-141	-143	-145
		-147	-149							
7	or	10or	11or	12or	13or	14or	15or	16or	17	
8	or	18	-22or	19	-23or	20	-24or	21	-25	
9	or	22or	23or	24or	25					
10		26								
11		27								
12		28	-3							
13		29	-8	-30	-32	-33	-36	-44	-45	
14		30	-8	-33	-35	-37	-28			
15		31	-8	-30	-32	-33	-38	-46	-47	
16		32	-8	-33	-39					
17		33	-8	-34	-36	-37	-38	-39		
18	or	36	-40or	37	-41or	38	-42or	39	-43	
19	or	40or	41or	42or	43					
20	or	44or	45or	46or	47					
21		34	-26							
22		35	-27							
23		48	-2							
24		49	-1							
25	or	50	-62	-86	-97	-106	-107			
	or	51	-62	-86	-99	-106	-107			
	or	51	-62	-86	98	-106	-107			
	or	51	-62	-86	-97	-106	-107			
	or	55	-86							
	or	63	-106	-107						
26	or	52	-57	-60	-64	-65	-66	-69	-73	-87
		-91	103	-126	-127	-100	-101			
	or	102	-57	-60	-64	-65	-66	-69	-73	-87
		-91	-126	-127						
	or	58	-64	-60						
	or	61	-64	-57						
	or	59	-69	-64	-126	-127				
	or	70	52	103	-126	-127				
	or	71	102	-126	-127					
	or	72	52	103	-126	-127				
	or	70	102	-126	-127					
	or	74	-57	-60	-64or	75	-57	-60	-64	
	or	76	-57	-60	-64or	77	-57	-60	-64	
	or	78	-57	-60	-64or	79	-57	-60	-64	
	or	80	-57	-60	-64or	81	-57	-60	-64	
	or	82	-57	-60	-64or	83	-57	-60	-64	

Figure C-6. (cont.)

	or	84	-57	-60	-64or	85	-57	-60	-64
	or	88	-57	-60	-64	-65	-66	52	103
	or	88	-57	-60	-64	-65	-66	102	
	or	87	-89	-90	-88	-65	-66	52	103
	or	87	-89	-90	-88	-65	-66	102	
	or	91	-94	-96	-73	102			
	or	91	-94	-96	-73	103			
27	or	53	-67or	54	-68				
28		56	-53	-54	-67	-68			
29		57	-58	-59					
30		60	-61	-59					
31	or	62	-63	-106or	64	-126or	86	-126	
32	or	65or	66						
33	or	67or	68						
34		69	-70	-71	-72	-64			
35		73	-74	-75	-76	-77	-78	-79	-80 -81
		-82	-83	-84	-85				
36	or	87	-88	89	-67	-68			
	or	87	-88	90	-67	-68			
37	or	91	-73	94or	91	-73	96		
38		97	99	-98	-62				
39	or	101	-102or	100	-102				
40	or	104	-65	-128	-130	-143	-145or	105	-66 -132
		-134	-147	-149					
41	or	106	-107or	108	-109or	110	-111or	112	-113
	or	114	-115or	116	-117or	118	-119or	120	-121
	or	122	-123or	124	-125or	126	-127or	128	-129
	or	130	-131or	132	-133or	134	-135or	137	-138
	or	139	-140or	141	-142or	143	-144or	145	-146
	or	147	-148or	149	-150				
42		107							
43		109							
44		111							
45		113							
46		115							
47		117							
48		119							
49		121							
50		123							
51		125							
52		127							
53		129							
54		131							
55		133							
56		135							
57		136	-4	-5	-6	-7	-26	-27	-28 -44
		-45	-46	-47	-9				

Figure C-6. (cont.)

```
58      138
59      140
60      142
61      144
62      146
63      148
64      150
-1
 1 1001    0    2  100    /box/z1001/surrounding/air-void
 2 1002    0    3  100    /box/z1002/bottom/base/pad
 3 1003    0    3  100    /box/z1003/upper/base/pad
 4 1004    0    3  100    /box/z1004/inner/alignment/pads
 5 1005    0    3  100    /box/z1005/inner/box
 6 1006    0    2  100    /box/z1006/inner/box/void-air
 7 1007    0    3  100    /box/z1007/outer/wall/alignment/pads
 8 1008    0    3  100    /box/z1008/base/pad/lift/eyelets
 9 1009    0    2  100    /box/z1009/eyelets/voids-air
10 1010    0    3  100    /box/z1010/inner/box/top/hatch
11 1011    0    3  100    /box/z1011/inner/box/side/hatch
12 1012    0    2  100    /box/z1012/inner/outer/cable/run/void-air
13 1013    0    3  100    /box/z1013/outer/wall/negative/y-axis
14 1014    0    3  100    /box/z1014/outer/wall/positive/x-axis
15 1015    0    3  100    /box/z1015/outer/wall/positive/y-axis
16 1016    0    3  100    /box/z1016/outer/wall/negative/x-axis
17 1017    0    3  100    /box/z1017/outer/top
18 1018    0    3  100    /box/z1018/outer/wall/lift/eyelets
19 1019    0    2  100    /box/z1019/outer/wall/lift/eyelets/void-air
20 1020    0    2  100    /box/z1020/inner/outer/drain/holes
21 1021    0    3  100    /box/z1021/outer/top/hatch
22 1022    0    3  100    /box/z1022/outer/wall/side/hatch
23 1023    0    1  100    /box/z1023/ground
24 1024    0    0    0    /box/z1024/external/void
25 1025    0    5  100    /phanton/z1025/flesh/head-neck
26 1025    0    5  100    /phanton/z1026/flesh/torso
27 1025    0    5   90    /phanton/z1027/flesh/legs
28 1028    0    5   90    /phanton/z1028/sex/organ
29 1029    0    4   90    /phanton/z1029/internal/left/lung
30 1029    0    4   90    /phanton/z1030/internal/right/lung
31 1031    0    6   90    /phanton/z1031/skeletal/skull-neck-spinal
32 1031    0    6   90    /phanton/z1032/skeletal/arms
33 1031    0    6   90    /phanton/z1033/skeletal/legs
34 1031    0    6   90    /phanton/z1034/sheletal/hip
35 1031    0    6   90    /phanton/z1035/skeletal/ribs
36 1031    0    6   80    /phanton/z1036/skeletal/pelvis
37 1037    0    6   80    /phanton/z1037/skeletal/shoulder-blades
38 1038    0    5   80    /phanton/z1038/flesh/throat
```

Figure C-6. (cont.)

39	1031	0	5	80	/phanton/z10349/flesh/breasts
40	1025	0	5	80	/phanton/z1040/flesh/arms
41	1106	0	8	100	/detectors/z1041/containers
42	1107	0	7	100	/detector/z1042/mid-head
43	1109	0	7	100	/detector/z1043/left-chest 1
44	1111	0	7	100	/detector/z1044/left-chest 2
45	1113	0	7	100	/detector/z1045/left-chest 3
46	1115	0	7	100	/detector/z1046/front/mid-gut 1
47	1117	0	7	100	/detector/z1047/fornt/mid-gut 2
48	1119	0	7	100	/detector/z1048/front/mid-gut 3
49	1121	0	7	100	/detector/z1049/rear/mid-gut 1
50	1123	0	7	100	/detector/z1050/rear/mid-gut 2
51	1125	0	7	100	/detector/z1051/rear/mid-gut 3
52	1127	0	7	100	/detector/z1052/inner/mid-gut
53	1129	0	7	100	/detector/z1053/rt. arm/outer
54	1131	0	7	100	/detector/z1054/rt. arm/inner
55	1133	0	7	100	/detector/z1055/left/arm/rear
56	1135	0	7	100	/detector/z1056/left/arm/front
57	1157	0	9	100	/box/z1157/2-inch/inner-liner
58	1158	0	7	100	/detector/z1058/shelf/inner
59	1159	0	7	100	/detector/z1059/shelf/middle
60	1160	0	7	100	/detector/z1060/shelf/outer
61	1160	0	7	100	/detector/z1061/right/arm/rear
62	1160	0	7	100	/detector/z1062/right/arm/front
63	1160	0	7	100	/detector/z1063/left/arm/inner
64	1160	0	7	100	/detector/z1064/left/arm/outer

Figure C-6. (cont.)

INTERNAL DISTRIBUTION

1. B. R. Appleton
2-6. J. M. Barnes
7. T. J. Burns
8-12. J. D. Drischler
13. C. M. Haaland
14. D. T. Ingersoll
15-19. J. O. Johnson
20. J. V. Pace
21. W. A. Rhoades
22. R. W. Roussin
23. R. T. Santoro
24. R. C. Ward
25-26. EPMD Reports Office
27-28. Laboratory Records Department
29. Laboratory Records ORNL-RC
30. Document Reference Section
31. Central Research Library
32. ORNL Patent Section

EXTERNAL DISTRIBUTION

33. Director, Defense Nuclear Agency
ATTN: RARP (Dr. D. L. Auton)
6801 Telegraph Road
Alexandria, VA 22310-3398

34. Dr. Roger W. Brockett
Wang Professor of Electrical Engineering
and Computer Science
Division of Applied Science
Harvard University
Cambridge, Massachusetts 02138

35. Dr. N. Ricky Byrn
Nicholes Research Corp.
4040 So. Memorial Parkway
Huntsville, AL 35802

36. Director, Harry Diamond Laboratory
ATTN: SLCHD-NW-P (Mr. John Corrigan)
2800 Powder Mill Road
Adelphi, MD 20783-1197

37. Electronics Division, NES
ATTN: Dr. Tom Cousins
Defence Research Establishment Ottawa
Ottawa, Ontario, Canada, K1A OZ4

38. Commander, U.S. Army Nuclear & Chemical Agency
ATTN: MONA-ZB (Dr. David Bash)
7500 Backlick Rd., Bldg. 2073
Springfield, VA 22150-3198

39. Establissment Technique Central de l' Armement
ATTN: Dr. Joel Dhermain
Centre d'Etudes du Boucher
16 bis Avenue Prieur de la Cote d'or
94114 Arcueil-Cedex, France

40. Dr. John J. Dorning
Department of Nuclear Engineering & Engineering Physics
Thorton Hall, McCormick Road
University of Virginia
Charlottesville, Va 22901

41. Science Applications International Corporation
ATTN: Dr. Stephen Egbert
10260 Campus Point Drive
San Diego, CA 92121

42. Commander, U.S. Army Combat Systems Test Activity
ATTN: STECS-NE (Mr. John Gerdes)
Aberdeen Proving Ground, MD 21005-5059

43. Ministry of Defence, Atomic Weapons Establishment
ATTN: Dr. Kevin G. Harrison
Building A72, Aldermaston,
Reading, Berkshire, United Kingdom, RG7 4PR

44. Commander, U.S. Army Combat Systems Test Activity
ATTN: STECS-NE (Dr. C. Heimbach)
Aberdeen Proving Ground, MD 21005-5059

45. Director, Bubble Technology Industries, Inc.
ATTN: Dr. Harry Ing
Highway 17
Chalk River, Ontario, Canada, KOJ 1JO

46. Science Applications International Corporation
ATTN: Mr. Dean C. Kaul
10260 Campus Point Drive
San Diego, CA 92121

47. Commander, U.S. Army Combat Systems Test Activity
ATTN: STECS-NE (Dr. A. Halim Kazi)
Aberdeen Proving Ground, MD 21005-5059

48. Director, Armed Forces Radiobiology Research Institute
ATTN: MRAD (CDR Kearsly)
Bethesda, MD 20814-5145

49. Director, Defense Nuclear Agency
ATTN: RARP (MAJ Robert Kehlet)
6801 Telegraph Road
Alexandria, VA 22310-3398

50. Director, Harry Diamond Laboratory
ATTN: SLCHD-NW-P (Mr. Klaus Kerris)
2800 Powder Mill Road
Adelphi, MD 20783-1197

51. US Army Center for EQ/RSTA
ATTN: AMSEL-RSK (Dr. Stanley Kronenberg)
Fort Monmouth, NY 07703

52. Establissment Technique Central de l' Armement
ATTN: Dr. Jacques Laugier
Centre d'Etudes du Boucher
16 bis Avenue Prieur de la Cote d'or
94114 Arcueil-Cedex, France

53. Dr. James E. Leiss
Route 2, Box 142C
Broadway, VA 22815

54. Dr. Neville Moray
Department of Mechanical and Industrial Engineering
University of Illinois
1206 West Green Street
Urbana, Il 61801

55. Director, Defense Nuclear Agency
ATTN: RARP (Ms. Joan Ma Pierre)
6801 Telegraph Road
Alexandria, VA 22310-3398

56. Naval Surface Warfare Center
ATTN: CODE R41 (Mr. Gordon Reil)
New Hampshire Road
White Oak, MD 20903-5000

57. Commander, U.S. Army Foreign Science & Technology Center
ATTN: UVA (Dr. Roger Rydin)
220 7th Street NE
Charlottesville, VA 22901-5396

58. HEAD, Nuclear Radiation Effects
ATTN: Dr. Ludwig Schaenzler
Wehrwissenschaftliche Dienststelle
Postfach 1320
3042 Munster
Federal Republic of Germany

59. David L. Tilson
U.S. Army SDC
ATTN: CSSD-SA-EV
P.O. BOx 1500
Huntsville, AL 35807

60. Commander, U.S. Army Foreign Science & Technology Center
ATTN: AIFRTA (Mr. Charles Ward)
220 7th Street NE
Charlottesville, VA 22901-5396

61. Dr. Mary F. Wheeler
Department of Mathematical Sciences
Rice University
P. O. Box 1892
Houston, Tx 77204-3476

62. Commander, U.S. Army Tank Automotive Command
ATTN: AMSTA-RSK (Mr. Greg Wolfe)
Bldg. 200
Warren, MI 48317-5000

63. Director, Defense Nuclear Agency
ATTN: RARP (Dr. Robert Young)
6801 Telegraph Road
Alexandria, VA 22310-3398

64. Office of the Assistant Manager for Energy
Research and Development
Department of Energy, Oak Ridge Operations
P.O. Box 2001
Oak Ridge, TN 37831

65-74. Office of Scientific and Technical Information
P.O. Box 62
Oak Ridge, TN 37830